



universität
wien

DISSERTATION

Maltolderivate als Liganden von Ruthenium(II)-Cymen Komplexen mit tumorhemmenden Eigenschaften: Der Einfluss der Ligand-Metall Bindungsstabilität auf die zytotoxische Aktivität

angestrebter akademischer Grad

Doktor der Naturwissenschaften (Dr. rer. nat.)

Verfasserin / Verfasser:	Dipl. Ing. Wolfgang Kandioller
Matrikel-Nummer:	9626363
Dissertationsgebiet (lt. Studienblatt):	Chemie (A091 419)
Betreuerin / Betreuer:	Univ.-Prof. Dr. Dr. Bernhard K. Keppler

Wien, am 14. Juli 2009



universität
wien

Ph.D. Thesis

Maltol-derived ruthenium(II)-cymene complexes with tumor inhibiting properties: The impact of ligand-metal bond stability on the anticancer activity

Submitted in part fulfillment of the requirements for the degree
Doctor of Sciences (Dr. rer. nat.)

Author:	Dipl. Ing. Wolfgang Kandioller
Matriculation number:	9626363
Doctoral subject	Chemistry (A091 419)
Supervisor:	Univ.-Prof. Dr. Dr. Bernhard K. Keppler

Vienna, July 10, 2009

This Ph.D. Thesis is based on following publications and submitted manuscripts, which are presented in the original format or the submitted manuscript.

Tuning the anticancer activity of maltol-derived ruthenium complexes by derivatization of the 3-hydroxy-4-pyrone moiety

Wolfgang Kandioller, Christian G. Hartinger, Alexey A. Nazarov, Johanna Kasser, Roland John, Michael A. Jakupec, Vladimir B. Arion, Paul J. Dyson, Bernhard B. Keppler
J. Organomet. Chem., **2009**, 694, 922-929

From pyrone to thiopyrone ligands – the in vitro anticancer activity of Ru(II) arene complexes in dependence of the ligand donor atoms

Wolfgang Kandioller, Christian G. Hartinger, Alexey A. Nazarov, Roland John, Michael A. Jakupec and Bernhard B. Keppler
Organometallics, **in press**

Maltol-derived ruthenium-cymene complexes with tumor inhibiting properties: The impact of ligand-metal bond stability on the anticancer activity

Wolfgang Kandioller, Christian G. Hartinger, Alexey A. Nazarov, Caroline Bartel, Matthias Skocic, Michael A. Jakupec, Vladimir B. Arion and Bernhard K. Keppler
Chem. Eur. J., submitted

Acknowledgements

I would like to thank

O. Prof. Dr. Dr. Keppler for giving me the opportunity to perform my Ph.D. thesis in his working group and for the interesting and challenging topic.

My supervisor Dr. Christian Hartinger for interesting and fruitful ideas and discussions and Dr. Alexey Nazarov for taking the role of Christian during his stay in Switzerland.

Dr. Kristof Meelich, Dr. Wolfgang Schmid, Mag. Sergey Abramkin, DI Amitava Kundu for recording NMR spectra, especially Dr. Michael Reithofer and Ao. Prof. Dr. Markus Galanski for the introduction in NMR measurements.

Alexander Roller and Prof. Arion for X-ray data collection and structure refinement, Mag. Anatoli Dobrov, Dr. Alexey Nazarov and Christian Hartinger for ESI-MS measurements and DI (FH) Caroline Bartel, Dr. Roland John and Dr. Michael Jakupec for the MTT assays.

All members and former colleagues of the working group, especially Hansi, Amitava, Elfi, Muhammad (2x), Christian K., Alex R., Werner, Sergey, Maria, and Andrea for the nice time.

I want to express my deepest gratitude to my whole family for supporting me in hard times and making all this possible.

My good friends Christian, Alex, Mario & Martin, Harti and Tanja for the good non-chemical entertainment.

For financial support:



Last but not least myself for keeping the head up high since 2002.

Abstract

Cancer is the second leading cause of death worldwide and has been over the last decades an area of intensive research. Platinum based chemotherapeutics as cisplatin, oxaliplatin or carboplatin are used in approximately 50% of all cancer treatments. Due to severe side effects of these drugs (e.g. nephrotoxicity, neurotoxicity, nausea, vomiting *etc.*) and intrinsic or acquired resistance, there is an intensive search for novel drugs to overcome these limitations. In the last decade, complexes with metal ions other than platinum, like gallium and ruthenium, have been investigated for their anticancer properties. These compounds have a general lower toxicity and from the chemical point of view more coordination sites compared to platinum. Several ruthenium(III) and gallium(III) complexes (KP46, trismaltolate gallium, KP1019, NAMI-A) entered clinical trials and gave promising results. It is supposed, that the active species of the Ru(III) drugs are Ru(II) analogues which are obtained by reduction with glutathione inside the tumor cell ("*Activation by Reduction*").

During the last years, the novel class of "piano-stool" configured Ru(II) arene complexes has found considerable interest. The arene ligand stabilizes the Ru(II) central atom and also provides an hydrophobic face for the passive transport inside the cell. By modifying the arene moiety, the solubility in water changes dramatically and the affinity to nucleobases can be tuned.

4-Pyrones have been used as chelating ligands for a long time, due to their high affinity towards metal ions. 3-Hydroxy-2-methyl-4-pyrone (maltol) is one of the best known compounds of this class, which forms stable and defined complexes with a high number of 2- and 3-valent metal ions, such as Fe(III), Ga(III), Zn(II), Al(III), Ru(III) *etc.* and based on of its well-studied biocompatibility a favorable toxicity profile is suggested.

Within this Ph.D. thesis, a series of novel Ru(II) arene complexes, bearing a pyrone or thiopyrone moiety as chelating ligand, were synthesized and characterized by 1D and 2D NMR spectroscopy, FT-IR spectroscopy, mass spectrometry, elemental analysis and, if single crystals were obtained, by X-ray diffraction analysis. The stability in aqueous solution, pK_a values of the aqua species and the interactions with small biomolecules (e.g. 5'-GMP, and various amino acids) were determined. The cytotoxic activity of the complexes towards the human cancer cell lines CH1 (ovarian carcinoma), SW480 (colon carcinoma) and A549 (lung carcinoma) was investigated by using the colorimetric MTT assays, expressed as the IC_{50} values and structure–activity relationships have been derived.

Zusammenfassung

Krebs ist die zweithäufigste Todesursache weltweit und in den letzten Jahrzehnten wurde nach immer neuen Behandlungsmöglichkeiten geforscht. Platinbasierende Zytostatika (Cisplatin, Carboplatin, Oxaliplatin) werden in ca. 50% aller Chemotherapien verwendet, aber wegen starker Nebenwirkungen (Nierenschädigung, Neurotoxizität, Übelkeit, Erbrechen, *etc.*) und Resistenzbildung werden neue Medikamente mit einer höheren Selektivität gegenüber der Krebszellen mit einer geringeren Toxizität bei normalen Zellen gesucht. Deswegen steigerte sich in den letzten Jahren das Interesse an Metallkomplexen mit anderen Zentralatomen als Platin, wie z. B. Ruthenium oder Gallium. Der Vorteil dieser neuen Verbindungen besteht in einer geringeren Toxizität und aus der Sicht des Chemikers in der höheren Koordinationszahl im Vergleich zu Platin. Eine Serie von Ru(III) und Ga(III) Komplexen (KP46, Trismaltolato-gallium, KP1019, NAMI-A) befindet sich derzeit in klinischen Studien mit sehr vielversprechenden Resultaten. Es wird vermutet, dass Ru(III) intrazellulär durch Glutathion zur aktiven Ru(II) Spezies reduziert wird („Activation by Reduction“ Hypothese).

Seit einiger Zeit findet die Klasse der Ru(II) Aren Komplexe immer größer werdendes Interesse. Der aromatische Ligand stabilisiert das Ru(II) Zentralatom und bietet eine hydrophobe Stelle für den passiven Transport in die Zelle. Durch die Modifikation des Arens kann die Löslichkeit der Verbindung und die Affinität zu Nukleobasen stark beeinflusst werden.

4-Pyrone werden aufgrund ihrer starken Affinität zu Metallionen seit langem als Chelatliganden verwendet. Maltol ist ein Vertreter dieser Substanzklasse der mit verschiedensten di- und trivalenten Metallionen, wie etwa Fe(III), Ga(III), Zn(II), Al(III), Ru(III), stabile und definierte Komplexe bildet und weiters eine hohe Biokompatibilität mit einem bevorzugten Toxizitätsprofil verbindet.

Im Rahmen meiner Doktorarbeit wurde eine Serie neuer Ru(II)-Aren Komplexe, mit Pyron- und Thiopyronderivaten als Liganden, hergestellt und mittels 1D/2D NMR Spektroskopie, FT-IR Spektroskopie, Massenspektrometrie, Elementaranalyse und im Fall von Einkristallen mit Kristallstrukturanalyse charakterisiert. Die Stabilität in wässriger Lösung und der pK_a Wert der reaktiven Aqua-Spezies wurden bestimmt und Untersuchungen bezüglich der Wechselwirkungen mit kleinen Biomolekülen (z.B. 5'-GMP und diverse Aminosäuren) durchgeführt. Die IC_{50} Werte der Komplexe bezüglich der humanen Krebszelllinien CH1 (Eierstockkrebs), SW480 (Dickdarmkrebs) und A549 (Lungenkrebs) wurden bestimmt und Struktur/Aktivitäts-Beziehungen abgeleitet.

Table of Contents

1.	Abbreviations	1
2.	Introduction	2
2.1.	Cancer – General considerations	2
2.2.	Carcinogenesis	3
2.3.	Different methods of cancer treatment	4
2.4.	Classes of chemotherapeutics	5
2.5.	Metal-based drugs	6
2.6.	Ruthenium complexes	7
2.7.	Overview of ruthenium(II)-arene complexes	10
2.8.	4-Pyr(id)ones as chelating ligands	16
3.	Published results	20
3.1.	Tuning the anticancer activity of maltol derived ruthenium complexes by derivatization of the 3-hydroxy-4-pyrone moiety	20
3.2.	From pyrone to thiopyrone ligands – the in vitro anticancer activity of Ru(II) arene complexes in dependence of the ligand donor atoms	30
3.3.	Maltol-derived ruthenium-cymene complexes with tumor inhibiting properties: The impact of ligand-metal bond stability on the anticancer activity	66
4.	Conclusion and Outlook	106
5.	Curriculum vitae	108

1. Abbreviations

1D	one-dimensional (NMR)	<i>J</i>	coupling constant (NMR)
2D	two-dimensional (NMR)	L-Cys	L-cysteine
AMP	adenosine 5'-mono-phosphate	L-His	L-histidine
brs	broad singlet (NMR)	L-Met	L-methionine
°C	degree Celsius	m	multiplet (NMR)
d	doublet (NMR)	mg	milligram
CDCl ₃	deuterated chloroform	min	minute
CMP	cytidine 5'-monophosphate	μM	micromolar
δ	chemical shift	mL	milliliter
d ₆ - DMSO	deuterated dimethyl sulfoxide	mM	millimolar
DNA	2'-deoxyribonucleic acid	mmol	millimol
D ₂ O	deuterated water	m.p.	melting point
<i>e.g.</i>	<i>exempli gratia</i> (for exam- ple)	MS	mass spectrometry
<i>et al.</i>	<i>et alii</i> (and others)	NMR	nuclear magnetic resonance (spectroscopy)
<i>etc.</i>	<i>et cetera</i> (and other things)	pH	p ondus H ydrogenii (power of hydrogen)
ESI	electrospray ionization	p <i>K_a</i>	log <i>K_a</i> (acid dissociation constant)
g	gram	ppm	parts per million
h	hour	RNA	ribonucleic acid
Gly	glycine	s	singlet (NMR)
GMP	guanosine 5'- monophosphate	t	triplet (NMR)
Hz	hertz	TMP	thymidine 5'-monophosphate
IR	infrared (spectroscopy)		

2. Introduction

2.1. Cancer – General considerations

Cancer is a class of diseases where cells with malignant character grow uncontrolled, followed by invasion of healthy tissues and often formation of metastases. Cancer is the second most prevalent death cause in the European Union. There were about 3.4 million incident cases of cancer and approximately 1.8 million deaths due to this disease registered in 2008. The most common cancers for men are prostate, lung and colorectal cancer and are responsible for about 50% of cancer deaths. In the case of women, breast, colorectal and lung cancer are predominant (Figure 1).

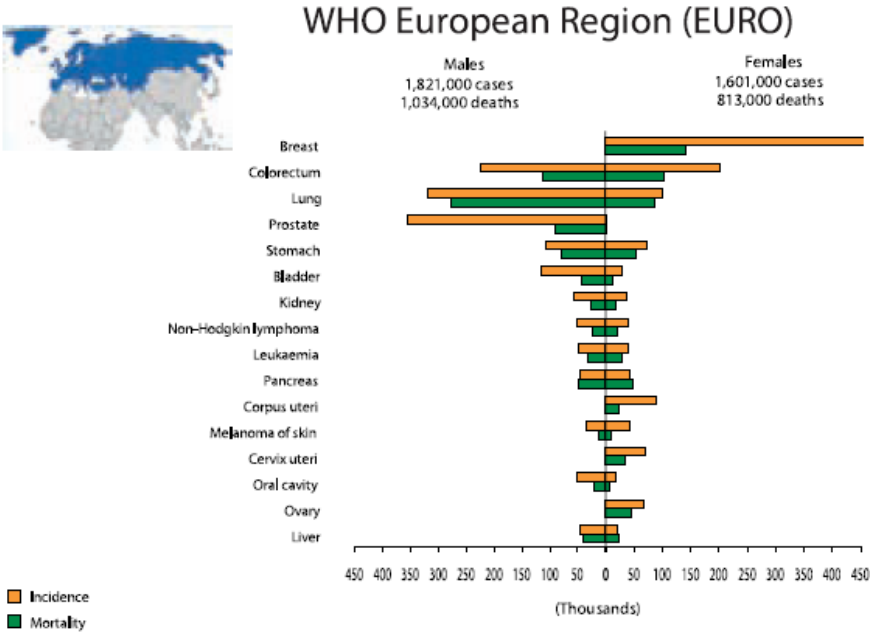


Figure 1: Cancer incidence and mortality rates in the EU¹

A similar trend is observed in Austria, where cancer causes 25.4% of all deaths. Over the last 20 years the number of cancer incidents increased by about 28%, whereas the mortality ratio

¹ WHO, world cancer report 2008

kept nearly stable (+1%)². This can be explained by the development of improved cancer therapeutics as well as by the better prevention and early diagnosis.

2.2. Carcinogenesis

Carcinogenesis (Figure 2) deals with the transformation of healthy to malignant cells and is a complex and until now not fully understood process over several stages: (i) Initiation, (ii) Promotion, (iii) Conversion, (iv) Progression.

Initiation is the first step, where mutagens modify DNA. If the damage is too serious that the repair mechanisms of the cell or the programmed cell death (apoptosis) fail, this irreversible mutation is given to the next cell generation and proto-oncogenes can be generated, which promote cell growth and mitosis. The same result is obtained by mutations of tumor suppressor genes, e.g. the p53 gene. Several severe mutations are necessary for the conversion of normal cells in malignant cells³.

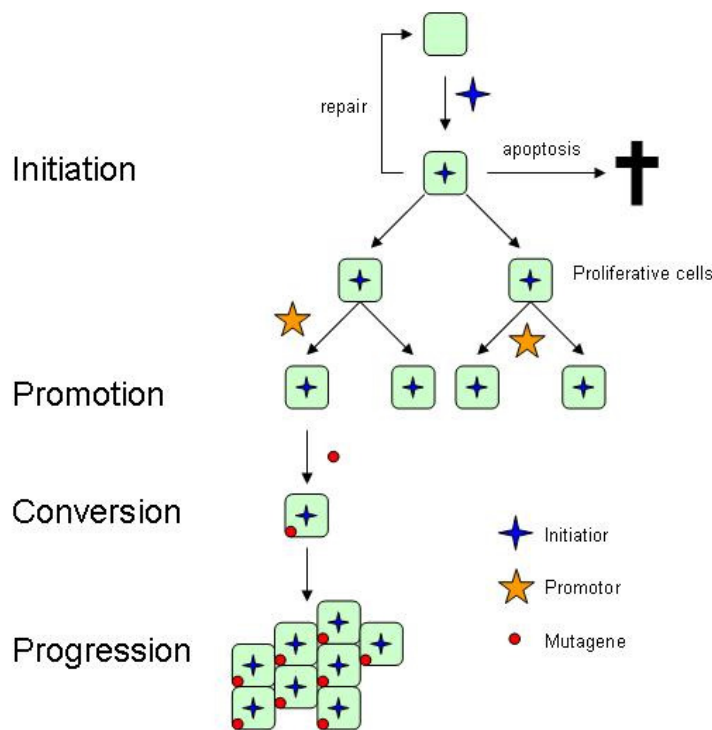


Figure 2: Carcinogenesis

² Statistik Austria, Jahrbuch der Gesundheitsstatistik 2007

³ C. Haskell, Cancer Treatment, Academic Press, New York 2008

The next step is the promotion by exo- or endogenous parameters (promoters) (alcohol, free radicals, hormones,...), which results in proliferation of the initialized cells. The preneoplastic cell population with identical mutations is restricted (benign tumor), but able to handicap organs or invade surrounding tissues. This stage is reversible, due to the dependence on a constant presence of the promoter. Additional mutations lead to the formation of malignant cells inside the benign tumor. This transformation could also occur directly after initiation and the appearance of benign tumors is not required. The next stage (Progression) is the fast and uncontrolled cell growth, activated by progressors. The tumor invades and damages healthy tissue and metastases are released into the blood or lymph stream.

2.3. Different methods of cancer treatment

Due to the fact, that cancer is a class of diseases, there will be no single cure. Various methods have been developed within the last century. Cancer treatment differs depending on the class, the state and the location of the tumor. The age and health state of the patient is important as well. The most common approaches for cancer treatment are:

- Surgery: only applicable for primary tumors and localized metastases
- Radiation therapy: can be used for every solid tumor and localized metastases, but damages healthy tissues and has severe side effects like damage of the epithelial surface, swelling as a consequence of inflammation ...
- Chemotherapy: chemicals which harm the cell replication by binding or intercalation to DNA, interaction and inhibition of proteins involved in the cell cycle (e.g. topoisomerase I and II)

In most cases, cancer is treated by a combination of the above listed methods to increase the chance of cure.

2.4. Classes of chemotherapeutics

Chemotherapy is a general term for treating diseases by using pharmaceutical compounds, but in general used for substances active in the treatment of cancer. The main targets of chemotherapeutics are often DNA or other crucial parameters for cell replication like Topoisomerase or inhibition of mitosis. In many cases, the drug interacts with DNA by formation of a covalent bond or by intercalation into the α -helix, which inhibits the DNA transcription and induces cell death. The following classes of compounds are used for clinical treatment⁴.

- Alkylating agents alkylate DNA and induce strain breaks, cross-linking of DNA, RNA and proteins
 - Triazines e.g. *Dacarbazine*
 - Nitrogen mustards e.g. *Cyclophosphamide*; *Chlorambucil*
 - Alkyl sulfonates e.g. *Busulfan*
 - Nitrosoureas e.g. *lomustine*, *carmustine*, *streptozocine*
 - Platinum(II) or (IV) complexes e.g. *Cisplatin*, *carboplatin*, *oxaliplatin* are often wrongly referred as alkylating agents.
- Anti-Metabolites mimic essential DNA nucleobases like modified purines or pyrimidines and induce cell cycle arrest
 - Folic acid analogues e.g. *methotrexate*
 - Pyrimidine analogues e.g. *5-fluorouracil*, *floxuridine*, *gemcitabine*
 - Purine analogues e.g. *Tioguanine*, *Fludarabine*
- Topoisomerase inhibitors: DNA replication and transcription is hindered e.g. *topotecan* (Topoisomerase I), *etoposide* (Topoisomerase II)

Other approaches for cancer treatment are for example hormone inhibitors (GnRH - analogs), mitosis inhibitors, cytotoxic antibiotics, antibodies, signal transduction and enzyme inhibitors.

⁴ C. M. Haskell, Cancer Treatment, Saunders, Philadelphia 2000

2.5. Metal-based drugs

Metal-based drugs have been used as therapeutic agents since early history and were applied in their simplest form, as salts. Li_2CO_3 is an important tool for the treatment of manic states and bipolar disorder and is in clinical application since the 1950ies. Lithium carbonate is administered orally and has a well established toxicity profile. Arsenic compounds have a long history in the treatment of various diseases. Salvarsan was used from 1910 to the 1930ies for the treatment of syphilis and was a milestone in the development of metal-based drugs. Trisenox (As_2O_3) was approved in 2000 by the Food and Drug Administration for the treatment of acute promyelocytic leukemia (APL). Further established metal compounds in clinical treatment are: (i) silver nitrate as disinfectant, (ii) mercury salts for their antibacterial and antifungal properties, (iii) gold complexes (Auranofin) for the treatment of chronic arthritis, (iv) bismuth salts as antacid and astringent agents, (v) antimony gluconate as antiparasitic drug, (vi) gallium salts as anticancer agents⁵.

Since the discovery of the antineoplastic effect of *cisplatin* by Barnett Rosenberg⁶, platinum based chemotherapeutics have been a field of intensive research for more than 40 years. Although several thousand compounds have been synthesized, only a small number has entered clinical trials⁷ and only two other compounds, *carboplatin* and *oxaliplatin* (Figure 3), are used worldwide for the treatment of cancer. These three compounds are used in the treatment of approximately 50% of all cancer cases.

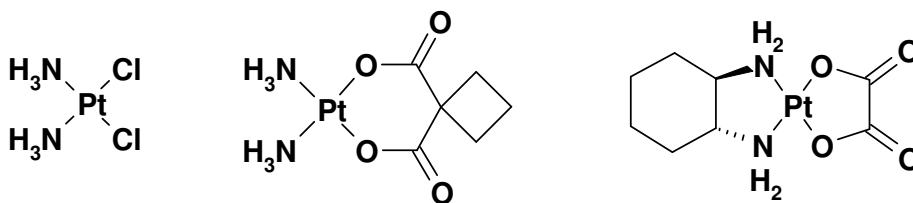


Figure 3: Platinum compounds used in clinical treatment; from left to right: cisplatin, carboplatin, oxaliplatin

Cisplatin is used for the treatment of small and non-small cell lung cancer, metastatic testicular tumors, bladder carcinoma, cervical and esophageal cancer. It is one of only few drugs with a high curative potential in cancer treatment. The activity profile of carboplatin is very

⁵ Z. Guo, P. J. Sadler, *Adv. Inorg. Chem.* **2000**, 49, 183.

⁶ Rosenberg, M.; VanCamp, L.; Krigas, T. *Nature* **1965**, 205, 698.

⁷ Galanski, M.; Jakupec, M. J.; Keppler, B. K. *Curr. Med. Chem.* **2005**, 18, 2075.

similar to cisplatin, but the lower toxicity leads to higher applicable doses. Oxaliplatin is used for the treatment of colorectal cancer in combination with 5-fluorouracil.

Nevertheless, it has to be kept in mind that platinum based drugs are only active in a small number of tumors and the side effects are severe. Frequently observed are nausea, vomiting, nephrotoxicity, neurotoxicity, myelosuppression, tinnitus and ototoxicity. Intrinsic and acquired resistance are also major drawbacks for this class of drugs. To overcome these problems, the development of novel chemotherapeutics with a different activity profile, mode of action, with lower toxicity and higher selectivity is essential for the improved treatment of cancer.

As a consequence, complexes with other metal ions than platinum have become an area of intensive research. Within our working group, the ruthenium complex KP1019 and the gallium complex KP46 have been synthesized and entered recently clinical trials with promising results⁸.

2.6. Ruthenium complexes

The cytotoxic potential of ruthenium complexes has been found three decades ago and the utilization of ruthenium offers several advantages over platinum-based chemotherapy⁹. First of all, ruthenium is stable in different oxidation states (II, III, IV) at physiological conditions and also the preparative chemistry is well developed. Ruthenium complexes have an octahedral coordination sphere in contrast to square-planar Pt(II). Ligand substitution kinetics are similar to Pt(II) compounds, but tunable due to the strong influence of the coordinated ligands. Ruthenium has the ability of mimicking iron, which leads to lower toxic side effects and a different mode of action.

The two most famous compounds (Figure 4) are imidazolium [*trans*-tetrachloro(dimethylsulfoxide)(imidazole)ruthenate(III)] (NAMI-A) and indazolium [*trans*-

⁸ F. Lentz, A. Drescher, A. Lindauer, M. Henke, R. A. Hilger, C. G. Hartinger, M. E. Scheulen, C. Dittrich, B. K. Keppler, U. Jaehde, *Anticancer Drugs* **2009**, *20*, 97.

⁹ R. Margalit, H. B. Gray, M. J. Clarke, L. Podbielski, *Chem.-Biol. Interact.* **1986**, *59*, 231.

tetrachlorobis(1H-indazole)ruthenate(III)] (KP1019). Both complexes adopt octahedral coordination geometry with Ru(III) as central ion. NAMI-A showed marked efficacy against metastases in preclinical models¹⁰, whereas KP1019 exhibits excellent activity especially in an autochthonous colorectal tumour model that resembles human colon tumors in its histological appearance and behavior against chemotherapeutics¹¹. Remarkable is the significantly lower toxicity and the general inactivity of platinum-based drugs for this kind of tumors.

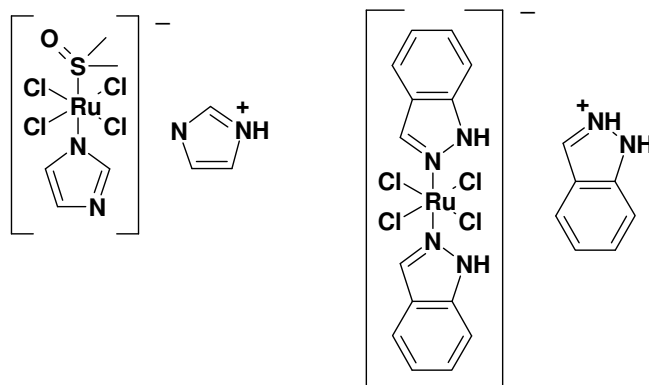


Figure 4: Ru(III) complexes in clinical trials; NAMI-A (left) and KP1019 (right)

The supposed mode of action of KP1019 involves intravenous application and subsequent quick binding to proteins, which is thought to be responsible for the general low toxicity. This fast attachment prevents KP1019 of hydrolysis, which would lead to the inactive and insoluble aqua-complex^{12,13}. For platinum chemotherapeutics, the interaction with blood proteins is supposed to be an important factor for side effects. The cellular uptake of the KP1019-transferrin adduct by endocytosis is thought to be enhanced by the increased number of transferrin receptors, which are expressed by the cancer cell as a consequence of the higher iron requirement of malignant cells. After release from the protein, the Ru(III) compound undergoes *in vivo* reduction to the kinetically more reactive Ru(II) species by glutathione or other biologic reducing agents. This “Activation by Reduction” step was supposed by Clarke three decades ago¹⁴. The needed reductive micro-environmental conditions for this conversion are

¹⁰ Alessio, E.; Mestroni, G.; Bergamo, A.; Sava, G. *Curr. Top. Med. Chem.* **2004**, *4*, 1525–1535.

¹¹ Berger, M. R.; Garzon, F. T.; Keppler, B. K.; Schmähl, D. *Anticancer Res.* **1989**, *9*, 761–766.

¹² K.-G. Lipponer, E. Vogel, B.K. Keppler, *Metal-Based Drugs* **1996**, *3*, 243.

¹³ B. Cebrian-Losantos, E. Reisner, C. R. Kowol, A. Roller, S. Shova, V. A. Arion, B. K. Keppler, *Inorg. Chem.* **2008**, *47*, 6513.

¹⁴ M. J. Clarke, *Met. Ions Biol. Syst.* **1980**, *11*, 231.

formed by the insufficient nutrient and blood supply (hypoxia). DNA does not seem to be the main target of KP1019, in contrast to platinum-based chemotherapeutics, although DNA damage was observed¹⁵. It was found, that the induction of apoptosis could also be explained by the intrinsic mitochondrial pathway¹⁶, but further investigations are necessary to elucidate the major target of KP1019.

As a consequence of the “*Activation by reduction*” hypothesis, Ru(II) complexes have been investigated for their cytotoxic potential. Ruthenium(II) can be easily oxidized and for stabilization of the metal center in oxidation state +2, the coordinating ligands play an important role. It is known, that Ru(II) reacts fast with sulfur and nitrogen functionalities, forming stable compounds. First, the close analogues of *cis*- and *transplatin* *cis*- and *trans*-Ru(DMSO)₄X₂ (X = Br, Cl) were synthesized and screened for their antiproliferative activity in C75B1 and BD2F1 cancer cell lines (lung carcinoma). The *trans* isomer was found to be 20-fold more active against metastases than the corresponding *cis* complex^{17,18}. Bi- and polypyridyl Ru(II) complexes have been investigated intensively and a large number of applications, related to the well documented photophysical and electrochemical properties, have been established. The use of typically commercially available polypyridyl ligands like 2,2'-bipyridine (bpy), 1,10-phenanthroline (phen) and 2,2':6'2''-terpyridine (terpy) yields highly stable Ru(II) complexes. The interaction with DNA or other biomolecules have been investigated for this class of compounds for more than 20 years and it depends strongly on the type of the polypyridyl chelate. The complex [Ru(bpy)₃]²⁺ shows only weak interaction with DNA (mainly electrostatic), while the interaction of [Ru(phen)₃]²⁺ is much stronger¹⁹. Another reported interaction with DNA of this class of complexes is intercalation, which depends on the size of the aromatic ring system of the polypyridyl ligands. The complex [Ru(bpy)₂(dppz)]²⁺ (dppz = dipyrido [3,2-a:2',3'-c]-phenazine) is luminescent when intercalated into DNA and used therefore as a light switching probe, whereas the complex [Ru(bpy)(dpq)]²⁺ (dpq =dipyrido [3,2-d:2c',3c'-f] quinoxaline) does not show this behavior.

¹⁵ S. Kapitza, M. A. Jakupec, M. Uhl, B. K. Keppler, B. Mariani, *Cancer Lett.* **2005**, 226, 115.

¹⁶ S. Kapitza, M. Pongratz, M. A. Jacubec, P. Heffeter, W. Berger, L. Lackinger, B. K. Keppler, B. Mariani, *J. Cancer. Res. Clin. Oncol.* **2005**, 46, 472.

¹⁷ E. Alessio, G. Mestroni, G. Nardin, W. M. Attia, M. Calligaris, G. Sava, S. Zorzet, *Inorg. Chem.* **1988**, 27, 4099.

¹⁸ G. Sava, S. Pacor, S. Zorzet, E. Alessio, G. Mestroni, *Pharmacol. Res.* **1989**, 21, 617.

¹⁹ J. M. Kelly, A. B. Tossi, D.J. McConnel, C. Oh Uigin, *Nucl. Acids Res.*, **1985**, 13, 6017.

2.7. Overview of ruthenium(II)-arene complexes

Iron(II) has similar chemical and physical properties as ruthenium(II) and therefore, stabilization can also be easily achieved for Ru(II) by η^6 -coordination of aromatic moieties, which leads to half sandwich complexes. The Ru(II) center adopts the so called “piano-stool” configuration, where the aromatic ring forms the seat and the remaining three ligands the legs (Figure 5).

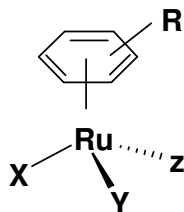


Figure 5: General formula of Ru(II) complexes with “piano-stool” configuration

This conformation offers the opportunity of derivatization at the arene moiety and the application of various mono- or bidentate ligands. In general, at least one halide is coordinated to the ruthenium, because the aquation, which leads to the formation of a highly reactive aqua species, seems to be essential for the activity, though also inert complexes with anticancer properties have been reported. This conversion to a charged complex is responsible for the good aqueous solubility, which is also an important factor for biological studies and possible clinical applications. Insertion of the arene moiety has important effects on the physical and chemical properties: (i) it offers a hydrophobic face which facilitates the passive transport *via* diffusion through the cell membrane and gives the possibility of intercalation with the DNA double-strand; (ii) it has a big influence on the ligand exchange kinetics and protein binding ability; (iii) it is inert toward ligand exchange reactions, but it is flexible site for derivatization²⁰.

This class of organometallic ruthenium compounds has been investigated for more than twenty years. One of the first reported complexes was $[\text{Ru}(\text{C}_6\text{H}_6)(\text{DMSO})\text{Cl}_2]$ (Figure 6). This complex shows strong inhibition of topoisomerase II, which is essential for structural organi-

²⁰ M. J. Clarke, *Coord. Chem. Rev.*, **2003**, 236, 209.

zation of the mitotic chromosomal scaffold during the cell replication process²¹. The coordination of PTA (1,3,5-triaza-7-phosphatricyclo[3.3.1.]decane) instead of DMSO yields the so called RAPTA complexes (Figure 6). *Dyson et al.* have shown, that this ligand exchange leads to largely increased aqueous solubility, interesting antimetastatic activities with high selectivity next to a low general toxicity. The PTA ligand is supposed to be responsible for the observed selectivity. It has been shown, that methylation of one PTA nitrogen leads to a large increase of toxicity²². The replacement of the chlorido ligands by oxalate or cyclobutane-1,1-dicarboxylate gives analogues of oxali- and carboplatin, which show minor influence on the biological activity²³.

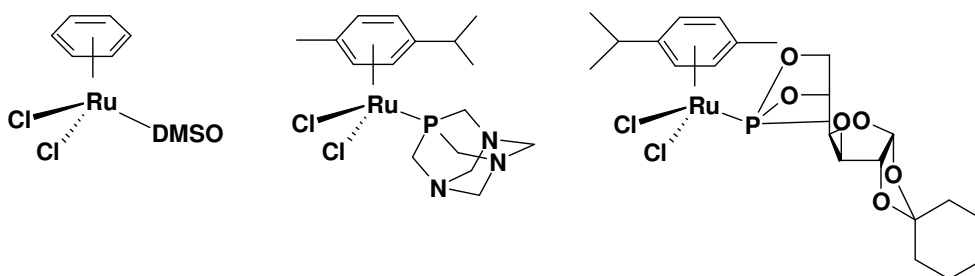


Figure 6: from left to right: $[\text{Ru}(\text{C}_6\text{H}_6)(\text{DMSO})\text{Cl}_2]$, RAPTA-C, KP1558

$\text{Ru}(\text{II})$ cymene complexes have been prepared, wherein the PTA has been replaced by 3,5,6-bicyclophosphite- α -D-glucofuranoside ligands. It has been shown that the cytotoxic activity can be tuned by the lipophilicity of the alkyl moiety of the phosphites. The ruthenium complex KP1558 (Figure 6) has shown among the tested derivatives the highest cytotoxic activity towards different cancer cell lines²⁴. Hydrolysis of these P-sugar containing $\text{Ru}(\text{II})$ complexes leads to the cleavage of one P-O bond. This degradation process can be inhibited by addition of sodium chloride, due to the reversibility of the first hydrolysis step of the $\text{Ru}(\text{II})$ center.

The complexes $[\text{Ru}(\eta^6\text{-}p\text{-cymene})(\text{X})(\text{Y})(\text{Z})]$ (X, Y or Z = halide, acetonitrile or isonicotinamide) with three monodentate ligands, have no significant activity against A2780 cancer cells. This lack of cytotoxicity can be explained by their high reactivity, which leads to fast

²¹ Y.N.V. Gopal, D. Jayaraju, A.K. Kondapi, *Biochemistry* **1999**, *38*, 4382

²² C. Scolaro, A. Bergamo, L. Brescacin, R. Delfino, M. Cocchietto, G. Laurenczy, T. J. Geldbach, G. Sava, P. J. Dyson, *J. Med. Chem.* **2005**, *48*, 4161.

²³ A. Casini, P. J. Dyson, L. Messori, *ChemMedChem* **2007**, *2*, 631.

²⁴ I. Berger, M. Hanif, A. A. Nazarov, C. G. Hartinger, R. O. John, M. L. Kuznetsov, M. Groessler, F. Schmitt, O. Zava, F. Biba, V. A. Arion, M. Galanski, M. A. Jakupec, L. Juillerat-Jeanneret, P. J. Dyson, B. K. Keppler, *Chem. Eur. J.* **2008**, *14*, 9046.

interaction with small biomolecules and potentially deactivates them before reaching the cellular target²⁵. Therefore, organometallic compounds of the general formula $[\text{Ru}(\eta^6\text{-arene})(\text{en})\text{X}]$ (Figure 7, arene = benzene or derivatives of benzene, en = ethylenediamine or derivatives, X = a halide), have been investigated by *Sadler et al* and it has been shown, that the coordination of the chelating ligand ethylenediamine leads to lower reactivity compared to monodentate ligands and interesting biological and chemical properties was observed²⁶.

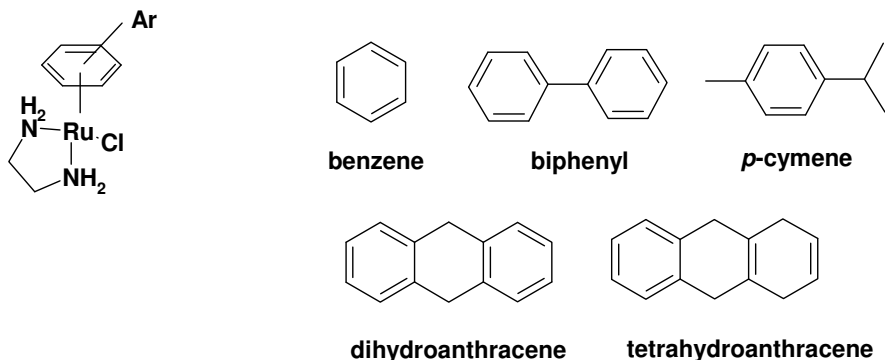


Figure 7: Ru(II) arene complexes (by *Sadler et al.*) with various arene ligands

The cytotoxic activity of these complexes against the human ovarian cancer cells A2780 depends on the size of the coordinated arene and benzene showed the lowest and tetrahydroanthracene the highest effect (Table 1).

Arene / Pt compound	X	Y	Z	IC ₅₀ (μM)
<i>p</i> -Cymene	isonicotineamide	Cl	Cl	>150
<i>p</i> -Cymene	en		Cl	10 ± 1.1
Benzene	en		Cl	17 ± 8.3
Tetrahydroanthracene	en		Cl	2 ± 0.4
<i>Carboplatin</i>				6 ± 0.7
<i>Cisplatin</i>				0.6 ± 0.06

Table 1: IC₅₀ values against A2780 cancer cells of Ru(II) arene complexes with the general formula $[\text{Ru}(\eta^6\text{-arene})(\text{X})(\text{Y})(\text{Z})]$ compared to *cis*- and *carboplatin*

²⁵ R. E. Morris, R. E. Aird, P. del S. Murdoch, H. Chen, J. Cummings, N. C. Hughes, S. Parsons, A. Parkin, G. Boyd, D. I. Jodrell, P. J. Sadler, *J. Med. Chem.* **2001**, *44*, 3616

²⁶ R.E. Aird, J. Cummings, A. A. Ritchie, M. Muir, R. E .Morris, H. Chen, P. J. Sadler, D. I. Jodrell, *Br. J. Cancer* **2002**, *86*, 1652

It has been shown, that hydrolysis plays an important role for the cytotoxic activity of some metal based drugs^{27,28}. The halido complexes often act as prodrugs and are activated by hydrolysis. Under physiological conditions, the aqua species react rapidly to biomolecules, which influences strongly pharmacodynamics and pharmacokinetics. The interaction with blood proteins, DNA (components) or small biomolecules has a protective effect and decreases the rate of degradation or side product formation²⁹. In the case of Ru(II), the formation of the highly reactive aqua complex proceeds *via* a dissociative process, the leaving group (normally the halide) is cleaved off, leading to a 16 electron complex, followed by interaction with the solvent molecule, yielding in an activated 18 electron aqua complex.

Next to the increased cytotoxicity by application of chelating ligands, another interesting feature for these group of Ru(II) arene complexes has been reported³⁰. The complex $[\text{Ru}(\eta^6\text{-biphenyl})(\text{en})\text{Cl}]^+$ was found to possess high selectivity towards small biomolecules. This compound binds selectively towards the *N7* of guanosine, to *N3* of thymidine and to *N1* and *N7* of inosine. Hence, no coordination towards adenosine and only weak interaction with *N3* of cytidine was observed. Furthermore, the reactivity at physiological pH decreases in the order $\text{G}(\text{N7}) > \text{I}(\text{N7}) > \text{I}(\text{N1})$, $\text{T}(\text{N3}) > \text{C}(\text{N3}) > \text{A}(\text{N7})$, $\text{A}(\text{N1})$. Therefore, “piano-stool” Ru(II) complexes are much more selective than the square-planar Pt(II) compounds. The interaction with nucleotides such as 5'-GMP (DNA building block and model for interactions with Pt(II) complexes) has been investigated and again selective binding towards *N7* was found, similarly to studies with nucleosides. In competition studies with 5'-AMP, 5'-CMP and 5'-TMP only the 5'-GMP adduct was observed.

The type of chelating ligand plays an important role and has a strong influence on the chemical, physical and biological properties of Ru(II) compounds. The exchange of ethylenediamine by acetylacetonate (acac) leads to neutral complexes (Figure 8), which have an increased electron density of the Ru(II) center, which facilitates ligand exchange and hydrolysis processes³¹. The solubility of these compounds is increased, due to the formation of the better soluble and

²⁷ Berners-Price, S. J.; Frenkiel, T. A.; Frey, U.; Ranford, J. D.; Sadler, P. J. *J. Chem. Soc., Chem. Comm.* **1992**, 10, 789.

²⁸ A. Küng, T. Pieper, R. Wissiack, E. Rosenberg, B. K. Keppler, *J. Biol. Inorg. Chem.* **2001**, 6, 292.

²⁹ A. R. Tmerbaev, C. G. Hartinger, S. S. Aleksenko, B. K. Keppler, *Chem. Rev.* **2006**, 106, 2224.

³⁰ H. Chen, J. A. Parkinson, R. E. Morris, P. J. Sadler *J. Am. Chem. Soc.* **2003**, 125, 173

³¹ R. Fernandez, M. Melchart, A. Habtemariam, S. Parsons, P. J. Sadler, *Chem. Eur. J.* **2004**, 10, 5173.

charged aqua complexes. Furthermore, the before mentioned selectivity towards nucleobases is changed. The complex $[\text{Ru}(\eta^6\text{-}p\text{-cymene})(\text{acac})\text{Cl}]$ shows higher affinity towards adenine than to guanine. These results give access to novel Ru(II) complexes with different affinities and therefore possibilities of tuning the activity of organometallic ruthenium drugs.

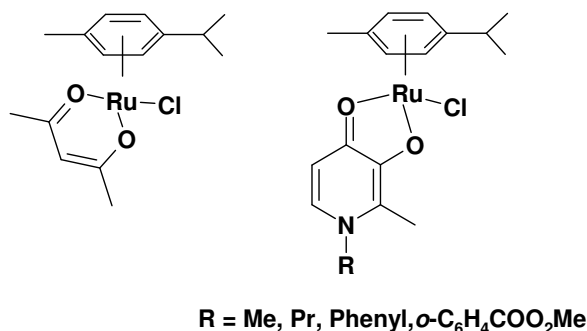


Figure 8: left: $[\text{Ru}(\text{cym})(\text{acac})\text{Cl}]$; right: 3-hydroxy-2-methyl-4-pyridone Ru(II) cymene complexes

During the last years, the main target of novel derivatives was the modification of the arene moiety, while the chelating ligand kept very simple and purchasable. *Severin et al.* were the first, who synthesized Ru(II) cymene complexes bearing 4-pyridones as chelating ligands³² (Figure 8), but they focused their investigations on the catalytic properties and not on the anti-cancer potential. Recently, a series of novel 4-pyridone derived chelating ligands and their Ru(II) complexes have been prepared. Investigations have shown that the coordination of pyridone moieties leads to highly active compounds with interesting biochemical features (Figure 9)³³.

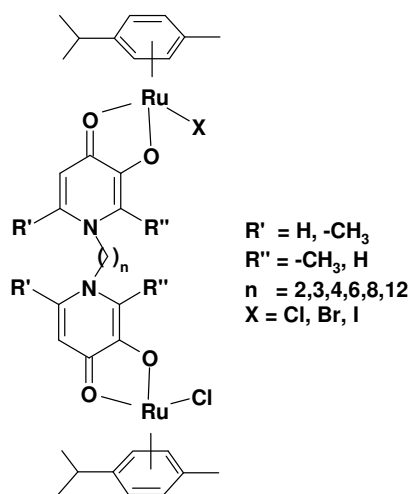


Figure 9: Dinuclear pyridone based Ru(II) cymene complexes

³² R. Lang, K. Polborn, T. Severin, K. Severin, *Inorg. Chem. Acta* **1999**, 294, 62.

³³ O. Novakova, A. A. Nazarov, C. G. Hartinger, B. K. Keppler, V. Brabec, *Biochem. Pharmacol.* **2009**, 77, 364.

The lipophilicity of the 3-hydroxy-2-methyl-4-pyridone derived chloro complexes, the corresponding IC₅₀ and log P values are shown in Table 2. It can be seen, that the cytotoxic activity correlates with the lipophilicity and can be tuned by increasing the length of the aliphatic chain between the two pyridones³⁴. The observed IC₅₀ values are in the same dimension as established Pt(II) anticancer drugs. These complexes undergo rapid hydrolysis to the more reactive aqua species and form rapidly adducts with DNA and model nucleotides, but no reaction with the small proteins cytochrome c or ubiquitin was observed³⁵. The pK_a values are in the same range (~ 9.70) as known for other Ru(II) complexes.

n	log P	IC ₅₀ [μM]	
		SW480	A2780
2	-1.42	76 ± 4	84 ± 3
3	-1.39	62 ± 14	25 ± 2
4	-1.33	28 ± 1	41 ± 2
6	-1.36	26 ± 8	30 ± 6
8	-1.28	2.5 ± 0.2	5.7 ± 0.5
12	-0.56	0.29 ± 0.05	1.5 ± 0.3

Table 2: log P and IC₅₀ values of dinuclear Ru(II) cymene complexes

Additional, mono and dinuclear Ru(II) cymene complexes derived from ethylmaltol and alloxal, based are currently under investigation^{36,37}.

³⁴ M. G. Mendoza-Ferri, C. G. Hartinger, R. E. Eichinger, N. Stolyarova, K. Severin, M. A. Jakupec, A. A. Nazarov, B. K. Keppler, *Organometallics* **2008**, *27*, 2405.

³⁵ M. G. Mendoza-Ferri, C. G. Hartinger, M. A. Mendoza, M. Groessl, A. E. Egger, R. E. Eichinger, J. B. Mangrum, N. P. Farrell, M. Maruszak, P. J. Bednarski, F. Klein, M. A. Jakupec, A. A. Nazarov, K. Severin, B. K. Keppler, *J. Med. Chem.* **2009**, *54*, 916.

³⁶ M. A. Shaheen, W. Kandjoller, M. G. Mendoza-Ferri, A. A. Nazarov, C. G. Hartinger, B. K. Keppler, *Chem. Biodiv.* **2008**, *5*, 2060.

³⁷ M. G. Mendoza-Ferri, C. G. Hartinger, A. A. Nazarov, W. Kandjoller, K. Severin, B. K. Keppler, *Appl. Organomet. Chem.* **2008**, *22*, 326.

2.8. 4-Pyr(id)ones as chelating ligands

4-Pyridones and their close analogues 4-pyrones are widely used as chelating ligands due to their high affinity towards a large range of di- and trivalent metal ions³⁸, which results in highly stable complexes. This ability can be explained by the pseudo-aromatic character of the ring system (Figure 10).

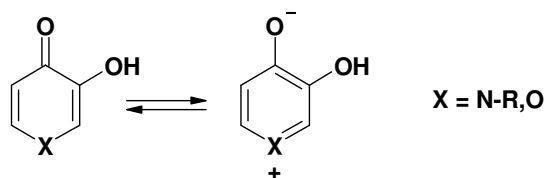


Figure 10: Mesomeric forms of 3-hydroxy-4-pyr(id)one

The conversion of pyrones to the corresponding pyridones can be performed easily and was described by *Harris et al*³⁹. It has been shown, that protection of the hydroxyl group via benzylation facilitates the reaction and the pH value of the reaction (~12) is essential for high yield. Cleavage of the benzyl group *via* hydrogenation affords the desired 4-pyridones. This synthetic route enabled a whole series of novel 4-pyridone-based chelating ligands^{40,41}. It was found, that 3-hydroxy-4-pyridones have a strong affinity towards iron⁴² and can therefore be used as regulating agent for iron overload disorders.

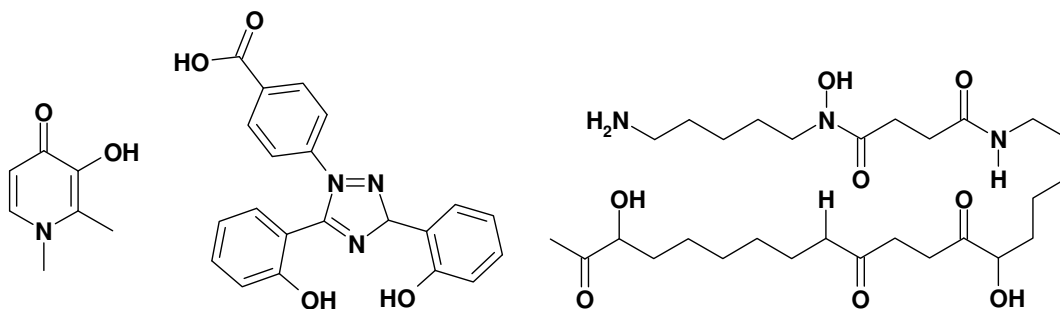


Figure 11: Compounds used for clinical treatment of iron overload. From left to right: Deferiprone (L1 or CP20), Desferasirox (Exjade or ICL670) and Desferoxamin (Desferal)

³⁸ K. H. Thompson, C. A. Barta, C. Orvig, *Chem. Soc. Rev.* **2006**, 35, 545.

³⁹ R. L. N. Harris, *Aust. J. Chem.* **1976**, 29, 1329.

⁴⁰ P. S. Dobbin, R. C. Hider, A. D. Hall, P. D. Tazlor, P. Sarpong, J. B. Porter, G. Xiao, D. van der Helm, *J. Med. Chem.* **1993**, 36, 2448.

⁴¹ L. S. Dehkordi, Z. D. Liu, R. C. Hider, *Eur. J. Med. Chem.* **2008**, 43, 1035.

⁴² W. C. Tsai, K. H. Ling, *J. Chin. Biochem. Soc.* **1973**, 2, 70

Deferiprone (1,2-dimethyl-3-hydroxypyrid-4-one) (Figure 11) was synthesized by *Kontoghiorghes et al.* in the early 1980ies⁴³ and is in clinical application since 2000 in Europe. The bidentate ligand forms 1:3 iron chelate complexes and it was found to be relatively non-toxic even at high doses (200 mg/kg). Deferiprone was the first drug for the treatment of iron overload that could be administered orally, furthermore the high selectivity towards iron is noteworthy. No significant increase in excretion of Cu, Zn, Mg, or Ca was detected⁴⁴. One major disadvantage of Deferiprone is the fast inactivation by phase II metabolism (glucuronidation)⁴⁵. Around 85% of the administered dose is recovered as the converted *O*-glucuronid in the urine. These insights in the deferiprone metabolism led to the synthesis of novel 4-hydroxypyridones, which do not undergo this inactivation.⁴⁶ In general, pyridones are used to remove metal ions and restore metal overload disorders; pyrone-based complexes act as metal source, due to their weaker bidentate binding.

The most common 4-pyrones are shown in Figure 12 and are generally characterized by their synthetic versatility. Derivatization at positions 2, 5 and 6 of the ring system and conversion to 4-pyridones can be easily accomplished. 4-Pyrones form thermodynamically stable complexes at physiological pH values⁴⁷.

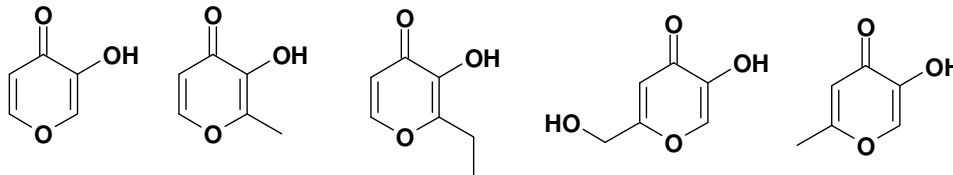


Figure 12: Most common and best studied 4-pyrone derivatives; from left to right: Pyromeconic acid, maltol, ethylmaltol, kojic acid, allomaltol

3-Hydroxy-2-methyl-4-pyrone (maltol) is one of the best studied compounds of this class and is known for its biocompatibility and favorable toxicity profile. It is used as food additive to impart the malty taste and aroma into bread, beer, cakes, *etc.* Next to its application in food

⁴³ G. J. Kontoghiorghes, L. Sheppard, *Inorg. Chim. Acta* **1987**, 136, L11.

⁴⁴ D. Cappellini, P. Patteroneri, *Annu. Rev. Med.* **2009**, 60, 25-38

⁴⁵ S. Singh, O. Epemolu, P. S. Dobbin, G. S. Tilbrook, B. L. Ellis, L. A. Damani, R. C. Hider, *Drug Metab. Dispos.* **1992**, 20, 256.

⁴⁶ Z. D. Liu, H. H. Khodr, D. Y. Liu, S. L. Liu, R. C. Hider, *J. Med. Chem.* **1999**, 42, 4814.

⁴⁷ R. D. Hancock, A. E. Martell, *Chem. Rev.* **1989**, 89, 1875.

industry, the maltol derived metal complexes with a series of two- and trivalent ions (Ga(III), Zn(II), Al(III), V(IV), etc.) have been investigated over the last decades.

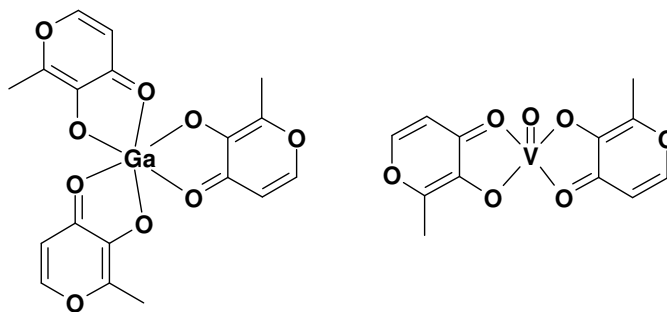


Figure 13: Maltol derived complexes under clinical investigations; from left to right: [Ga(Mal)₃], [VO(Mal)₂].

Gallium citrate is used since the 1960's as a soft tumor imaging agent⁴⁸, but in the last decades, the focus shifted towards its coordination compounds, since antineoplastic abilities of GaCl₃ and Ga(NO₃)₃ were observed. In contrast to the early investigated gallium salts, [Ga(Mal)₃] (Figure 13) can be administered orally, has a higher bioavailability⁴⁹, due to stabilization towards hydrolysis, which is the major hindrance for absorption, and less side effects.

Another example to increase the metal uptake by coordination is the bis(maltolato)oxovanadium(IV) complex (Figure 13), which is the first vanadium-based insulin enhancing compound, due to the ability of vanadium ions to mimic insulin *in vivo*⁵⁰ and *in vitro*⁵¹. The anti-diabetic potential of this complex is significantly higher than of the sodium vanadate salt and is currently tested in clinical trials⁵² (together with the ethylmaltol analogue).

Although pyrone complexes have been investigated intensively over the last decades, only the organometallic compound [Ru(arene)(Mal)Cl] has been tested for its anticancer activity and there is still a need for further investigations on the potential of this class of compounds.

⁴⁸ R. E. Coleman, *Cancer* **1991**, 67, 1261.

⁴⁹ L. R. Bernstein, T. Tanner, C. Godfrey, B. Noll, *Meta -Based Drugs* **2000**, 7, 33.

⁵⁰ Y. Shechter, *Diabetes* **1990**, 39, 1.

⁵¹ K. H. Thompson, J. H. McNeill, C. Orvig, *Chem. Rev.* **1999**, 99, 2561.

⁵² C. E. Heyliger, A. G. Tahiliani, J. H. McNeill, *Science* **1985**, 227, 1474.

The conversion of 3-hydroxy-4-pyr(id)ones to the corresponding thio compound has been described in literature and the most common are (i) addition of 1 eq Lawesson's reagent⁵³ and the (ii) reaction with an excess of P₄S₁₀⁵⁴ under various conditions⁵⁵. It has been shown, that the reaction of two equivalents of Lawesson's reagent with 4-pyrone leads to highly interesting dithiopyrones⁵⁶.

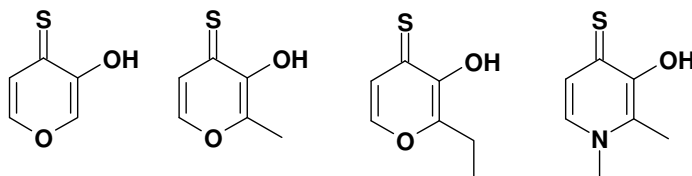


Figure 14: 3-Hydroxy-4-thiopyr(id)ones; from left to right: Thiopyromeconic acid, thiomaltol, thioethylmaltol, 3-hydroxy-1,2-dimethylpyridin-4(1H)-thione

3-Hydroxy-4-thiopyr(id)ones (Figure 14) are a new class of soft chelating agents and their metal complexes are under intensive investigations. Coordination compounds with Ga³⁺ and Ho³⁺ may be used as contrast agents for MRI imaging⁵⁴. The corresponding Zn²⁺ and VO²⁺ complexes showed encouraging in vitro results as anti-diabetic agents⁵⁷.

⁵³ S. Chaves, M. Gil, S. Canario, R. Jelic, M. J. Romao, J. Trincão, E. Herdtweck, J. Sousa, C. Diniz, P. Fresco, M. A. Santos, *Dalton Trans.* **2008**, 1773.

⁵⁴ V. Monga, B. O. Patrick, C. Orvig, *J. Inorg. Chem.* **2005**, *44*, 2666.

⁵⁵ J. A. Lewis, D. T. Puerta, S. M. Cohen, *Inorg. Chem.* **2003**, *74*, 7455.

⁵⁶ D. Brayton, F. E. Jacobsen, S. M. Cohen, P. J. Farmer, *Chem. Comm.* **2006**, 206.

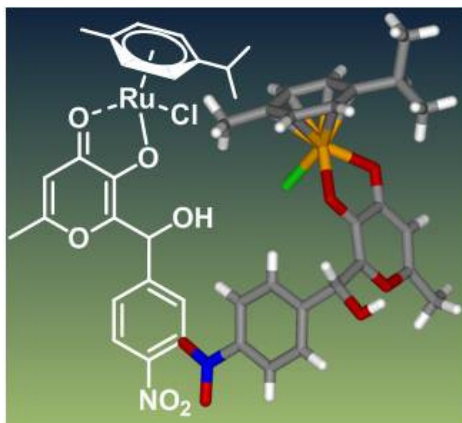
⁵⁷ A. Katoh, T. Tsukahara, R. Saito, K. K. Ghosh, Y. Yoshikawa, Y. Kojima, A. Tamura, H. Sakurai, *Chem. Lett.* **2002**, 114.

3. Published results

3.1. Tuning the anticancer activity of maltol derived ruthenium complexes by derivatization of the 3-hydroxy-4-pyrone moiety

Journal of Organometallic Chemistry, 2009, 694, 922-929

Graphical Abstract



Organometallic ruthenium(II) complexes based on maltol-derived ligands were synthesized and their hydrolysis behavior, reaction to the DNA model 5'-GMP, and anticancer activity against human tumor cell lines was tested. Promising anticancer activity was observed, with the lipophilicity of the compounds appearing to be the determining parameter of anticancer activity.



Tuning the anticancer activity of maltol-derived ruthenium complexes by derivatization of the 3-hydroxy-4-pyrone moiety

Wolfgang Kandioller^a, Christian G. Hartinger^{a,b,*}, Alexey A. Nazarov^{a,b,*}, Johanna Kasser^a, Roland John^a, Michael A. Jakupec^a, Vladimir B. Arion^a, Paul J. Dyson^b, Bernhard K. Keppler^a

^a University of Vienna, Institute of Inorganic Chemistry, Waehringer Str. 42, A-1090 Vienna, Austria

^b Institut des Sciences et Ingénierie Chimiques, Ecole Polytechnique Fédérale de Lausanne (EPFL), CH-1015 Lausanne, Switzerland

ARTICLE INFO

Article history:

Received 12 September 2008

Received in revised form 9 October 2008

Accepted 10 October 2008

Available online 17 October 2008

Dedicated to Prof. Gérard Jaouen on the occasion of his 65th birthday.

Keywords:

Antitumor agents

Bioorganometallic chemistry

Ruthenium(II)-arene complex

Pyrone

Hydrolysis

5'-GMP binding

ABSTRACT

Organometallic ruthenium(II)-arene complexes coordinated to maltol-derived ligands were prepared and their anticancer activity against human tumor cell lines was studied. In addition, their hydrolysis behavior and reaction with 5'-GMP was tested and compared to the parent compound chlorido[2-methyl-3-(oxo-κO)-pyran-4(1H)-onato-κO4](η⁶-p-cymene)ruthenium(II) (Ru-maltol). Improved stability and *in vitro* anticancer activity at maintained GMP binding capability were observed, in comparison to the Ru-maltol complex.

© 2008 Elsevier B.V. All rights reserved.

1. Introduction

Platinum complexes play an important role in the treatment of cancer and are included into *ca.* 50% of the therapeutic schemes [1]. Due to severe side effects, high toxicity, limited activity in common tumor types and tumor resistance, non-platinum complexes are undergoing intensive research as chemotherapeutics and also as radiodiagnostics [2–7]. Ruthenium compounds are the most widely developed alternatives, and (H₂Ind) *trans*-[RuCl₄(HInd)₂] (KP1019, HInd = indazole; Fig. 1) and (H₂Im) *trans*-[RuCl₄(DMSO)(HIm)] (NAMI-A, HIm = imidazole) have entered clinical trials [4,8,9]. Both compounds exhibit only low side effects, which might be due to selective uptake *via* the transferrin cycle [10–15] and/or activation by reduction [16] in the reductive environment typical of neoplastic tissue.

More recently stable organometallic compounds moved into the focus of interest [5]. Beside, for example, titanium, iron and

gold compounds [17–19], some of which underwent clinical trials, Ru(II) species, such as RAPTA type complexes, have been observed to exhibit anticancer activity, tunable by careful selection of the ligand sphere [3,20–32]. These studies resulted in compounds with interesting modes of action, for example potentially targeting kinases [25,29,30], or drug resistance pathways [27,33] and light activated systems [34,35], and a number of encouraging *in vivo* studies have been reported [3,5,21,22,36,37]. More recently, dinuclear pyridinone-based Ru(II) complexes, such as PyrRu₂¹² (Fig. 1), were observed to exhibit increased cytotoxicity due to jointly acting Ru(II)-arene moieties [31,32,38]. By varying the spacer length between the two ruthenium centers, compounds with mild to high cytotoxicity were obtained. Recent studies on their DNA binding properties revealed different modes of action for compounds only varying in the length of the spacer between the Ru(II)-arene fragments [31,32,38]. Other maltol-derived compounds have proven medicinal potential in the treatment of β-thalassemia and diabetes, and as radiodiagnostics [39] and, when coordinated to a Ga(III) center, in chemotherapy [2], or in form of a VO(maltolato) complex as a medication against diabetes type II [40,41].

The coordination ability of maltol-derived ligands with particular affinities for divalent and trivalent metal ions allows very stable complexes to be prepared [31,32,42–45], which can easily be

* Corresponding authors. Address: University of Vienna, Institute of Inorganic Chemistry, Waehringer Str. 42, A-1090 Vienna, Austria. Tel.: +43 1 4277 52609; fax: +43 1 4277 52680 (C.G. Hartinger).

E-mail addresses: christian.hartinger@univie.ac.at (C.G. Hartinger), alex.nazarov@univie.ac.at (A.A. Nazarov).

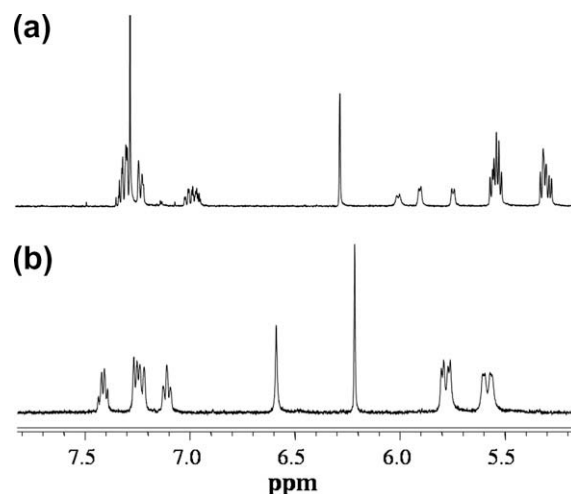
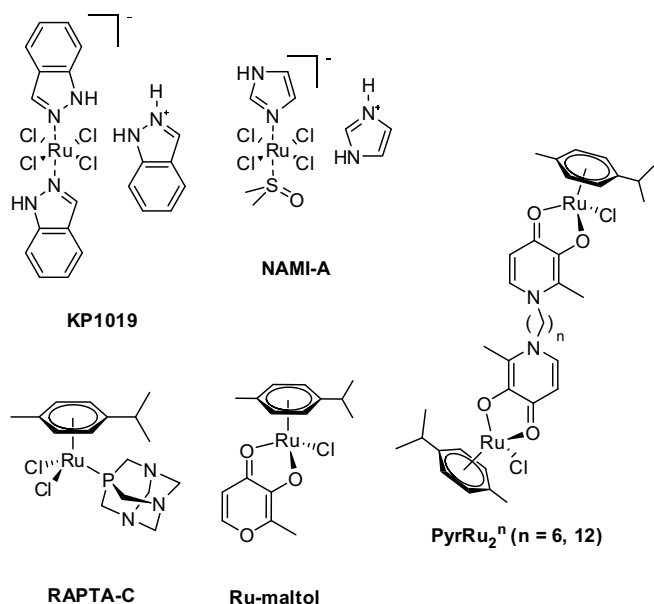


Fig. 2. ¹H NMR of 3d in (a) CDCl₃ and (b) D₂O.

Fig. 1. Structural formulae of the ruthenium anticancer drug candidates KP1019, NAMI-A, RAPTA-C, Ru-maltol and PyrRu₂ⁿ.

varied for modulation of important parameters such as solubility, hydrophobicity, etc.

In the present work, the synthesis of mononuclear Ru(II)-arene complexes with novel maltol-derived ligands is reported. The substitution pattern of the aryl part of the ligand was found to be crucial for controlling both the *in vitro* anticancer activity and complex solubility.

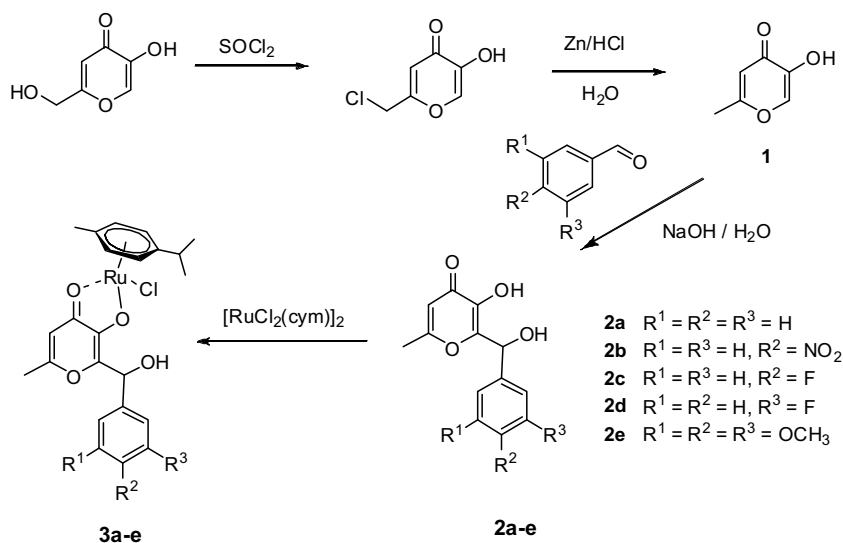
2. Results and discussion

2.1. Synthesis and characterization of the Ru(II)-*p*-cymene complexes

The synthesis of the precursor allomaltol **1** was performed in two steps, starting from kojic acid by reaction with thionylchloride followed by the reduction with zinc under acidic conditions (Scheme 1) [46]. Due to the higher reactivity of position 2 compared to 5 in the pyrone ring of **1**, functionalization can easily be

achieved in a similar fashion to the aldol reaction. Compound **1** was deprotonated with NaOH, and the anionic species obtained was reacted immediately with the corresponding aldehyde, yielding ligands **2a–e** after addition of HCl and recrystallization (yield 64–90%). The reaction occurs only in sufficient yield at pH 10.5. The air and light stable complexes (>1 year) **3a–e** were obtained by deprotonation of the corresponding ligand with sodium methoxide and addition of the bis(dichlorido(η⁶-*p*-cymene)ruthenium(II)). A slight excess of ligand (10%) was added in order to facilitate purification, and all complexes were obtained in good yield (52–73%).

The compounds were characterized by IR and 1D and 2D NMR spectroscopy, mass spectrometry and elemental analysis. All complexes possess two stereogenic centers and were isolated as mixtures of two diastereomers (*R/R*, *S/S* and *R/S*, *S/R*), as observed by NMR spectroscopy in aprotic solvents, where both forms are distinguishable. The separation of the diastereomers by fractional crystallization or chromatography was not successful. As a representative example, the ¹H NMR of **3d** in CDCl₃ and in D₂O is shown in Fig. 2. In CDCl₃ two sets of signals are observed for the hydrogens of the coordinated arene ring and for the *m*-fluoro substituted phenyl group. In D₂O, the spectrum comprises a single



Scheme 1. Synthesis of pyrone-based ligands and their ruthenium(II)-arene complexes.

set of signals, presumably due to fast inversion of the metal center, leading to epimerization of the diastereomers [47,48]. The ^1H NMR signal of the OH proton was observed to be split in aprotic solvents into two doublets with $\Delta\delta = 0.2$ ppm, which may be due to the formation of a hydrogen bond between the aliphatic –OH group of the ligand and the coordinated alcoholate of the pyrone ring (Fig. 2).

The IR spectra of the ligands **2a–e** show C=O, C=C and C–O stretching bands at 1654–1120 cm^{-1} [49]. The O–H stretching bands were observed as broad bands in the range 3420–3280 cm^{-1} . The spectra of **3a–d** contained four bands in the region of 1610–1460 cm^{-1} , which are typical for maltolato complexes [50,51]. Upon complexation the C=O stretching bands appear shifted by 40 cm^{-1} to lower wavenumbers. In the case of **3e** strong overlapping of the latter signals with those assignable to the methoxy groups was observed. In the spectra of the complexes the bands attributed to the OH stretching are in the range 3400–3340 cm^{-1} and are of significantly lower intensity due to deprotonation and coordination of one of the OH groups to the Ru centers.

ESI mass spectra of **3a–e** were recorded in methanol in the positive ion mode. For all compounds the most abundant peaks were assigned to $[\text{M}–\text{Cl}]^+$ ions, which had the appropriate ruthenium isotopic pattern.

2.2. Crystal structure determination

The molecular structure of **3b** was determined by X-ray diffraction analysis (Fig. 3), and the metal center was found to adopt the expected pseudo-octahedral “piano-stool” geometry. In the phenyl substituted maltolato complex **3b** and PyrRu_2^6 a short and a long Ru–O bond have been observed (Table 1), whereas in chlorido-[3-(oxo- κO)-2-methyl-4-pyridinonato- κO4](η^6 -*p*-cymene)ruthenium(II) (Ru-maltol, Fig. 1) the two Ru–O bond lengths are almost identical. This observation might be explained by a lengthening of the Ru–O2 bond in the Ru-maltol complex due to the involvement of this oxygen donor atom in a strong intermolecular H-bond (donor–acceptor distance of 2.805(2) Å, and a donor–hydrogen–acceptor angle of 174°). The Ru–Cl bond length in **3b** of 2.4310(4) Å is similar to that in Ru-maltol, whereas the bond observed for the pyridinone complex PyrRu_2^6 is slightly shorter [31]. Although the Ru–Cl bond lengths in the above mentioned structures are very different, the rate of hydrolysis is rapid in all cases (see below).

2.3. Hydrolysis, pK_a and GMP binding

Due to the low solubility of **3a–e** in water (Table 2), all NMR experiments on the hydrolytic stability were performed in a 5%

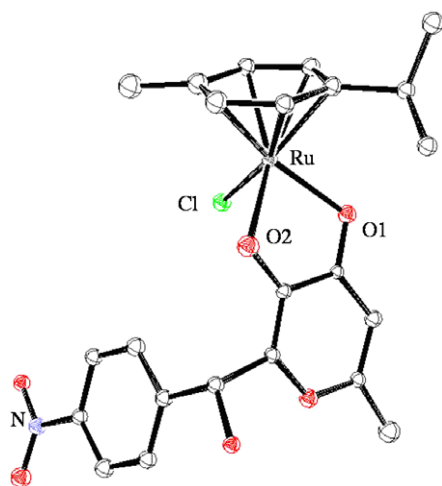


Fig. 3. ORTEP plot of the molecular structure of **3b** at 50% probability level.

Table 1

Selected bond lengths (Å) and angles (°) of **3b** and comparisons with the dinuclear complex PyrRu_2^6 and the structurally related Ru-maltol complex chlorido[3-(oxo- κO)-2-methyl-4-pyridonato- κO4](η^6 -*p*-cymene)ruthenium(II).

	3b	PyrRu_2^6 ^a	Ru-maltol ^b
Ru–Cl	2.4310(4)	2.4186(10)	2.4329(5)
Ru–O1	2.1179(10)	2.101(3)	2.1035(13)
Ru–O2	2.0766(10)	2.074(3)	2.0901(13)
O1–Ru–O2	78.82(4)	79.63(11)	78.79(5)
O1–Ru–Cl	83.35(3)	83.90(8)	83.42(4)
Cl–Ru–O2	85.51(3)	85.11(8)	85.89(4)

^a From Ref. [31].

^b From Ref. [28].

Table 2

Solubility in PBS and IC_{50} values of **3a–e** and of Ru-maltol in the human cancer cell lines CH1, SW480 and A549.

Compound	Solubility (mg/mL)	IC_{50} (μM)		
		CH1	SW480	A549
3a	0.25	50 ± 9	67 ± 10	172 ± 5
3b	Insoluble	–	–	–
3c	0.1	24 ± 4	44 ± 10	98 ± 4
3d	0.1	29 ± 2	57 ± 8	138 ± 6
3e	1	48 ± 6	84 ± 7	220 ± 14
Ru-maltol	>10	>100	>100	–

DMSO- d_6 /D $_2$ O solution. Coordination of DMSO to the ruthenium center was not observed (data not shown). NMR spectra of the complexes with and without addition of AgNO_3 (used to remove the chlorido ligand) are identical, indicating that the hydrolysis proceeds immediately upon dissolving in water. The aqua complexes are stable in aqueous solution, whereas the Ru-maltol complex reacts to form a dimeric ruthenium compound [28], indicating that the hydroxyl-methyl-aryl substituent in position 2 of the pyrone ring inhibits the formation of dimeric species.

The pK_a values of the aqua complexes of **3a–e** were estimated by titration with NaOD to afford the corresponding hydroxido compounds by monitoring the deprotonation process by ^1H NMR spectroscopy (Table 3). To generate the aqua species, the complexes were dissolved in D $_2$ O containing 5% DMSO- d_6 . The chemical shifts of the $\text{Ar}_{\text{cym}}\text{-H2/H6}$ proton signal of the arene ring (e.g., from 5.75 ppm at pH 3.21 to 5.49 at pH 11.00 for **3c**) were plotted against the pD value. The pK_a values (in D $_2$ O) were determined from the inflection point of the sigmoid curve (see Fig. 4 for the titration curve of **3c**) and corrected for the difference between D $_2$ O and water to yield the pK_a (using Eq. (1), see Section 4). The pK_a values of **3a–e** were determined to be between 8.99 and 9.80, with the substitution of the aryl moiety of the ligand having only a minor influence. The pK_a values are similar to those of the parent compound Ru-maltol (pK_a 9.23) [28] and the dinuclear pyridinone-type ruthenium arene complexes (pK_a 9.60–9.83) [31].

The reaction of **3a–e** with the DNA model compound 5'-GMP was investigated by ^1H and ^{31}P NMR spectroscopy to evaluate the potential of DNA as an intracellular target, as reported for other Ru complexes and also the clinically established Pt compounds

Table 3

pK_a values of complexes **3a–e**.

Compound	pK_a
3a	9.05 ± 0.02
3b	9.80 ± 0.03
3c	8.99 ± 0.01
3d	9.56 ± 0.01
3e	9.64 ± 0.02

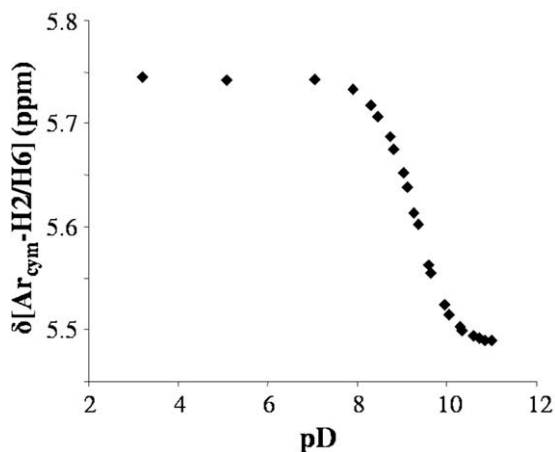


Fig. 4. Titration curve of **3c** used to determine the pK_a .

[1,16,52,53]. Stepwise addition of 5'-GMP to the aqua complexes (in aqueous solutions) resulted in the formation of 5'-GMP adducts within seconds. After addition of an equimolar amount of the reagent, three new signals for the H8 of 5'-GMP were observed in the ^1H NMR spectra between 7.7 and 7.9 ppm in a ratio of 1:1:2 (Fig. 5). The signals may be assigned to the four stereoisomers formed by the coordination of 5'-GMP to the ruthenium center. The change of the H8 signal in the ^1H NMR spectrum from 8.15 ppm to approximately 7.80 ppm indicates coordination *via* the N7 atom of the guanine [53]. The ^{31}P NMR spectrum contains 3 peaks between 3.7 and 3.1 ppm in 1:1:2 ratio in agreement with the ^1H NMR spectra.

2.4. *In vitro* evaluation

The *in vitro* anticancer activity of **3a** and **3c–e** was determined in SW480 (colon carcinoma), CH1 (ovarian carcinoma) and A549 (non-small cell lung carcinoma) human cancer cells using the colorimetric MTT assay, yielding IC_{50} values mostly in the 10^{-5} M range (Table 2). Due to the low solubility of **3b** it was not possible to determine its anticancer activity.

CH1 cells were found to be the most sensitive to all four ruthenium complexes, and in all cell lines **3c** was the most active compound with an IC_{50} value of 24 μM in the ovarian cancer cell line (Fig. 6). In general, it appears as the solubility in medium/DMSO

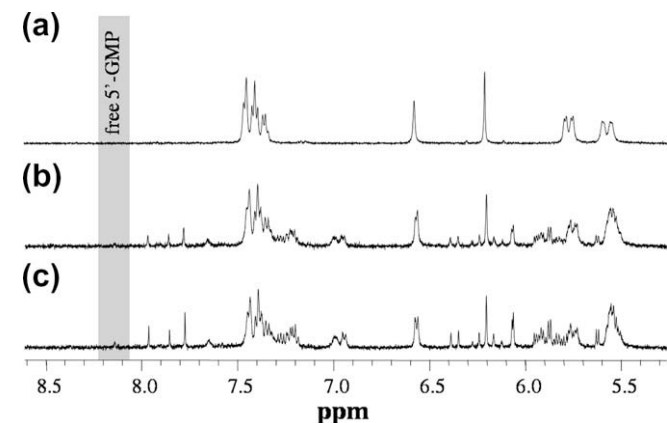


Fig. 5. 5'-GMP binding of **3d** studied by ^1H NMR spectroscopy after addition of (a) 0 eq, (b) 1 eq, and (c) an excess of 5'-GMP to a D_2O solution of the Ru complex.

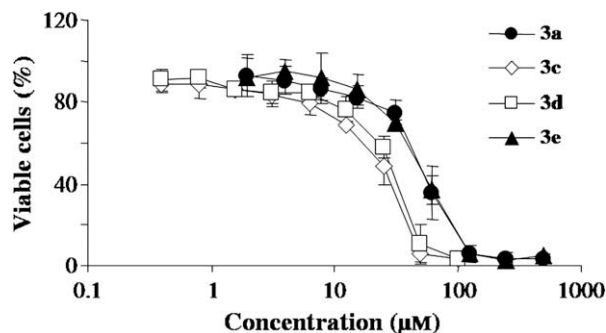


Fig. 6. Concentration–effect curves of **3a** and **3c–e** in CH1 ovarian carcinoma cells.

as a measure of lipophilicity determines the *in vitro* anticancer activity of the compounds (Table 2). Furthermore, the substituent on the aryl moiety of the ligand appears to influence the activity of the ruthenium complex in all tested cell lines: **3c** and **3d** with their electron withdrawing substituents exhibit a higher cytotoxic activity in CH1 cells than **3a**. In contrast, electron-donating substituents such as the methoxy groups in **3e** do not significantly influence the activity in CH1 cells and are even disadvantageous in SW480 and A549 cells. In comparison to the parent compound Ru-maltol, the compounds bearing substituents at the 2-position are more cytotoxic, which may also be due to the increased lipophilicity of the compounds (Table 2). However, in order to establish definitive structure–activity relationships a higher number of compounds need to be studied.

3. Conclusions

Ruthenium complexes have been established as potential drug candidates for treatment of cancer. Herein, ruthenium(II)-*p*-cymene complexes with 2-substituted 3-hydroxypyran-4(1*H*)-one ligands have been evaluated for potential anticancer activity. The complexes hydrolyze rapidly in aqueous solutions, in a process involving substitution of the chlorido ligand by an aqua ligand. Substitution of the 2-position of the pyrone moiety results in increased stability of the aqua complexes in aqueous solution in comparison to Ru-maltol which affords dimeric species. The reaction of the Ru moiety toward 5'-GMP is very fast, and binding occurs selectively at the N7 of the guanine. Complexes **3a** and **3c–e** exhibit moderate cytotoxicity against SW480 and CH1 human tumor cell lines, and poor activity against A549 cells, suggesting a certain degree of selectivity. The aryl moiety seems to be relevant for determining the *in vitro* activity of the compounds with electron withdrawing substituents at the phenyl moiety decreasing the IC_{50} value and electron donating groups having the opposite effect. There appears to be a correlation between the electronic effect of the substituents on the maltol-derived ligands, and the *in vitro* activity, but a larger library of compounds should be studied to confirm this hypothesis.

4. Experimental

4.1. Materials and methods

All solvents were dried and distilled prior to use. Ruthenium(III) chloride (Johnson Matthey), kojic acid (Fluka), benzaldehyde (Fluka), *p*-nitrobenzaldehyde (Aldrich), *p*-fluorobenzaldehyde (Fluka), *m*-fluorobenzaldehyde (Fluka), 3,4,5-trimethoxybenzaldehyde (Aldrich) and sodium methoxide (Aldrich) were purchased and used without further purification. Bis[dichlorido(η^6 -*p*-cymene)ruthenium(II)], 2-chloromethyl-5-hydroxypyran-4(1*H*)-one (chlorokojic acid), and 5-hydroxy-2-methyl-pyran-4(1*H*)-one

(allomaltol, **1**) were synthesized as described elsewhere [46,54]. Melting points were determined with a Büchi B-540 apparatus and are uncorrected. Elemental analyses were carried out with a Perkin Elmer 2400 CHN Elemental Analyzer at the Microanalytical Laboratory of the University of Vienna. NMR spectra were recorded at 25 °C on a Bruker FT-NMR spectrometer Avance III™ 500 MHz at 500.10 MHz (¹H), 125.75 MHz (¹³C) and 202.44 MHz (³¹P) in DMSO-*d*₆, D₂O or CDCl₃. The 2D NMR spectra were measured in a gradient-enhanced mode. An esquire₃₀₀₀ ion trap mass spectrometer (Bruker Daltonics, Bremen, Germany), equipped with an orthogonal ESI ion source, was used for MS measurements. The solutions were introduced *via* flow injection using a Cole-Parmer 74900 single-syringe infusion pump (Vernon Hills, IL). The ESI-MS instrument was controlled by means of the ESQUIRECONTROL software (version 5.2), and all data were processed using DATAANALYSIS software (version 3.2) (both Bruker Daltonics). IR spectra were measured in KBr matrix (4000–400 cm⁻¹) with a Bruker Vertex 70 FT-IR spectrometer.

Single crystals of **3b** were grown from MeOH, and X-ray diffraction measurement was performed on a Bruker X8 APEXII CCD diffractometer at 100 K. The single crystal was positioned at 40 mm from the detector, and 2965 frames were measured, each for 3 s over 1° scan width. The data were processed using the SAINT software package [55]. Crystal data, data collection parameters, and structure refinement details are given in Table 4. The structure was solved by direct methods and refined by full-matrix least-squares techniques. Non-hydrogen atoms were refined with anisotropic displacement parameters. H atoms were inserted at calculated positions and refined with a riding model. The following computer programs were used: structure solution, SHELXS-97 [56]; refinement, SHELXL-97 [57]; molecular diagrams, ORTEP-3 [58]; computer, Pentium IV; scattering factors [59].

Table 4
Crystal data and details of data collection for **3b**.

Chemical formula	C ₂₃ H ₂₄ ClNO ₆ Ru
<i>M</i> (g mol ⁻¹)	546.95
Temperature (K)	100(2)
Crystal size (mm)	0.30 × 0.30 × 0.20
Crystal color, shape	Orange, block
Crystal system	Triclinic
Space group	P $\bar{1}$ (No 2)
<i>a</i> (Å)	7.4276(4)
<i>b</i> (Å)	12.5755(5)
<i>c</i> (Å)	12.6091(6)
α (°)	72.009(2)
β (°)	87.811(3)
γ (°)	74.210(2)
<i>V</i> (Å ³)	1076.55(9)
<i>Z</i>	2
<i>D</i> _c (g cm ⁻³)	1.687
μ (cm ⁻¹)	8.94
<i>F</i> (000)	556
θ Range for data collection (°)	2.04–30.07
<i>h</i> range	–10/10
<i>k</i> range	–17/17
<i>l</i> range	–17/17
Number of reflections used in refinement	6280
Number of parameters	295
<i>R</i> _{int}	0.0354
<i>R</i> ₁ ^a	0.0212
<i>wR</i> ₂ ^b	0.0532
GOF ^c	1.007
Residuals (e ⁻ Å ⁻³)	0.592, –0.490

$$^a R_1 = \sum ||F_o| - |F_c|| / \sum |F_o|.$$

$$^b wR_2 = \{ \sum [w(F_o^2 - F_c^2)^2] / \sum w(F_o^2)^2 \}^{1/2}.$$

^c GOF = $\{ \sum [w(F_o^2 - F_c^2)^2] / (n - p) \}^{1/2}$, where *n* is the number of reflections and *p* is the total number of parameters refined.

4.2. Synthesis

4.2.1. General procedure for the reaction of allomaltol with the aldehydes

Allomaltol **1** (1 eq) and NaOH (1.1 eq) were dissolved in water and stirred for 5 min. Afterwards, the aldehyde (1.1 eq) was added dropwise to the reaction mixture. The solution was adjusted to pH 10.5 with 5 M NaOH solution and stirred at r.t. for 12 h. The reaction mixture was acidified to pH 1 with conc. HCl and the resulting precipitate was collected by filtration. If no precipitation occurred, the reaction mixture was extracted with CH₂Cl₂ (3 × 20 mL). The combined organic layers were washed twice with saturated NaHCO₃ (30 mL) and water (30 mL), dried over Na₂SO₄, filtered and concentrated *in vacuo*. The crude product was purified by recrystallization.

4.2.1.1. 2-[(4-Hydroxy-phenyl-methyl)-3-hydroxy-6-methyl-pyran-4(1H)-one (2a). The reaction was performed according to the general procedure using **1** (2.0 g, 15.8 mmol) and benzaldehyde (1.8 mL, 17.5 mmol). The crude product was recrystallized from 2-propanol affording a white powder (3.3 g, 90%). M.p. 170–172 °C (decomp.); ¹H NMR (DMSO-*d*₆) δ : 2.18 (s, 3H, CH₃), 5.99 (d, *J* = 4.5 Hz, 1H, CHOHPH), 6.14 (d, *J* = 5.0 Hz, 1H, CHOHPH), 6.19 (s, 1H, CH), 7.27 (t, *J* = 7.5 Hz, 1H, Ph-H4'), 7.35 (t, *J* = 7.5 Hz, 2H, Ph-H3'/H5'), 7.40 (d, *J* = 7.5 Hz, 2H, Ph-H2'/H6'); ¹³C NMR (DMSO-*d*₆) δ : 19.7 (CH₃), 66.3 (CHPhOH), 111.6 (CH₃C=CH), 126.4 (Ph-C2'), 127.8 (Ph-C4'), 128.7 (Ph-C3') 141.0 (CH₃C=CH), 141.8 (Ph-C1'), 151.0 (HOHC=COH), 165.0 (CHOH), 174.3 (C=O); IR (KBr, cm⁻¹, selected bands): 3323, 1654, 1607, 1562, 1256, 1209; Elemental Anal. Calc. for C₁₃H₁₂O₄ · 0.2H₂O: C, 66.20; H, 5.30. Found: C, 66.24; H, 5.33%.

4.2.1.2. 2-[(4-Nitrophenyl)-hydroxy-methyl]-3-hydroxy-6-methyl-pyran-4(1H)-one (2b). The reaction was performed according to the general procedure using **1** (1.00 g, 7.9 mmol) and 4-nitrobenzaldehyde (1.32 g, 8.7 mmol, in 2 mL dioxane). The crude product was purified by recrystallization from 2-propanol affording yellow crystals (1.41 g, 64%). M.p. >200 °C decomp.; ¹H NMR (DMSO-*d*₆) δ : 2.17 (s, 3H, CH₃), 6.13 (s, 1H, CHOHA_r), 6.21 (s, 1H, CH), 6.50 (brs, 1H, CHOHA_r), 7.66 (d, *J* = 8.8 Hz, 2H, Ar-H2'/H6'), 8.23 (d, *J* = 8.6 Hz, 2H, Ar-H3'/H5'), 9.34 (s, 1H, COH); ¹³C NMR (DMSO-*d*₆) δ : 20.1 (CH₃), 66.2 (CHOHA_r), 112.1 (CH₃C=CH), 124.4 (Ar-C2'/C6'), 128.0 (Ar-C3'/C5'), 141.9 (CH₃C=CH), 147.7 (Ar-C1'), 149.8 (Ar-C4'), 150.2 (HOHC=COH), 165.6 (CHOH), 174.7 (C=O); IR (KBr, cm⁻¹, selected bands): 3281, 1650, 1606, 1563, 1347, 1220; Elemental Anal. Calc. for C₁₃H₁₁NO₆ · 0.1H₂O: C, 55.95; H, 4.04; N, 5.01. Found: C, 55.90; H, 3.98; N, 4.98%.

4.2.1.3. 2-[(4-Fluorophenyl)-hydroxy-methyl]-3-hydroxy-6-methyl-pyran-4(1H)-one (2c). The reaction was performed according to the general procedure using **1** (1.00 g, 8.0 mmol) and 4-fluorobenzaldehyde (1.08 g, 8.8 mmol, in 1 mL dioxane), affording colorless crystals (1.80 g, 91%). M.p. 158–160 °C; MS (ESI⁻) *m/z* 249 [M–H]⁻; ¹H NMR (DMSO-*d*₆) δ : 2.19 (s, 3H, CH₃), 5.99 (s, 1H, CHOHA_r), 6.20 (s, 1H, CH), 6.19 (brs, 1H, CHOHA_r), 7.18 (t, *J* = 9.0 Hz, 2H, Ar-H3'/H5'), 7.43 (dd, *J* = 9.0 Hz, *J* = 3.0 Hz, Ar-H2'/H6'), 9.10 (brs, 1H, COH); ¹³C NMR (DMSO-*d*₆) δ : 19.7 (CH₃), 66.7 (CHOHA_r), 111.6 (CH₃C=CH), 115.5 (*J* = 21.5 Hz, Ar-C3'), 128.4 (*J* = 8.1 Hz, Ar-C2'), 138.0 (*J* = 3.0 Hz, Ar-C1'), 141.0 (CH₃C=CH), 150.7 (HOHC=COH), 161.9 (*J* = 242.0 Hz, Ar-C4'), 165.1 (CHOH), 174.3 (C=O); IR (KBr, cm⁻¹, selected bands): 3293, 1652, 1607, 1564, 1508, 1219; Elemental Anal. Calc. for C₁₃H₁₁FO₄ · ¼H₂O: C, 61.30; H, 4.55. Found: C, 61.56; H, 4.39%.

4.2.1.4. 2-[(3-Fluorophenyl)-hydroxy-methyl]-3-hydroxy-6-methyl-pyran-4(1H)-one (2d). The reaction was performed according to

the general procedure using **1** (0.50 g, 4.0 mmol) and 3-fluorobenzaldehyde (0.54 g, 4.4 mmol, in 1 mL dioxane) affording colorless crystals (0.85 g, 85%). M.p. 170–172 °C; $^1\text{H NMR}$ (DMSO- d_6) δ : 2.27 (s, 3H, CH₃), 6.01 (s, 1H, CHOAr), 6.20 (s, 1H, CH), 6.40 (brs, CHOAr) 7.10 (m, Ar-H4'), 7.18–7.21 (m, 2H, Ar-H2'/H6'), 7.38 (q, $J = 8.0$ Hz, Ar-H5'), 9.15 (brs, 1H, COH); $^{13}\text{C NMR}$ (DMSO- d_6) δ : 19.7 (CH₃), 66.8 (CHOAr), 111.7 (CH₃C=CH) 113.0 ($J = 22.1$ Hz, Ar-C2'), 114.6 ($J = 21.3$ Hz, Ar-C4'), 122.4 ($J = 3.0$ Hz, Ar-C6'), 130.7 ($J = 8.2$ Hz, Ar-C5') 141.2 (CH₃C=CH), 144.8 ($J = 8.3$ Hz, Ar-C1'), 150.4 (HOCHC=COH), 162.0 ($J = 242.1$ Hz, Ar-C3'), 165.1 (CHOH), 174.3 (C=O); IR (KBr, cm^{-1} , selected bands): 3293, 1655, 1609, 1561, 1252, 1208; Elemental Anal. Calc. for C₁₃H₁₁FO₄ · 1/4H₂O: C, 61.30; H, 4.55. Found: C, 61.30; H, 4.45%.

4.2.1.5. 2-[(3,4,5-Trimethoxyphenyl)-hydroxy-methyl]-3-hydroxy-6-methyl-pyran-4(1H)-one (2e). The reaction was performed according to the general procedure using **1** (0.40 g, 3.2 mmol) and 3,4,5-trimethoxybenzaldehyde (0.68 g, 3.5 mmol, in 5 mL dioxane) affording a pale yellow solid (0.78 g, 69%). M.p. 182–184 °C; $^1\text{H NMR}$ (DMSO- d_6) δ : 2.22 (s, 3H, CH₃), 3.64 (s, 3H, 4'-OCH₃), 3.76 (s, 6H, 3'/5'-OCH₃), 5.95 (d, $J = 5.2$ Hz, 1H, CHOAr), 6.15 (d, $J = 5.2$ Hz, 1H, CHOAr), 6.20 (s, 1H, CH), 6.71 (s, 2H, Ar-H3'/H5'), 9.05 (brs, 1H, COH); $^{13}\text{C NMR}$ (DMSO- d_6) δ : 19.7 (CH₃), 56.3 (3'/5'-OCH₃), 60.5 (4'-OCH₃), 66.4 (CHOAr), 103.7 (Ar-C2'/C6'), 111.6 (CH₃C=CH), 137.2 (Ar-C1'), 137.4 (Ar-C4'), 140.0 (CH₃C=CH), 150.8 (HOCHC=COH), 153.2 (Ar-C3'/C5'), 165.0 (CHOH), 174.3 (C=O); IR (KBr, cm^{-1} , selected bands): 3416, 3293, 1646, 1600, 1558, 1226, 1126; Elemental Anal. Calc. for C₁₆H₁₈O₇ · 1/4H₂O: C, 58.80; H, 5.71. Found: C, 58.84; H, 5.42%.

4.2.2. General procedure for the synthesis of the Ru(II) complexes

The maltol-derived ligand (0.73 mmol) and sodium methoxide (43 mg, 0.80 mmol) were dissolved in methanol (15 mL) and stirred for 5 min under inert atmosphere to give a clear solution. Afterwards, bis[dichlorido(η^6 -*p*-cymene)ruthenium(II)] (200 mg, 0.33 mmol) was dissolved in CH₂Cl₂ (5 mL) and added dropwise to the reaction mixture which was stirred for further 5 (for **3a**) or 18 h. The reaction mixture was concentrated *in vacuo*, and the residue was extracted with CH₂Cl₂ (3 × 15 mL). The combined organic layers were filtered, and the solvent was removed. The crude product was purified by recrystallization or precipitation.

4.2.2.1. Chlorido[2-(hydroxy-phenyl-methyl)-6-methyl-3-(oxo- κ O)-pyran-4(1H)-onato- κ O4](η^6 -*p*-cymene)ruthenium(II) (3a). The reaction was performed according to the general complexation protocol using **2a** (168 mg, 0.73 mmol). The crude product was recrystallized from EtOAc/*n*-hexane affording a red crystalline solid (240 mg, 73%). M.p. 160–165 °C decomp.; MS (ESI⁺) m/z 391 [M–Cl]⁺; $^1\text{H NMR}$ (CDCl₃) δ : 1.30–1.38 (m, 6H, CH₃), 2.19 (s, 3H, CH₃,_{pyr}), 2.33 (s, 3H, CH₃,_{cym}), 2.93 (m, 1H, CH(CH₃)₂,_{cym}), 5.28–5.33 (m, 2H, Ar_{cym}-H3/H5), 5.52–5.57 (m, 2H, Ar_{cym}-H2/H6), 5.81 (s, 1H, CHOHPH), 5.86 (s, 1H, CHOHPH), 6.27 (s, 1H, CH), 7.30–7.50 (m, 5H, Ph); $^{13}\text{C NMR}$ (CDCl₃) δ : 18.6 (CH₃), 19.8 (CH₃,_{cym}), 22.3 (CH₃,_{cym}), 31.2 (CH(CH₃)₂), 72.9 (CHOHPH), 78.2 (Ar_{cym}-C3/C5), 80.2 (Ar_{cym}-C2/C6), 95.8 (Ar_{cym}-C4), 99.5 (Ar_{cym}-C1), 109.4 (CH), 127.1 (Ph-C2), 128.0 (Ph), 128.5 (Ph), 141.5 (CH₃C=CH), 152.9 (Ph-C1), 155.1 (HOCHC=COH), 164.2 (CHOH), 185.0 (C=O); IR (KBr, cm^{-1} , selected bands): 3394, 1604, 1561, 1503, 1476, 1259, 1206; Elemental Anal. Calc. for C₂₃H₂₅ClO₄Ru: C, 55.03; H, 5.02. Found: C, 54.73; H, 5.02%.

4.2.2.2. Chlorido[2-[(4-nitrophenyl)-hydroxy-methyl]-6-methyl-3-(oxo- κ O)-pyran-4(1H)-onato- κ O4](η^6 -*p*-cymene)ruthenium(II) (3b). The reaction was performed according to the general complexation protocol using **2b** (197 mg, 0.73 mmol). The crude product was recrystallized from EtOAc/diethyl ether/*n*-hexane

affording an orange powder (250 mg, 70%). M.p. 180–185 °C decomp.; MS (ESI⁺) m/z 512 [M–Cl]⁺; $^1\text{H NMR}$ (CDCl₃) δ : 1.31–1.40 (m, 6H, CH₃,_{cym}), 2.19 (s, 3H, CH₃,_{pyr}), 2.34 (s, 3H, CH₃,_{cym}), 2.92 (m, 1H, CH(CH₃)₂), 5.29–5.35 (m, 2H, Ar_{cym}-H3/H5); 5.51–5.58 (m, 2H, Ar_{cym}-H2/H6), 5.93 (bs, 1H, CHOAr), 5.99 (bs, 1H, CHOAr), 6.30 (s, 1H, CH), 7.67–7.70 (m, 2H, Ar_{cym}-H2/H6), 8.20–8.25 (m, 2H, Ar_{cym}-H3'/H5'); $^{13}\text{C NMR}$ (CDCl₃) δ : 18.6 (CH₃,_{pyr}), 19.9 (CH₃,_{cym}), 22.5 (CH₃,_{cym}), 31.2 (CH(CH₃)₂), 71.7 (CHOAr), 78.0 (Ar_{cym}-C3/C5), 80.3 (Ar_{cym}-C2/C6), 95.7 (Ar_{cym}-C4), 99.4 (Ar_{cym}-C1), 109.5 (CH), 123.6 (Ar-C2/C6), 127.5 (Ar-C3/C5), 148.0 (Ar-C1), 148.6 (Ar-C4), 151.0 (CH₃C=CH), 155.5 (HOCHC=COH), 164.7 (CHOH), 185.2 (C=O); IR (KBr, cm^{-1} , selected bands): 3342, 1603, 1564, 1513, 1477, 1256, 1205; Elemental Anal. Calc. for C₂₃H₂₄ClNO₆Ru: C, 50.51; H, 4.42; N, 2.56. Found: C, 50.35; H, 4.39; N, 2.51%.

4.2.2.3. Chlorido[2-[(4-fluorophenyl)-hydroxy-methyl]-6-methyl-3-(oxo- κ O)-pyran-4(1H)-onato- κ O4](η^6 -*p*-cymene)ruthenium(II) (3c). The reaction was performed according to the general complexation protocol using **2c** (183 mg, 0.73 mmol). The crude product was recrystallized from EtOAc/diethyl ether/*n*-hexane, affording an orange powder (240 mg, 71%). M.p. 90–95 °C decomp.; MS (ESI⁺) m/z 485 [M–Cl]⁺; $^1\text{H NMR}$ (CDCl₃) δ : 1.30–1.38 (m, 6H, CH₃,_{cym}), 2.20 (s, 3H, CH₃,_{pyr}), 2.33 (s, 3H, CH₃,_{cym}), 2.92 (m, 1H, CH(CH₃)₂), 5.28–5.33 (m, 2H, Ar_{cym}-H3/H5), 5.53–5.57 (m, 2H, Ar_{cym}-H2/H6), 5.76 (bs, 1H, CHOAr), 5.89 (bs, 1H, CHOAr), 6.28 (s, 1H, CH), 6.99–7.07 (m, 2H, Ar-H3/H5), 7.46–7.48 (m, 2H, Ar-H2/H6); $^{13}\text{C NMR}$ (CDCl₃) δ : 18.6 (CH₃,_{pyr}), 19.8 (CH₃,_{cym}), 22.4 (CH₃,_{cym}), 31.2 (CH(CH₃)₂), 72.2 (CHOAr), 78.1 (Ar_{cym}-C3/C5), 80.2 (Ar_{cym}-C2/C6), 95.7 (Ar_{cym}-C4), 99.3 (Ar_{cym}-C1), 109.4 (CH), 115.3 ($J = 22.3$ Hz, Ar-C3/C5), 128.5 ($J = 8.0$ Hz, Ar-C2/C6), 137.3 ($J = 4.1$ Hz, Ar-C1), 152.2 (CH₃C=CH), 155.2 (HOCHC=COH), 162.5 ($J = 245.7$ Hz, Ar-C4), 164.0 (CHOH), 185.0 (C=O); IR (KBr, cm^{-1} , selected bands): 3387, 1603, 1563, 1507, 1477, 1219; Elemental Anal. Calc. for C₂₃H₂₄ClFO₄Ru: C, 53.13; H, 4.65. Found: C, 52.86; H, 4.62%.

4.2.2.4. Chlorido[2-[(3-fluorophenyl)-hydroxy-methyl]-6-methyl-3-(oxo- κ O)-pyran-4(1H)-onato- κ O4](η^6 -*p*-cymene)ruthenium(II) (3d). The reaction was performed according to the general complexation protocol using **2d** (183 mg, 0.73 mmol). The crude product was recrystallized from EtOAc/diethyl ether/*n*-hexane affording an orange powder (250 mg, 73%). M.p. 160–165 °C decomp.; MS (ESI⁺) m/z 485 [M–Cl]⁺; $^1\text{H NMR}$ (CDCl₃) δ : 1.30–1.38 (m, 6H, CH₃,_{cym}), 2.20 (s, 3H, CH₃,_{pyr}), 2.33 (s, 3H, CH₃,_{cym}), 2.92 (m, 1H, CH(CH₃)₂), 5.30 (m, 2H, Ar_{cym}-H3/H5), 5.54 (m, 2H, Ar_{cym}-H2/H6), 5.83 (brs, 1H, CHOAr), 6.01 (brs, 1H, CHOAr), 6.28 (s, 1H, CH), 6.99 (m, 1H, Ar-H4), 7.22–7.33 (m, 3H, Ar-H2/H5/H6); $^{13}\text{C NMR}$ (CDCl₃) δ : 18.6 (CH₃,_{pyr}), 19.8 (CH₃,_{cym}), 22.2 (CH₃,_{cym}), 31.2 (CH(CH₃)₂), 72.4 (CHOAr), 78.1 (Ar_{cym}-C3/C5), 80.2 (Ar_{cym}-C2/C6), 95.7 (Ar_{cym}-C4), 99.4 (Ar_{cym}-C1), 109.4 (CH), 113.9 ($J = 22.3$ Hz, Ar-C2), 114.7 ($J = 22.2$ Hz, Ar-C4), 122.3 ($J = 3.0$ Hz, Ar-C6), 129.9 ($J = 7.4$ Hz, Ar-C5), 144.0 ($J = 7.2$ Hz, Ar-C1), 152.1 (CH₃C=CH), 155.2 (HOCHC=COH), 162.8 ($J = 262.4$ Hz, Ar-C3), 164.2 (CHOH), 185.0 (C=O); IR (KBr, cm^{-1} , selected bands): 3396, 1604, 1562, 1504, 1476, 1250, 1203; Elemental Anal. Calc. for C₂₃H₂₄ClFO₄Ru: C, 53.13; H, 4.65. Found: C, 53.11; H, 4.65%.

4.2.2.5. Chlorido[2-[(3,4,5-trimethoxyphenyl)-hydroxy-methyl]-6-methyl-3-(oxo- κ O)-pyran-4(1H)-onato- κ O4](η^6 -*p*-cymene)ruthenium(II) (3e). The reaction was performed according to the general complexation protocol using **2e** (234 mg, 0.73 mmol). The crude product was recrystallized from EtOAc/*n*-hexane, affording an orange powder (200 mg, 54%). M.p. 160–165 °C decomp.; MS (ESI⁺) m/z 557 [M–Cl]⁺; $^1\text{H NMR}$ (CDCl₃) δ : 1.37–1.39 (m, 6H, CH₃,_{cym}), 2.22 (s, 3H, CH₃,_{pyr}), 2.32 (s, 3H, CH₃,_{cym}), 2.93 (m, 1H, CH(CH₃)₂),

3.82 (s, 3H, 4'-OCH₃), 3.89 (s, 6H, 3'/5'-OCH₃) 5.29–5.31 (m, 2H, Ar_{cym}-H3/H5), 5.89 (m, 1H, CHOHAr), 6.30 (s, 1H, CH), 6.72 (s, 2H, Ar-H2/H6); ¹³C NMR (CDCl₃) δ: 18.6 (CH₃,_{pyr}), 19.8 (CH₃,_{cym}), 22.3 (CH₃,_{cym}), 31.2 (CH(CH₃)₂), 56.4 (3'/5'-OCH₃), 60.7 (4'-OCH₃), 71.8 (CHOHAr), 77.8 (Ar_{cym}-C3/C5), 80.5 (Ar_{cym}-C2/C6), 95.4 (Ar_{cym}-C4), 99.0 (Ar_{cym}-C1), 104.3 (Ar-C2/C6), 109.4 (CH), 136.8 (Ar-C1), 137.8 (Ar-C4), 152.8 (CH₃C=CH), 153.3 (Ar-C3/C5), 155.2 (HOCH=COH), 164.1 (CHOH), 185.0 (C=O); IR (KBr, cm⁻¹, selected bands): 3383, 1603, 1567, 1510, 1473, 1417, 1326, 1238, 1124; Elemental Anal. Calc. for C₂₆H₃₁ClO₇Ru: C, 52.75; H, 5.28. Found: C, 52.80; H, 5.32%.

4.3. GMP binding

Complexes **3a–e** (1–2 mg/mL) were dissolved in D₂O containing 5% DMSO-*d*₆. The solution was titrated with a 5'-GMP solution (10 mg/mL) in 50 μL increments, and the reaction was monitored by ¹H and ³¹P NMR spectroscopy until unreacted 5'-GMP was detected.

4.4. pK_a determination

Complexes **3a–e** were dissolved in D₂O containing 5% DMSO-*d*₆. The pH value was measured directly in the NMR tubes with an Eco Scan pH6 pH meter equipped with a glass-micro combination pH electrode (Orion 9826BN) and calibrated with standard buffer solutions of pH 4.00, 7.00 and 10.00. The pH titration was performed by addition of NaOD (0.4–0.0004% in D₂O) and DNO₃ (0.4–0.0004% in D₂O). The observed shifts of the Ar_{cym}-H2/H6 protons of the arene ring in the ¹H NMR spectra were plotted against the pH value, and the obtained curves were fitted using the Henderson-Hasselbalch equation with Excel software (Microsoft® Office Excel 2003, SP3, Microsoft Corporation). The experimentally obtained pK_a values were corrected with Eq. (1) [60], in order to convert the pK_a in D₂O to corresponding pK_a values in aqueous solutions.

$$pK_z = 0.929pK_{z^*} + 0.42 \quad (1)$$

4.5. Cytotoxicity in cancer cell lines

4.5.1. Cell lines and conditions

CH1 cells originate from an ascites sample of a patient with a papillary cystadenocarcinoma of the ovary and were a generous gift from Lloyd R. Kelland, CRC Centre for Cancer Therapeutics, Institute of Cancer Research, Sutton, UK. SW480 (adenocarcinoma of the colon) and A549 (non-small cell lung cancer) cells were kindly provided by Brigitte Marian (Institute of Cancer Research, Department of Medicine I, Medical University of Vienna, Austria). All cell culture reagents were obtained from Sigma–Aldrich Austria. Cells were grown in 75 cm² culture flasks (Iwaki) as adherent monolayer cultures in Minimal Essential Medium (MEM) supplemented with 10% heat-inactivated fetal calf serum, 1 mM sodium pyruvate, 4 mM L-glutamine and 1% non-essential amino acids (100×). Cultures were maintained at 37 °C in a humidified atmosphere containing 5% CO₂.

4.5.2. MTT assay conditions

Cytotoxicity was determined by the colorimetric MTT (3-(4,5-dimethyl-2-thiazolyl)-2,5-diphenyl-2H-tetrazolium bromide, purchased from Fluka) microculture assay. For this purpose, cells were harvested from culture flasks by trypsinization and seeded into 96-well microculture plates (Iwaki). Cell densities of 1.5 × 10³ cells/well (CH1), 2.5 × 10³ cells/well (SW480) and 4 × 10³ cells/well (A549) were chosen in order to ensure exponential growth throughout drug exposure. Cells were allowed to settle in drug-free complete culture medium for 24 h. Stocks of the test compounds in

DMSO were diluted in complete culture medium such that the maximum DMSO content did not exceed 1% (this procedure yielded opaque but colloidal solutions from which no precipitates could be separated by centrifugation). These dilutions were added in 200 μL aliquots to the microcultures after removal of the pre-incubation medium, and cells were exposed to the test compounds for 96 h. At the end of exposure, all media were replaced by 100 μL/well RPMI1640 culture medium (supplemented with 10% heat-inactivated fetal bovine serum and 4 mM L-glutamine) plus 20 μL/well MTT solution in phosphate-buffered saline (5 mg/mL). After incubation for 4 h, the supernatants were removed, and the formazan crystals formed by vital cells were dissolved in 150 μL DMSO per well. Optical densities at 550 nm were measured with a microplate reader (Tecan Spectra Classic), using a reference wavelength of 690 nm. The quantity of vital cells was expressed in terms of T/C values by comparison to untreated control microcultures, and 50% inhibitory concentrations (IC₅₀) were calculated from concentration–effect curves by interpolation. Evaluation is based on means from three independent experiments, each comprising six replicates per concentration level.

Acknowledgments

We thank the University of Vienna, the Hochschuljubiläumsstiftung Vienna (H1556–2006), the Theodor-Körner-Fonds, the Austrian Council for Research and Technology Development, the FFG – Austrian Research Promotion Agency (Project FA 526003), the FWF – Austrian Science Fund (Schrödinger Fellowship J2613–N19 [C.G.H.], project P18123–N11), the EPFL, and COST D39 for financial support. We gratefully acknowledge Alexander Roller for collecting and refining the X-ray diffraction data and Prof. Markus Galanski for recording the NMR spectra.

Appendix A. Supplementary material

CCDC 701753 contains the supplementary crystallographic data for **3b**. These data can be obtained free of charge from The Cambridge Crystallographic Data Centre via www.ccdc.cam.ac.uk/data_request/cif. Supplementary data associated with this article can be found, in the online version, at [doi:10.1016/j.jorganchem.2008.10.016](https://doi.org/10.1016/j.jorganchem.2008.10.016).

References

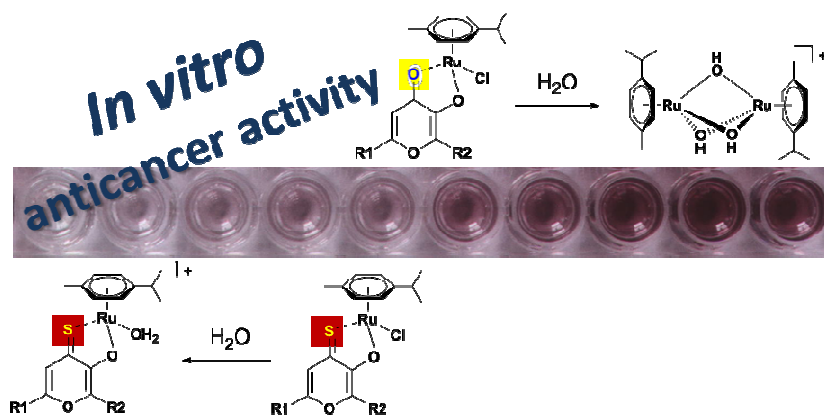
- [1] M.A. Jakupec, M. Galanski, V.B. Arion, C.G. Hartinger, B.K. Keppler, Dalton Trans. (2008) 183.
- [2] M.A. Jakupec, B.K. Keppler, Curr. Top. Med. Chem. 4 (2004) 1575.
- [3] W.H. Ang, P.J. Dyson, Eur. J. Inorg. Chem. (2006) 4003.
- [4] C.G. Hartinger, S. Zorbas-Seifried, M.A. Jakupec, B. Kynast, H. Zorbas, B.K. Keppler, J. Inorg. Biochem. 100 (2006) 891.
- [5] C.G. Hartinger, P.J. Dyson, Chem. Soc. Rev. (2008) doi:10.1039/B707077M.
- [6] U. Schatzschneider, N. Metzler-Nolte, Angew. Chem., Int. Ed. 45 (2006) 1504.
- [7] R. Alberto, Top. Curr. Chem. 252 (2005) 1.
- [8] J.M. Rademaker-Lakhai, D. van den Bongard, D. Pluim, J.H. Beijnen, J.H. Schellens, Clin. Cancer Res. 10 (2004) 3717.
- [9] C.G. Hartinger, M.A. Jakupec, S. Zorbas-Seifried, M. Groessl, A. Egger, W. Berger, H. Zorbas, P.J. Dyson, B.K. Keppler, Chem. Biodiversity 5 (2008) 2140.
- [10] M. Pongratz, P. Schluga, M.A. Jakupec, V.B. Arion, C.G. Hartinger, G. Allmaier, B.K. Keppler, J. Anal. At. Spectrom. 19 (2004) 46.
- [11] A.R. Timerbaev, A.V. Rudnev, O. Semenova, C.G. Hartinger, B.K. Keppler, Anal. Biochem. 341 (2005) 326.
- [12] M. Sulyok, S. Hann, C.G. Hartinger, B.K. Keppler, G. Stingeder, G. Koellensperger, J. Anal. At. Spectrom. 20 (2005) 856.
- [13] C.G. Hartinger, S. Hann, G. Koellensperger, M. Sulyok, M. Grössl, A.R. Timerbaev, A.V. Rudnev, G. Stingeder, B.K. Keppler, Int. J. Clin. Pharmacol. Ther. 43 (2005) 583.
- [14] A.R. Timerbaev, C.G. Hartinger, S.S. Aleksenko, B.K. Keppler, Chem. Rev. 106 (2006) 2224.
- [15] K. Polec-Pawlak, J.K. Abramski, O. Semenova, C.G. Hartinger, A.R. Timerbaev, B.K. Keppler, M. Jarosz, Electrophoresis 27 (2006) 1128.
- [16] P. Schluga, C.G. Hartinger, A. Egger, E. Reisner, M. Galanski, M.A. Jakupec, B.K. Keppler, Dalton Trans. (2006) 1796.

- [17] A. Vessieres, S. Top, W. Beck, E. Hillard, G. Jaouen, Dalton Trans. (2006) 529.
- [18] K. Strohhfeldt, M. Tacke, Chem. Soc. Rev. 37 (2008) 1174.
- [19] A. Casini, C. Hartinger, C. Gabbiani, E. Mini, P.J. Dyson, B.K. Keppler, L. Messori, J. Inorg. Biochem. 102 (2008) 564.
- [20] C.S. Allardyce, P.J. Dyson, D.J. Ellis, S.L. Heath, Chem. Commun. (2001) 1396.
- [21] C. Scolaro, A. Bergamo, L. Brescacin, R. Delfino, M. Cocchietto, G. Laurenczy, T.J. Geldbach, G. Sava, P.J. Dyson, J. Med. Chem. 48 (2005) 4161.
- [22] Y.K. Yan, M. Melchart, A. Habtemariam, P.J. Sadler, Chem. Commun. (2005) 4764.
- [23] W.H. Ang, E. Daldini, C. Scolaro, R. Scopelliti, L. Juillerat-Jeanerret, P.J. Dyson, Inorg. Chem. 45 (2006) 9006.
- [24] C. Scolaro, T.J. Geldbach, S. Rochat, A. Dorcier, C. Gossens, A. Bergamo, M. Cocchietto, I. Tavernelli, G. Sava, U. Rothlisberger, P.J. Dyson, Organometallics 25 (2006) 756.
- [25] J.É. Debreczeni, A.N. Bullock, G.E. Atilla, D.S. Williams, H. Bregman, S. Knapp, E. Meggers, Angew. Chem. 45 (2006) 1580.
- [26] C. Scolaro, A.B. Chaplin, C.G. Hartinger, A. Bergamo, M. Cocchietto, B.K. Keppler, G. Sava, P.J. Dyson, Dalton Trans. (2007) 5065.
- [27] C.A. Vock, W.H. Ang, C. Scolaro, A.D. Phillips, L. Lagopoulos, L. Juillerat-Jeanerret, G. Sava, R. Scopelliti, P.J. Dyson, J. Med. Chem. 50 (2007) 2166.
- [28] A.F.A. Peacock, M. Melchart, R.J. Deeth, A. Habtemariam, S. Parsons, P.J. Sadler, Chem. Eur. J. 13 (2007) 2601.
- [29] W.F. Schmid, R.O. John, V.B. Arion, M.A. Jakupec, B.K. Keppler, Organometallics 26 (2007) 6643.
- [30] W.F. Schmid, R.O. John, G. Mühlgassner, P. Heffeter, M.A. Jakupec, M. Galanski, W. Berger, V.B. Arion, B.K. Keppler, J. Med. Chem. 50 (2007) 6343.
- [31] M.G. Mendoza-Ferri, C.G. Hartinger, R.E. Eichinger, N. Stolyarova, K. Severin, M.A. Jakupec, A.A. Nazarov, B.K. Keppler, Organometallics 27 (2008) 2405.
- [32] M.G. Mendoza-Ferri, C.G. Hartinger, A.A. Nazarov, W. Kandioller, K. Severin, B.K. Keppler, Appl. Organomet. Chem. 22 (2008) 326.
- [33] W.H. Ang, A. De Luca, C. Chapuis-Bernasconi, L. Juillerat-Jeanerret, M. Lo Bello, P.J. Dyson, ChemMedChem 2 (2007) 1799.
- [34] F. Schmitt, P. Govindaswamy, G. Suess-Fink, W.H. Ang, P.J. Dyson, L. Juillerat-Jeanerret, B. Therrien, J. Med. Chem. 51 (2008) 1811.
- [35] W.H. Ang, E. Daldini, L. Juillerat-Jeanerret, P.J. Dyson, Inorg. Chem. 46 (2007) 9048.
- [36] P.J. Dyson, G. Sava, Dalton Trans. (2006) 1929.
- [37] S. Chatterjee, S. Kundu, A. Bhattacharyya, C.G. Hartinger, P.J. Dyson, J. Biol. Inorg. Chem. 13 (2008) 1149.
- [38] O. Nováková, A.A. Nazarov, C.G. Hartinger, B.K. Keppler, V. Brabec, Biochem. Pharmacol., in press, doi:10.1016/j.bcp.2008.10.021.
- [39] K.H. Thompson, C. Orvig, Dalton Trans. (2006) 761.
- [40] K. Saatchi, K.H. Thompson, B.O. Patrick, M. Pink, V.G. Yuen, J.H. McNeill, C. Orvig, Inorg. Chem. 44 (2005) 2689.
- [41] K.H. Thompson, C.A. Barta, C. Orvig, Chem. Soc. Rev. 35 (2006) 545.
- [42] Z.-S. Lu, J. Burgess, R. Lane, Transition Met. Chem. 27 (2002) 239.
- [43] D.T. Puerta, M. Botta, C.J. Jocher, E.J. Werner, S. Avedano, K.N. Raymond, S.M. Cohen, J. Am. Chem. Soc. 128 (2006) 2222.
- [44] C.-T. Yang, S.G. Sreerama, W.-Y. Hsieh, S. Liu, Inorg. Chem. 47 (2008) 2719.
- [45] M. Backlund, J. Ziller, P.J. Farmer, Inorg. Chem. 47 (2008) 2864.
- [46] Y. Ma, W. Luo, P.J. Quinn, Z. Liu, R.C. Hider, J. Med. Chem. 47 (2004) 6349.
- [47] A.P. Abbott, G. Capper, D.L. Davies, J. Fawcett, D.R. Russell, J. Chem. Soc., Dalton Trans. (1995) 3709.
- [48] R. Lang, K. Polborn, T. Severin, K. Severin, Inorg. Chim. Acta 294 (1999) 62.
- [49] M.D. Aytémir, U. Calis, M. Ozalp, Arch. Pharm. (Weinheim, Ger.), 337 (2004) 281.
- [50] W.-Y. Hsieh, C.M. Zaleski, V.L. Pecoraro, P.E. Fanwick, S. Liu, Inorg. Chim. Acta 359 (2006) 228.
- [51] J.L. Lamboy, A. Pasquale, A.L. Rheingold, E. Melendez, Inorg. Chim. Acta 360 (2007) 2115.
- [52] U. Warnke, C. Rappel, H. Meier, C. Kloft, M. Galanski, C.G. Hartinger, B.K. Keppler, U. Jaehde, ChemBioChem 5 (2004) 1543.
- [53] A. Dorcier, C.G. Hartinger, R. Scopelliti, R.H. Fish, B.K. Keppler, P.J. Dyson, J. Inorg. Biochem. 102 (2008) 1066.
- [54] M.A. Bennett, T.N. Huang, T.W. Matheson, A.K. Smith, Inorg. Synth. 21 (1982) 74.
- [55] M.R. Pressprich, J. Chambers, SAINT + Integration Engine, Program for Crystal Structure Integration, Madison, 2004.
- [56] G.M. Sheldrick, SHELXS-97, Program for Crystal Structure Solution, University Göttingen, Germany, 1997.
- [57] G.M. Sheldrick, SHELXL-97, Program for Crystal Structure Refinement, University Göttingen, Germany, 1997.
- [58] L.J. Farrugia, J. Appl. Crystallogr. 30 (1997) 565.
- [59] International Tables for X-ray Crystallography, Kluwer Academic Press, Dordrecht, The Netherlands, 1992.
- [60] A. Krezel, W. Bal, J. Inorg. Biochem. 98 (2004) 161.

3.2. From pyrone to thiopyrone ligands – the *in vitro* anticancer activity of Ru(II) arene complexes in dependence of the ligand donor atoms

Organometallics, in press

Graphical Abstract



Ru(II)-arene complexes with pyrone-derived ligands are rendered active against cancer cells by replacement of the coordinated *O,O* donor with an *S,O* donor. The different stabilities of these systems may explain the observed influence of the donor atoms on the anticancer activity *in vitro*.

From pyrone to thiopyrone ligands – rendering maltol-derived Ru(II)-arene complexes anticancer active *in vitro*

Wolfgang Kandioller,^a Christian G. Hartinger,^{a,*} Alexey A. Nazarov,^{a,b,*} Maxim L. Kuznetsov,^c Roland John,^a Caroline Bartel,^a Michael A. Jakupec,^a Vladimir B. Arion^a and Bernhard K. Keppler^a

^a University of Vienna, Institute of Inorganic Chemistry, Waehringer Str. 42, A-1090 Vienna, Austria.

^b Institut des Sciences et Ingénierie Chimiques, Ecole Polytechnique Fédérale de Lausanne (EPFL), CH-1015 Lausanne, Switzerland.

^c Centro de Química Estrutural, Complexo I, Instituto Superior Técnico, Technical University of Lisbon, Av. Rovisco Pais, 1049-001 Lisbon, Portugal.

christian.hartinger@univie.ac.at, alex.nazarov@univie.ac.at.

RECEIVED DATE (to be automatically inserted after your manuscript is accepted if required according to the journal that you are submitting your paper to)

(Thio)pyrone-Ru(II)-arene anticancer agents

ABSTRACT.

Ru(II)-arene complexes with maltolato ligands are inactive in tumor cell lines, probably due to formation of dimeric species. Switching from pyrones to thiopyrones renders such compounds active against cancer cells. These complexes are significantly more stable in aqueous solution, as shown by ESI-MS and NMR spectroscopy and confirmed by DFT calculations, and do not undergo dimer formation. The different stabilities of these systems may explain the observed influence of the donor atoms on the anticancer activity *in vitro*.

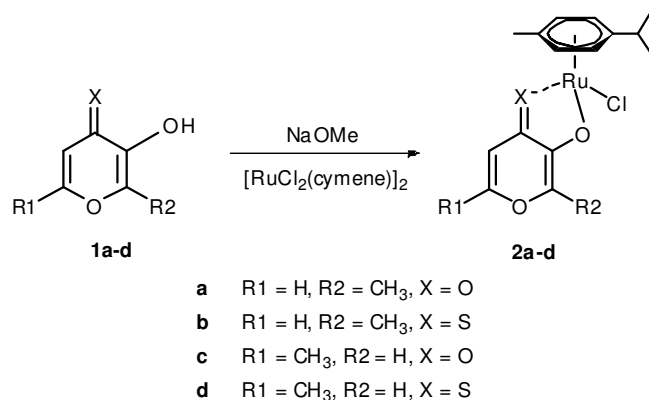
KEYWORDS.

Cancer, Ruthenium-arene complexes, Aquation, Density functional calculations, Thiopyrones.

Metal complexes are playing an important role in the treatment of cancer, and many promising compounds have been developed in recent years.¹⁻⁴ Ruthenium complexes have been shown to be among the most promising candidates for new metal-based anticancer drugs. Two of them, KP1019 and NAMI-A, are currently undergoing clinical trials.^{2,5} Their low general toxicity might be explained by their modes of action, including protein binding and activation by reduction.⁵⁻⁷

More recently, bioorganometallic chemistry has emerged as a new source of anticancer metallodrugs, with titanocene dichloride being the prototype agent of this compound class.^{4,8,9} Furthermore, organometallic Ru(II) compounds, that are stabilized in their +2 oxidation state by coordination of an arene ligand, have been investigated for their anticancer properties. These piano-stool complexes have been pioneered by the Dyson and Sadler groups,^{10,11} who developed compounds with pta (1,3,5-triaza-7-phoshatricyclo[3.3.1.1]decane) and en (ethylenediamine) ligands, respectively.¹⁰ For the $[(\eta^6\text{-arene})\text{Ru}(\text{II})(\text{X})(\text{Y})]$ complexes, DNA base selectivity strongly depends on the character of the chelating ligand Y – exchange of the neutral ethylenediamine by anionic acetylacetonate shifts the affinity from guanine to adenine.¹² Besides en and pta complexes, maltol-derived mono- and polynuclear ruthenium and osmium complexes have been developed.¹³⁻¹⁵ The linking of two pyridone moieties opened up new possibilities for tuning the *in vitro* anticancer activity and lipophilicity, and compounds with interdplex cross-linking capacity were obtained.^{14,16-18} In the case of the mononuclear Ru(II) complexes, an increase in cytotoxic activity was achieved by derivatization of the pyrone ring with lipophilic aromatic substituents.¹³

In order to study the Ru–ligand interaction and its effect on the *in vitro* anticancer activity, Ru(II)–cymene complexes (Scheme 1) with pyrones and their corresponding, more lipophilic thiopyrones as chelating agents were prepared.^{15,19} Such (thio)pyrone systems found already application in medicinal chemistry.^{20,21} The Ru(II)–cymene complexes were obtained in good yields (64–85%) by deprotonation of the ligand with sodium methoxide and reaction with bis[dichlorido(η^6 -*p*-cymene)ruthenium(II)]. The reaction was performed with a slight excess of ligand to facilitate the purification. All complexes have been fully characterized by 1D and 2D NMR spectroscopy, mass spectrometry and elemental analysis.



Scheme 1. Synthesis of the complexes **2a–d**.

Single crystals of **2b** were obtained from ethyl acetate, and the molecular structure was determined by X-ray diffraction analysis. The ruthenium center was found to adopt piano-stool configuration (Figure 1; Supporting Information). Due to the larger sulfur atom in **2b** as compared to the oxygen in maltol-derived ligands, the Ru–S bond (2.3730(3) Å) is significantly longer than the Ru–O bond (2.0808(10) Å). This leads to a strong distortion of the 5-membered chelate ring of the complex. The length of the Ru–Cl bond in **2b** (2.4331(4) Å) is comparable to the corresponding bond lengths of pyrone and pyridone Ru(II)–arene complexes.^{14,15}

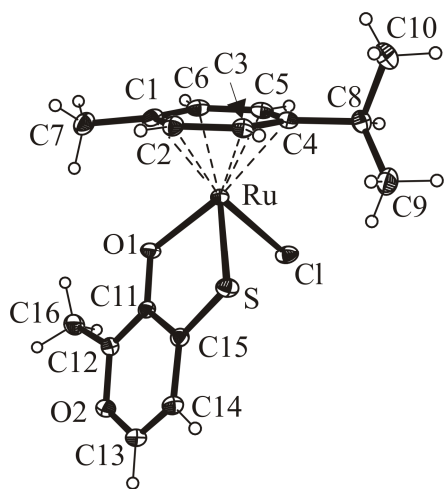


Figure 1. ORTEP plot of the molecular structure of **2b**.

The antiproliferative activities of **2a–d** were investigated in the human tumor cell lines SW480 (colon carcinoma) and CH1 (ovarian carcinoma) by using the colorimetric MTT assay (Figure 2). The IC₅₀ values are presented in Table 1. As reported earlier,¹⁴ the maltol complex **2a** shows limited cytotoxic activity, and the allomaltol derivative **2c** has IC₅₀ values > 200 μM. In contrast, the thiopyrone complexes **2b** and **2d** are at least by an order of magnitude (in IC₅₀) more active than their pyrone analogues. For complexes **2b** and **2d**, an inverted sensitivity of SW480 cells and CH1 cells was observed, which contrasts with a broad spectrum of other compounds, but parallels that observed with Ru(II)–arene complexes containing an 8-quinolinolato ligand.²² The substitution pattern influences the activity, as inferred from the 2.7–3.9 times higher activity of **2b** as compared to **2d**. These compounds are less cytotoxic than other ruthenium complexes,²³ but still in a reasonable range of activity *in vitro* when compared to other Ru–arene species.²² However, the *in vitro* activity is only a first indication for potential activity and the results need to be reproduced *in vivo*.

Table 1. Antiproliferative activity, ΔG of hydrolysis and bond energies (kcal/mol) of **2a–d** (**2'a–d**).

		2a	2b	2c	2d
IC₅₀ [μM]	CH1	81 ± 14	13 ± 4	239 ± 22	35 ± 8
	SW480	159 ± 41	5.1 ± 0.5	359 ± 119	20 ± 7
		2'a	2'b	2'c	2'd
ΔG_{hydr}		4.2	3.3	4.9	3.6
E(Ru–Cl)		10.6	7.1	11.1	7.9
E(Ru–O/S)_(O/S=C)		26.8	34.6	26.4	34.4
E(Ru–O)_(O–C)		36.9	35.7	36.6	36.2

The *in vitro* inactivity of the maltolato complexes has been attributed to the formation of dimers in aqueous solution.¹³ Accordingly, hydrolysis/stability in water were investigated by NMR spectroscopy in D₂O or 10% DMSO-*d*₆/D₂O solutions for the maltol and thiomaltol compounds, respectively. The

complexes **2a–d** hydrolyze within seconds to charged complexes by exchange of the chlorido ligand with a water molecule (Figure 2). No coordination of DMSO-*d*₆ was observed, and identical NMR spectra were obtained by activation of **2a** and **2c** with an equimolar amount of AgNO₃, which confirms the obtained results. Similarly to **2a**,¹³ the formation of a dimeric species was observed for **2c** (Figure 2, top left), as demonstrated by ESI-MS with a sample of 25 μM; this concentration was chosen in order to obtain a mass spectrum containing both the intact complex and the dimeric species. The amount of formed side product depends on the concentration, time and pH value of the solution and its formation can be prevented by addition of an equimolar amount of imidazole, as also demonstrated by means of ESI-MS (Figure 2, top right).

Hydrolysis of **2b** and **2d** in 10% DMSO-*d*₆/D₂O results in the rapid formation of aqua species, which are stable for more than 24 h, and in contrast to the maltolato complexes, no dimers have been observed. To explain these observations, theoretical DFT calculations (B3LYP, Gaussian 03 program package,²⁴ see Supporting Information for computational details) of the metal–ligand bond energies have been performed. They reveal that the Ru–S_(S=C) bond energies in the model complexes **2'b** and **2'd** (bearing benzene instead of cymene in **2b** and **2d**) are by 7.8–8.0 kcal/mol higher than the Ru–O_(O=C) bond energies in **2'a** and **2'c**, respectively. In contrast, the Ru–O_(O=C) bond energies in thiopyrone complexes are lower than those in pyrone species but only by 0.4–1.2 kcal/mol. The stronger binding of thiopyrones to Ru as compared to pyrones explains why thiopyrone complexes are stable in aqueous solution while pyrone complexes undergo decomposition with release of the ligands **1a** and **1c**.

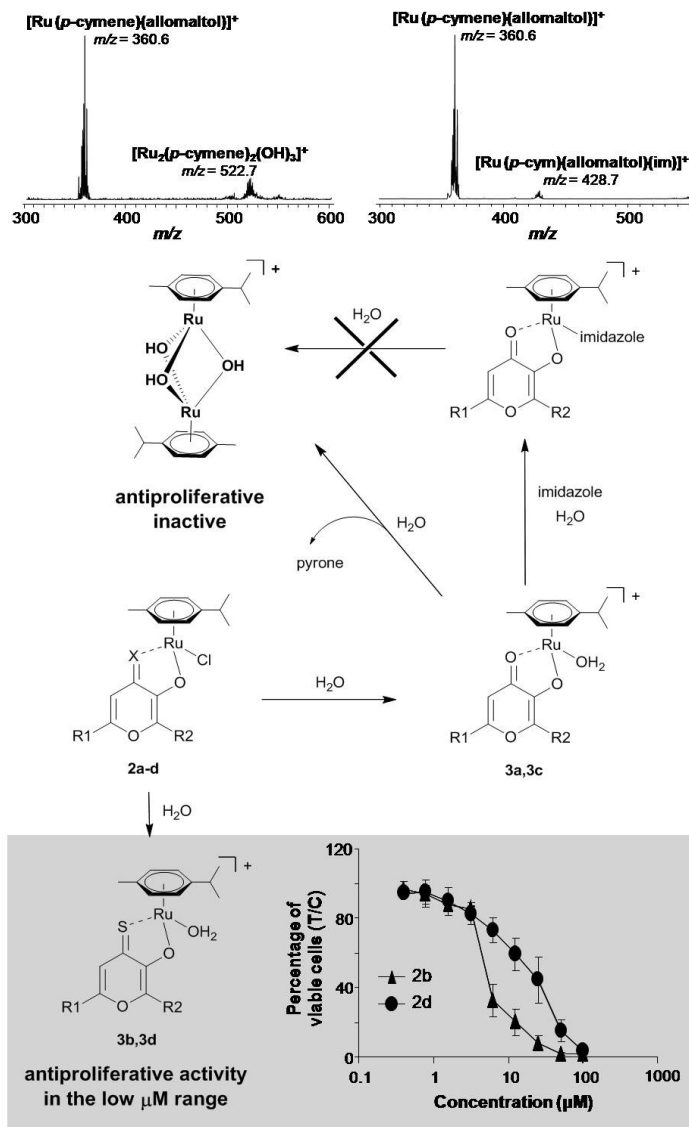


Figure 2. The hydrolysis of Ru-(thio)pyronato complexes (X = O or S) yields in the case of the pyrone ligands the dimeric $[\text{Ru}_2(\text{cym})_2(\text{OH})_3]^+$ species (as demonstrated by ESI-MS; top left). When the aqua complexes **3a** and **3c** are reacted with imidazole, no dimerization was observed (top right), as is the case for the thiopyrone compounds **3b** and **3d**, which show significant cytotoxic activity in human cancer cell lines (bottom right).

Theoretical calculations of **2'a-d** and **3'a-d** show that ΔG values for the substitution of chloride with H_2O are only slightly positive (3.3–4.9 kcal/mol). Taking into account the large excess of water,

complexes **3a–d** are the predominant species in aqueous solutions. Lower Ru–Cl bond energies in **2'b** and **2'd** as compared to **2'a** and **2'c**, respectively, correlate with ΔG values of hydrolysis (Table 1).

Summarizing, the modification of the first ligand sphere and therewith of the stability of the complexes influences significantly the *in vitro* anticancer activity. Pyrone and thiopyrone compounds behave quite differently in water (dimer formation) and when reacted with biological molecules. These features have important implications for the mode of action of the compounds and result in considerably active thiopyrone vs. minimally active pyrone complexes. Furthermore, complexes **2b** and **2d** are slightly more active in SW480 cells, though CH1 cells are in our experience more chemosensitive to the vast majority of metal-based and other tumor-inhibiting compounds tested so far.

ACKNOWLEDGMENT

We thank the Hochschuljubiläumsstiftung Vienna, the Theodor-Körner-Fonds, COST D39 and the Austrian Science Fund (Schrödinger Fellowship J2613-N19 [C.G.H.] and project P18123–N11) for financial support and the computer center of the University of Vienna for computer time at the Linux-PC cluster Schroedinger III. This research was supported by a Marie Curie Intra European Fellowship within the 7th European Community Framework Programme project 220890-SuRuCo (A.A.N.). We gratefully acknowledge Alexander Roller for collecting the X-ray diffraction data.

Supporting Information Available. General procedure for the synthesis of the complexes, characterization, elemental analysis data, X-ray diffraction data, computational details. CCDC 720741 contains the supplementary crystallographic data for this paper. This material is available free of charge via the Internet at <http://pubs.acs.org>.

References.

1. Guo, Z.; Sadler, P. J. *Adv. Inorg. Chem.* **2000**, *49*, 183-306.
2. Alessio, E.; Mestroni, G.; Bergamo, A.; Sava, G. *Curr. Top. Med. Chem.* **2004**, *4*, 1525-35.
3. Jakupec, M. A.; Galanski, M.; Arion, V. B.; Hartinger, C. G.; Keppler, B. K. *Dalton Trans.* **2008**, 183-194.
4. Strohfeldt, K.; Tacke, M. *Chem. Soc. Rev.* **2008**, *37*, 1174-1187.
5. Hartinger, C. G.; Zorbas-Seifried, S.; Jakupec, M. A.; Kynast, B.; Zorbas, H.; Keppler, B. K. *J. Inorg. Biochem.* **2006**, *100*, 891-904.
6. Groessl, M.; Reisner, E.; Hartinger, C. G.; Eichinger, R.; Semenova, O.; Timerbaev, A. R.; Jakupec, M. A.; Arion, V. B.; Keppler, B. K. *J. Med. Chem.* **2007**, *50*, 2185-2193.
7. Dyson, P. J.; Sava, G. *Dalton Trans.* **2006**, 1929-1933.
8. Hartinger, C. G.; Dyson, P. J. *Chem. Soc. Rev.* **2009**, *38*, 391-401.
9. Jaouen, G., *Bioorganometallics*. Wiley-VCH: Weinheim, 2006; p 444.
10. Ang, W. H.; Dyson, P. J. *Eur. J. Inorg. Chem.* **2006**, 4003-4018.
11. Yan, Y. K.; Melchart, M.; Habtemariam, A.; Sadler, P. J. *Chem. Commun.* **2005**, 4764-4776.
12. Fernandez, R.; Melchart, M.; Habtemariam, A.; Parsons, S.; Sadler, P. J. *Chem. Eur. J.* **2004**, *10*, 5173-5179.
13. Peacock, A. F. A.; Melchart, M.; Deeth, R. J.; Habtemariam, A.; Parsons, S.; Sadler, P. J. *Chem. Eur. J.* **2007**, *13*, 2601-2613.

14. Mendoza-Ferri, M. G.; Hartinger, C. G.; Eichinger, R. E.; Stolyarova, N.; Jakupec, M. A.; Nazarov, A. A.; Severin, K.; Keppler, B. K. *Organometallics* **2008**, *27*, 2405-2407.
15. Kandioller, W.; Hartinger, C. G.; Nazarov, A. A.; Kasser, J.; John, R.; Jakupec, M. A.; Arion, V. B.; Dyson, P. J.; Keppler, B. K. *J. Organomet. Chem.* **2009**, *694*, 922-929.
16. Mendoza-Ferri, M. G.; Hartinger, C. G.; Nazarov, A. A.; Kandioller, W.; Severin, K.; Keppler, B. K. *Appl. Organomet. Chem.* **2008**, *22*, 326-332.
17. Mendoza-Ferri, M. G.; Hartinger, C. G.; Mendoza, M. A.; Groessler, M.; Egger, A.; Eichinger, R. E.; Mangrum, J. B.; Farrell, N. P.; Maruszak, M.; Bednarski, P. J.; Klein, F.; Jakupec, M. A.; Nazarov, A. A.; Severin, K.; Keppler, B. K. *J. Med. Chem.* **2009**, *52*, 916-925.
18. Nováková, O.; Nazarov, A. A.; Hartinger, C. G.; Keppler, B. K.; Brabec, V. *Biochem. Pharmacol.* **2009**, *77*, 364-374.
19. Lewis, J. A.; Puerta, D. T.; Cohen, S. M. *Inorg. Chem.* **2003**, *42*, 7455-7459.
20. Lewis, J. A.; Mongan, J.; McCammon, J. A.; Cohen, S. M. *ChemMedChem* **2006**, *1*, 694-697.
21. Thompson, K. H.; Barta, C. A.; Orvig, C. *Chem. Soc. Rev.* **2006**, *35*, 545-556.
22. Schuecker, R.; John, R. O.; Jakupec, M. A.; Arion, V. B.; Keppler, B. K. *Organometallics* **2008**, *27*, 6587-6595.
23. Jakupec, M. A.; Reisner, E.; Eichinger, A.; Pongratz, M.; Arion, V. B.; Galanski, M.; Hartinger, C. G.; Keppler, B. K. *J. Med. Chem.* **2005**, *48*, 2831-2837.
24. *Gaussian 03, Revision D.01*, Gaussian, Inc.: Wallingford CT, 2004.

Scheme 1. Synthesis of the complexes **2a–d**.

Figure 1. ORTEP plot of the molecular structure of **2b**.

Figure 2. Hydrolysis scheme of Ru-(thio)pyronato complexes; X = O or S.

Table 1. Antiproliferative activity, ΔG of hydrolysis and bond energies (kcal/mol) of **2a–d** (**2'a–d**).

		2a	2b	2c	2d
IC50 [μM]	CH1	> 100	13 \pm 4	239 \pm 22	34 \pm 8
	SW480	> 100	5.1 \pm 0.5	359 \pm 119	20 \pm 7
		2'a	2'b	2'c	2'd
ΔG_{hydr}		4.2	3.3	4.9	3.6
E(Ru–Cl)		10.6	7.1	11.1	7.9
E(Ru–O/S)_(O/S=C)		26.8	34.6	26.4	34.4
E(Ru–O)_(O–C)		36.9	35.7	36.6	36.2

Supporting Information

From pyrone to thiopyrone ligands – rendering
maltol-derived Ru(II)-arene complexes anticancer
active *in vitro*

Wolfgang Kandioller,^a Christian G. Hartinger^{a,*} Alexey A. Nazarov,^{a,b,*} Maxim L. Kuznetsov,^c
Roland John,^a Caroline Bartel,^a Michael A. Jakupec,^a Vladimir B. Arion,^a Bernhard K. Keppler^a

^a University of Vienna, Institute of Inorganic Chemistry, Austria.

^b Institut des Sciences et Ingénierie Chimiques, Ecole Polytechnique Fédérale de Lausanne,
Switzerland.

^c Centro de Química Estrutural, Complexo I, Instituto Superior Técnico, Technical University of
Lisbon, 1049-001 Lisbon, Portugal.

Table of contents

1. General Procedure for the Synthesis of the Complexes.....	3
2. Characterization.....	3
2.1. Elemental Analysis Data.....	3
2.2. X-Ray Diffraction Data.....	4
2.3. Mass Spectrometric Characterization of the Dimeric Hydrolysis Product.....	5
3. Computational Details.....	6
4. References	22

1. General Procedure for the Synthesis of the Complexes

The maltol-derived ligand (1 eq) and sodium methoxide (1.1 eq) were dissolved in methanol and stirred for 5 min under inert atmosphere to give a clear solution. Afterwards, bis[dichlorido(η^6 -*p*-cymene)ruthenium(II)] (0.9 eq) was dissolved in CH₂Cl₂ and added dropwise to the reaction mixture, which was stirred for further 4 h. The red solution was concentrated in *vacuo* and the residue was extracted with CH₂Cl₂. The combined organic layers were filtered and the solvent was removed. The crude product was purified by precipitation.

2. Characterization

2.1. Elemental Analysis Data

Compound	C [%]		H [%]		N [%]		S [%]	
	calc.	found	calc.	found	calc.	found	calc.	found
2a C ₁₆ H ₁₉ ClO ₃ Ru	48.55	48.45	4.84	4.63	0.00	<0.05	0.00	<0.05
2b C ₁₆ H ₁₉ ClO ₂ RuS	46.65	47.03	4.65	4.57	0.00	<0.05	7.78	7.67
2c C ₁₆ H ₁₉ ClO ₃ Ru	48.55	48.12	4.84	4.79	0.00	<0.05	0.00	<0.05
2d C ₁₆ H ₁₉ ClO ₂ RuS	46.65	46.24	4.65	4.61	0.00	<0.05	7.78	8.04

2.2. X-Ray Diffraction Data

Chemical formula	C ₁₆ H ₁₉ ClO ₂ RuS
M (g mol ⁻¹)	411.89
Temperature (K)	100(2)
Crystal size (mm)	0.30 × 0.22 × 0.15
Crystal color, shape	red, block
Crystal system	monoclinic
Space group	<i>P</i> 2 ₁ / <i>n</i>
<i>a</i> (Å)	8.3191(2)
<i>b</i> (Å)	14.8407(4)
<i>c</i> (Å)	12.9576(3)
β (°)	99.769(1)
<i>V</i> (Å ³)	1576.56(7)
<i>Z</i>	4
<i>D</i> _c (g cm ⁻³)	1.735
μ (cm ⁻¹)	12.97
F(000)	932
θ range for data collection (°)	2.72–30.09
<i>h</i> range	-11/11
<i>k</i> range	-20/20
<i>l</i> range	-18/18
No. refls. used in refinement	4622
No. parameters	192
<i>R</i> _{int}	0.0287
<i>R</i> ₁ ^a	0.0175
w <i>R</i> ₂ ^b	0.0432
GOF ^c	1.047
residuals, e ⁻ Å ⁻³	0.438, -0.408

^a $R_1 = \Sigma||F_o| - |F_c||/\Sigma|F_o|.$

^b $wR_2 = \{\Sigma[w(F_o^2 - F_c^2)^2]/w\Sigma(F_o^2)^2\}^{1/2}.$

^c GOF = $\{\Sigma[w(F_o^2 - F_c^2)^2]/(n - p)\}^{1/2}$, where *n* is the number of reflections and *p* is the total number of parameters refined.

2.3. Mass Spectrometric Characterization of the Dimeric Hydrolysis Product

The mass spectrometry data on the dimer formation was collected from samples prepared in H₂O (2.5 mM, 250 μM, 25 μM and 2.5 μM). The samples were introduced into the MS by flow injection and the spectra were recorded in the positive ion mode.

The abundance of the peak assigned to the dimeric $[\text{Ru}_2(\text{cym})_2(\text{OH})_3]^+$ ion was dependent on the concentration, temperature and pH. The lower the concentration, the more abundant was the peak in the MS. However, at 2.5 μM the signal to noise ratio limited the analysis of the sample and a concentration of 25 μM was identified as ideal for the experiment. In addition, the higher the pH, the quicker the dimer was formed, and also longer incubation time yielded higher amounts of the dimer (an optimum of 18 h was found).

3. Computational Details

The full geometry optimization of all structures has been carried out at the DFT level of theory using Becke's three-parameter hybrid exchange functional^{S1} in combination with the gradient-corrected correlation functional of Lee, Yang and Parr^{S2} (B3LYP) with the help of the Gaussian-03^{S3} program package. Symmetry operations were not applied for all structures. The geometry optimization was carried out using a quasi-relativistic Stuttgart pseudopotential described 28 core electrons and the appropriate contracted basis set (8s7p6d)/[6s5p3d]^{S4} for the ruthenium atom and the 6-31G(d) basis set for other atoms. Then single-point calculations were performed in the basis of the found equilibrium geometries using the 6-31+G(d,p) basis set for non-metal atoms. The experimental X-ray structure of **2b** (this work) was chosen as the starting geometry for the optimizations. The Hessian matrix was calculated analytically for all optimized structures in order to prove the location of correct minima (no "imaginary" frequencies), and to estimate thermodynamic parameters, the latter were calculated at 25 °C.

Solvent effects were taken into account at the single-point calculations based on the gas-phase equilibrium geometries at the CPCM-B3LYP/6-31+G(d,p)//gas-B3LYP/6-31G(d) level of theory using the polarizable continuum model in the CPCM version^{S5,S6} with H₂O as a solvent and UAKS atomic radii. The Gibbs free energies in solution (G_s) were estimated by addition of the solvation energy δG_{solv} to gas-phase Gibbs free energies (G_g).

The Ru–O_(O/S=C) bond energies have been calculated using the expression:

$$E_{\text{bs}}(\text{Ru-O/S}_{(\text{O/S=C})}) = E_s(\mathbf{R2'a-d}) - E_s(\mathbf{2'a-d})$$

where **R2'a-d** corresponds to complexes **2'a-d** but in which the organic ligand was rotated around the C(2)–O(1) bond by 50° so that the Ru–O/S_(O/S=C) bond becomes broken while other bond lengths and angles remain the same (except the angle RuO(4)C(3)). The torsion angle RuO(1)C(2)C(3) is –11.29° in **2'a**, –61.29° in **R2'a**, –11.71° in **2'b**, –61.71° in **R2'b**, –10.67° in **2'c**, –60.67° in **R2'c**, –10.47° in **2'd** and –60.47° in **R2'd**.

The Ru–O_(O-C) bond energies have been calculated using the expression:

$$E_{\text{bs}}(\text{Ru-O}_{(\text{O-C})}) = E_s(\mathbf{R'2'a-d}) - E_s(\mathbf{2'a-d})$$

where **R'2'a–d** corresponds to complexes **2'a–d** but in which the organic ligand was rotated around the C(3)O(4) bond by 50° so that the Ru–O_(O-C) bond becomes broken while other bond lengths and angles remain the same (except the angle RuO(1)C(2)). The torsion angle RuO(4)C(3)C(2) is 7.43° in **2'a**, 57.43° in **R'2'a**, 5.06° in **2'b**, 55.06° in **R'2'b**, 7.62° in **2'c**, 57.62° in **R'2'c**, 4.65° in **2'd** and 54.65° in **R'2'd**. It is necessary to mention that in **R2'a–d** and **R'2'a–d** the distances between any atom of the organic ligand (except the donor one) and the Ru atoms are not smaller than 2.7 Å. Thus, there are no new steric interactions in **R2'a–d** and **R'2'a–d** between the organic ligand and the metal, which might affect the bond energies calculated by this method. The equilibrium geometries and the main calculated bond lengths of **2'b** are in perfect agreement with the experimental X-ray structural data for **2b** (this work). The maximum deviation of the theoretical and experimental parameters is 0.03 Å for the Ru–S bond, whereas the difference for the other bonds does not exceed 0.018 Å, often falling within the 3σ interval of the X-ray data.

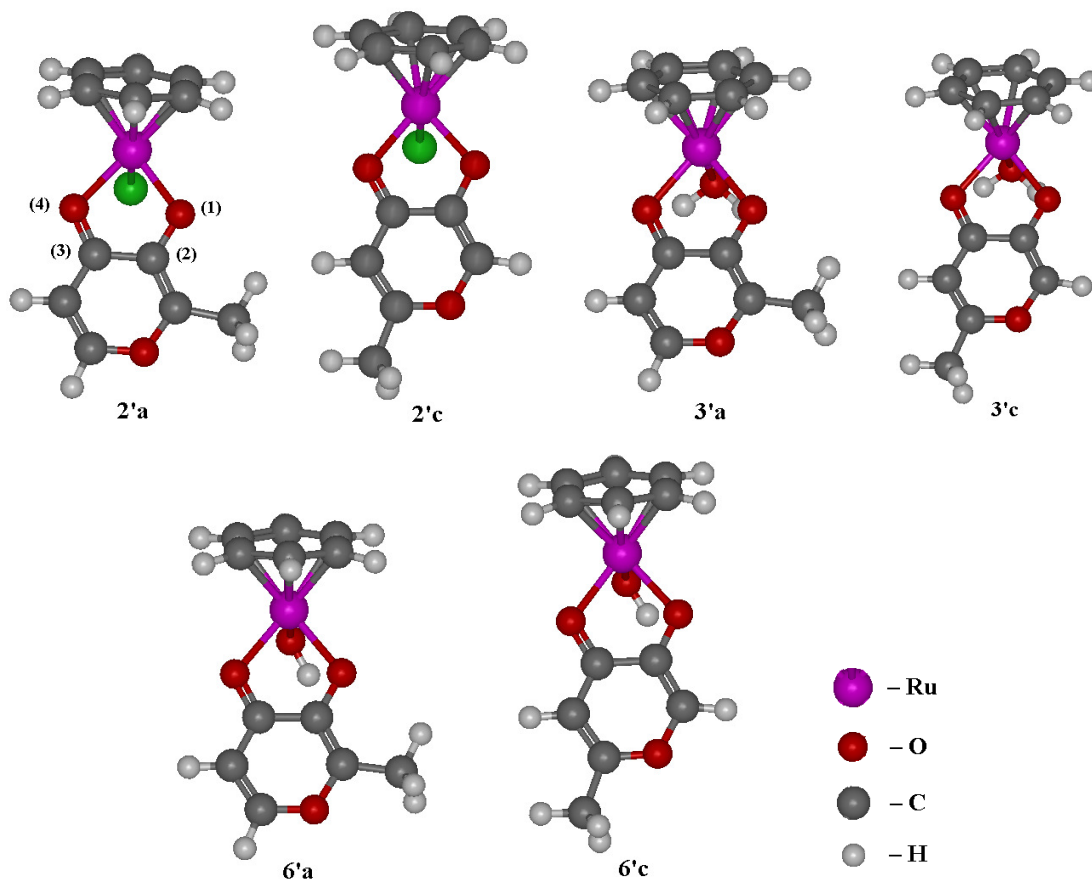


Figure S1. Equilibrium structures of the calculated pyrone complexes with numbering of selected atoms. Structures of the thiopyrone species are similar.

Table S1. Total energies, enthalpies and Gibbs free energies for the gas-phase and H₂O solution (Hartree) of the calculated structures.

	$E_g(6-31G^*)$	$E_g(6-31+G^{**})$	E_s	H_g	G_g	G_s
H ₂ O	-76.408953	-76.433933	-76.445244	-76.384013	-76.406114	-76.417425
H ₃ O ⁺	-76.689084	-76.707574	-76.880432	-76.650930	-76.673921	-76.846779
Cl ⁻	-460.252233	-460.274726	-460.388702	-460.249873	-460.267256	-460.381232
2'a	-1244.752725	-1244.785467	-1244.808913	-1244.528795	-1244.589480	-1244.612926
3'a	-860.753112	-860.793688	-860.870726	-860.503495	-860.565452	-860.642490
6'a	-860.334699	-860.375987	-860.401011	-860.099002	-860.160042	-860.185066
2'b	-1567.725128	-1567.756490	-1567.779352	-1567.503125	-1567.566512	-1567.589374
3'b	-1183.730680	-1183.769920	-1183.844267	-1183.482906	-1183.545901	-1183.620248
6'b	-1183.306404	-1183.346214	-1183.370216	-1183.072593	-1183.135279	-1183.159281
2'c	-1244.752547	-1244.785001	-1244.810377	-1244.528703	-1244.589490	-1244.614866
3'c	-860.753388	-860.793873	-860.871775	-860.503809	-860.565338	-860.643240
6'c	-860.334962	-860.375987	-860.402292	-860.099323	-860.159878	-860.186183
2'd	-1567.724717	-1567.755941	-1567.780854	-1567.502724	-1567.565314	-1567.590227
3'd	-1183.730836	-1183.769955	-1183.844913	-1183.483090	-1183.545807	-1183.620765
6'd	-1183.305917	-1183.345628	-1183.371532	-1183.072164	-1183.134632	-1183.160536

Table S2. Cartesian coordinates (Å) of the calculated equilibrium structures of the complexes.**2'a**

Ru	1.263322	0.694785	-0.519390
Cl	1.374085	-0.465312	-2.629825
O	-0.416880	-4.063596	0.661424
O	1.691882	-1.147331	0.357558
O	-0.675472	-0.156716	-0.366232
C	0.514582	2.612129	0.215428
H	-0.525502	2.801025	0.462731
C	1.386707	2.093188	1.216396
H	1.025632	1.911221	2.222159
C	0.960126	2.817668	-1.124385
C	0.654991	-1.955006	0.333449
C	3.150286	1.839025	-0.511609
H	4.116683	1.451678	-0.811736
C	2.270846	2.404604	-1.479495
H	2.567746	2.416597	-2.522253
C	0.716202	-3.293023	0.665089
C	-0.627787	-1.390052	-0.036275
C	1.945719	-4.042041	1.044665
C	2.686740	1.666359	0.826154
C	-1.772412	-2.236598	0.008715
H	-2.751390	-1.850441	-0.250400
C	-1.605752	-3.543512	0.347178
H	-2.395156	-4.284071	0.388949
H	0.270580	3.164560	-1.884815
H	3.305871	1.127837	1.536769
H	2.810721	-3.388637	0.917558
H	2.074586	-4.930063	0.414116
H	1.907385	-4.378948	2.089088

2'b

Ru	1.311265	1.074878	-0.584596
Cl	1.585380	0.268461	-2.853205
O	0.199127	-4.111449	-0.092515
O	1.756894	-0.889542	-0.016866
S	-0.923355	0.187195	-0.684385
C	0.626566	3.105734	-0.092816
H	-0.381855	3.477768	-0.242354
C	0.968193	2.454108	1.140894
H	0.221299	2.332404	1.917449
C	1.572633	3.203882	-1.140782
C	0.832516	-1.800777	-0.152710
C	3.210563	1.957615	0.218089
H	4.157778	1.436866	0.303131
C	2.875177	2.627813	-0.974360
H	3.558666	2.608682	-1.815571
C	1.151731	-3.148082	0.000793
C	-0.535299	-1.458826	-0.439011
C	2.523238	-3.659617	0.274238
C	2.238548	1.853998	1.272011
C	-1.485600	-2.508966	-0.497450
H	-2.530512	-2.298922	-0.697998
C	-1.079855	-3.797919	-0.329182
H	-1.713150	-4.674206	-0.378468
H	1.288608	3.629337	-2.095956
H	2.463328	1.255175	2.148550
H	3.244729	-3.142351	-0.366324
H	2.573882	-4.736334	0.093249
H	2.820276	-3.464546	1.313727

2'c

Ru	-1.151625	0.008824	-0.011704
Cl	-0.529393	2.337869	-0.011134
O	3.941668	-0.150756	0.973138
O	0.350649	-0.249553	1.414042
O	0.559083	-0.245173	-1.247858
C	-2.257874	-1.525794	-1.124459
H	-1.829779	-2.141372	-1.909460
C	-2.175773	-1.957723	0.224155
H	-1.706814	-2.902648	0.473799
C	-2.818445	-0.250902	-1.461588
C	1.545361	-0.198260	0.878599
C	-3.123316	0.218972	0.947565
H	-3.352854	0.924950	1.736720
C	-3.232982	0.614668	-0.423011
H	-3.527238	1.630929	-0.659553
C	2.720385	-0.165406	1.585370
C	1.642077	-0.218542	-0.572679
H	2.801174	-0.138805	2.662921
C	-2.571788	-1.052529	1.257840
C	2.937307	-0.230092	-1.158556
H	3.037444	-0.248889	-2.237712
C	4.048836	-0.181882	-0.362313
C	5.469139	-0.148971	-0.830593
H	-2.819485	0.089184	-2.490771
H	-2.372576	-1.307805	2.293789
H	5.966748	0.766294	-0.489553
H	5.512981	-0.184888	-1.921247
H	6.031111	-0.998978	-0.426422

2'd

Ru	-1.231863	-0.015157	0.007590
Cl	-0.680801	-1.222759	2.034205
O	3.968665	-0.986851	-0.720975
O	0.377358	-1.042998	-0.849886
S	0.513373	1.524754	0.621406
C	-2.773611	1.547767	-0.079924
H	-2.692489	2.531021	0.371626
C	-2.293755	1.339614	-1.417663
H	-1.852753	2.162051	-1.969024
C	-3.285753	0.467857	0.678823
C	1.588285	-0.647267	-0.580181
C	-2.805744	-1.071592	-1.187955
H	-2.726602	-2.079703	-1.578384
C	-3.305278	-0.848522	0.109910
H	-3.593579	-1.689516	0.729834
C	2.694119	-1.386209	-0.959248
C	1.849064	0.600079	0.103658
H	2.645964	-2.341401	-1.462920
C	-2.279022	0.030414	-1.945517
C	3.196325	0.981885	0.304096
H	3.425140	1.914838	0.807563
C	4.226396	0.175746	-0.102890
C	5.687667	0.435654	0.076102
H	-3.576341	0.612269	1.712226
H	-1.806202	-0.160367	-2.903074
H	6.148853	-0.346781	0.690023
H	5.845213	1.399357	0.564910
H	6.203869	0.442509	-0.891019

3'a

Ru	0.542595	0.869164	-1.297307
O	0.863722	-0.284744	-3.158545
O	0.568095	-3.801425	0.917138
O	1.675126	-0.716227	-0.592778
O	-0.946313	-0.558204	-0.966198
C	-0.821978	2.589070	-0.990829
H	-1.905151	2.527369	-0.973834
C	-0.080028	2.336034	0.210515
H	-0.601733	2.109000	1.133685
C	-0.149981	2.801675	-2.212459
C	0.914244	-1.712020	-0.142083
C	2.025665	2.517168	-1.070826
H	3.104591	2.419233	-1.115509
C	1.280326	2.747157	-2.248637
H	1.791765	2.805761	-3.203994
C	1.415848	-2.816790	0.517402
C	-0.502166	-1.616212	-0.367688
C	2.844982	-3.079115	0.837987
C	1.334853	2.299114	0.163227
C	-1.334745	-2.678081	0.071837
H	-2.406663	-2.648670	-0.085351
C	-0.749521	-3.734996	0.701903
H	-1.267748	-4.603953	1.087337
H	-0.712460	2.923592	-3.131534
H	1.895782	2.020470	1.049194
H	0.060002	-0.792540	-3.374001
H	1.532081	-0.938949	-2.873121
H	3.434668	-2.181570	0.643601
H	3.242332	-3.898571	0.225732
H	2.957788	-3.368209	1.888475

3'b

Ru	0.417749	1.437329	-0.680957
O	0.690447	0.616449	-2.732596
O	-0.353340	-3.657867	0.631411
O	1.066015	-0.499848	-0.284624
S	-1.720534	0.389320	-0.716314
C	-0.337352	3.517909	-0.403714
H	-1.318483	3.886937	-0.682231
C	-0.140818	2.892866	0.870979
H	-0.976230	2.782742	1.553723
C	0.724806	3.554930	-1.331917
C	0.165310	-1.433785	-0.029450
C	2.209943	2.427504	0.272977
H	3.156077	1.951336	0.506673
C	2.013185	3.027914	-0.982714
H	2.808169	3.021037	-1.720745
C	0.564343	-2.692832	0.417590
C	-1.230471	-1.190308	-0.215629
C	1.968525	-3.116537	0.666736
C	1.117229	2.334539	1.198702
C	-2.140883	-2.246358	0.023592
H	-3.207721	-2.109826	-0.114418
C	-1.662220	-3.452238	0.441511
H	-2.251814	-4.332234	0.662687
H	0.557153	3.944916	-2.330248
H	1.244199	1.800222	2.134027
H	-0.177494	0.357521	-3.096427
H	1.154013	-0.220284	-2.529789
H	2.397713	-3.596155	-0.223470
H	2.010656	-3.837722	1.487722
H	2.581348	-2.244516	0.903923

3'c

Ru	0.582223	1.957559	-0.498825
O	0.859757	0.932151	-2.440570
O	0.261203	-2.871958	1.328016
O	1.598215	0.254869	0.097622
O	-1.006426	0.610536	-0.291805
C	-0.655681	3.696221	0.076705
H	-1.735105	3.675683	0.187099
C	0.172687	3.307771	1.179375
H	-0.274819	3.026118	2.125950
C	-0.086422	3.994761	-1.181372
C	0.769416	-0.719394	0.453009
C	2.165405	3.512222	-0.271452
H	3.229648	3.372889	-0.424125
C	1.327409	3.875317	-1.353039
H	1.754837	3.991263	-2.343935
C	1.158750	-1.907428	1.013762
C	-0.641831	-0.517963	0.223457
H	2.176894	-2.192962	1.242125
C	1.576391	3.216503	0.995178
C	-1.539708	-1.555543	0.567148
H	-2.603353	-1.432255	0.399398
C	-1.055909	-2.716819	1.116914
C	-1.859491	-3.901326	1.539468
H	-0.721503	4.227425	-2.028778
H	2.198614	2.831107	1.796408
H	0.031021	0.494391	-2.708050
H	1.484378	0.217220	-2.206498
H	-1.533103	-4.798667	1.001856
H	-2.920134	-3.736506	1.340989
H	-1.725601	-4.092836	2.610190

3'd

Ru	0.891711	1.867919	-0.069241
O	1.112943	1.254112	-2.194564
O	0.175806	-3.340433	0.756447
O	1.562461	-0.090642	0.117317
S	-1.245989	0.810892	-0.142065
C	0.194553	3.956200	0.328314
H	-0.755764	4.388235	0.034662
C	0.306125	3.230676	1.557622
H	-0.566547	3.104085	2.189322
C	1.302562	4.012521	-0.544457
C	0.675659	-1.050072	0.304048
C	2.660789	2.711035	1.035862
H	3.572769	2.173574	1.273274
C	2.553539	3.413642	-0.177621
H	3.384853	3.431570	-0.873982
C	1.063216	-2.340567	0.604473
C	-0.734966	-0.804650	0.187702
H	2.088180	-2.664877	0.727965
C	1.523602	2.596558	1.903909
C	-1.623690	-1.886282	0.354426
H	-2.693838	-1.735548	0.265433
C	-1.147747	-3.144263	0.638183
C	-1.953464	-4.381942	0.847623
H	1.197398	4.476450	-1.519618
H	1.585393	1.994175	2.803528
H	0.240101	1.020195	-2.563044
H	1.591518	0.407967	-2.087381
H	-1.664439	-5.156755	0.128522
H	-3.017475	-4.169394	0.727863
H	-1.785476	-4.785803	1.852600

6'a

Ru	0.666795	0.911335	-1.291045
O	1.192454	-0.092283	-2.930925
O	0.478820	-3.898491	0.789796
O	1.663356	-0.647456	-0.257866
O	-0.889001	-0.575433	-1.081271
C	-0.744957	2.502950	-0.714590
H	-1.792844	2.343760	-0.479684
C	0.219501	2.452611	0.322782
H	-0.082047	2.267869	1.347580
C	-0.358573	2.695025	-2.083365
C	0.896989	-1.692115	-0.041895
C	2.011859	2.628574	-1.396816
H	3.062027	2.578196	-1.659564
C	1.020017	2.760870	-2.410226
H	1.321306	2.768726	-3.452336
C	1.326847	-2.836856	0.600918
C	-0.484192	-1.631283	-0.499489
C	2.696633	-3.070763	1.137627
C	1.595034	2.438856	-0.039656
C	-1.315192	-2.768421	-0.261548
H	-2.347620	-2.767258	-0.591990
C	-0.788119	-3.851241	0.368876
H	-1.321800	-4.767922	0.589289
H	-1.107305	2.688597	-2.867089
H	2.343197	2.223576	0.716819
H	1.530155	-0.948833	-2.620310
H	3.299705	-2.177086	0.967567
H	3.180502	-3.922445	0.642197
H	2.672427	-3.285990	2.213557

6'b

Ru	0.586766	1.401966	-0.737999
O	1.161099	0.539890	-2.459334
O	-0.497575	-3.664910	0.695515
O	1.032362	-0.476585	0.155264
S	-1.570701	0.330685	-1.049646
C	-0.340369	3.314239	-0.204793
H	-1.406692	3.515194	-0.242256
C	0.236906	2.833924	1.005978
H	-0.379420	2.666573	1.881835
C	0.448075	3.507798	-1.383820
C	0.129896	-1.410170	0.154133
C	2.398260	2.575537	-0.191770
H	3.414865	2.200393	-0.209466
C	1.819579	3.130338	-1.360432
H	2.391414	3.147414	-2.282199
C	0.431647	-2.676953	0.660814
C	-1.199833	-1.194614	-0.362378
C	1.766527	-3.062556	1.196818
C	1.581829	2.395921	0.975006
C	-2.127104	-2.263332	-0.277679
H	-3.142656	-2.141482	-0.638768
C	-1.741089	-3.460745	0.245505
H	-2.361684	-4.341978	0.343293
H	-0.011336	3.854014	-2.302090
H	1.994052	1.872718	1.832124
H	0.550442	-0.188740	-2.655542
H	1.955146	-2.587083	2.168868
H	2.552673	-2.715310	0.518225
H	1.833934	-4.146706	1.318228

6'c

Ru	0.683632	1.979794	-0.451454
O	1.099876	1.003903	-2.139870
O	0.179014	-2.893896	1.426807
O	1.584894	0.312634	0.496917
O	-0.977948	0.602034	-0.262145
C	-0.592273	3.650685	0.211440
H	-1.645597	3.563932	0.459592
C	0.381234	3.485088	1.228659
H	0.082130	3.284210	2.251122
C	-0.212934	3.867057	-1.155469
C	0.750186	-0.679461	0.682441
C	2.155258	3.589879	-0.515356
H	3.193761	3.466585	-0.799386
C	1.161739	3.839431	-1.504493
H	1.446715	3.865595	-2.550881
C	1.082714	-1.881468	1.256548
C	-0.638006	-0.504099	0.262168
H	2.067194	-2.148317	1.615219
C	1.745697	3.379812	0.841211
C	-1.538169	-1.589686	0.473093
H	-2.573006	-1.489642	0.165633
C	-1.098145	-2.751460	1.043201
C	-1.920933	-3.973038	1.306713
H	-0.971381	3.949199	-1.925435
H	2.486106	3.075219	1.574262
H	1.410027	0.124844	-1.865273
H	-1.522610	-4.834383	0.757746
H	-2.956037	-3.810520	0.998537
H	-1.906397	-4.227973	2.372724

6'd

Ru	0.830690	1.932275	-0.040419
O	0.620333	1.601591	-2.006970
O	0.307819	-3.408883	0.486267
O	1.558715	-0.066380	0.060701
S	-1.289649	0.775911	0.272915
C	0.457922	4.105144	0.051779
H	-0.348833	4.626441	-0.449840
C	0.255253	3.529133	1.348452
H	-0.718093	3.618902	1.820949
C	1.696772	3.886108	-0.610550
C	0.725490	-1.044480	0.236396
C	2.481787	2.545756	1.296018
H	3.213371	1.860826	1.713044
C	2.715871	3.109819	-0.002236
H	3.616506	2.860868	-0.551022
C	1.151180	-2.362219	0.304196
C	-0.703037	-0.825378	0.374024
H	2.182077	-2.673839	0.207255
C	1.291112	2.815684	2.013669
C	-1.533646	-1.953220	0.575746
H	-2.604602	-1.820820	0.686180
C	-1.012687	-3.219871	0.623483
C	-1.774642	-4.491827	0.815314
H	1.812018	4.203798	-1.641492
H	1.113124	2.360399	2.981140
H	0.114964	0.782002	-2.128312
H	-1.639777	-5.161203	-0.042544
H	-2.840537	-4.282109	0.929070
H	-1.425821	-5.026047	1.706951

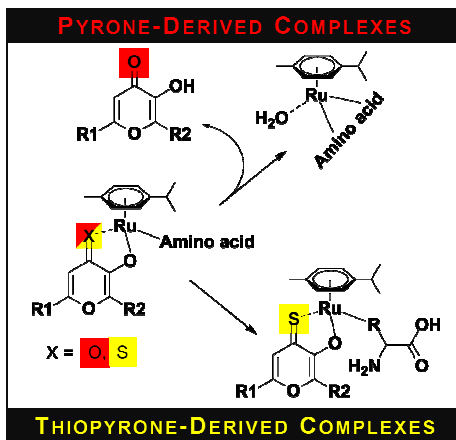
4. References

- S1. A. D. Becke, *J. Chem. Phys.*, 1993, **98**, 5648-5652.
- S2. C. Lee, W. Yang and R. G. Parr, *Phys. Rev. B: Condens. Matter*, 1988, **37**, 785-789.
- S3. M. J. Frisch, G. W. Trucks, H. B. Schlegel, G. E. Scuseria, M. A. Robb, J. R. Cheeseman, J. Montgomery, J. A., T. Vreven, K. N. Kudin, J. C. Burant, J. M. Millam, S. S. Iyengar, J. Tomasi, V. Barone, B. Mennucci, M. Cossi, G. Scalmani, N. Rega, G. A. Petersson, H. Nakatsuji, M. Hada, M. Ehara, K. Toyota, R. Fukuda, J. Hasegawa, M. Ishida, T. Nakajima, Y. Honda, O. Kitao, H. Nakai, M. Klene, X. Li, J. E. Knox, H. P. Hratchian, J. B. Cross, V. Bakken, C. Adamo, J. Jaramillo, R. Gomperts, R. E. Stratmann, O. Yazyev, A. J. Austin, R. Cammi, C. Pomelli, J. W. Ochterski, P. Y. Ayala, K. Morokuma, G. A. Voth, P. Salvador, J. J. Dannenberg, V. G. Zakrzewski, S. Dapprich, A. D. Daniels, M. C. Strain, O. Farkas, D. K. Malick, A. D. Rabuck, K. Raghavachari, J. B. Foresman, J. V. Ortiz, Q. Cui, A. G. Baboul, S. Clifford, J. Cioslowski, B. B. Stefanov, G. Liu, A. Liashenko, P. Piskorz, I. Komaromi, R. L. Martin, D. J. Fox, T. Keith, M. A. Al-Laham, C. Y. Peng, A. Nanayakkara, M. Challacombe, P. M. W. Gill, B. Johnson, W. Chen, M. W. Wong, C. Gonzalez and J. A. Pople, *Gaussian 03, Revision D.01*, (2004) Gaussian, Inc., Wallingford.
- S4. D. Andrae, U. Haeussermann, M. Dolg, H. Stoll and H. Preuss, *Theor. Chim. Acta*, 1990, **77**, 123-141.
- S5. J. Tomasi and M. Persico, *Chem. Rev.*, 1994, **94**, 2027-2094.
- S6. V. Barone and M. Cossi, *J. Phys. Chem. A*, 1998, **102**, 1995-2001.

3.3. Maltol-derived ruthenium-cymene complexes with tumor inhibiting properties: The impact of ligand-metal bond stability on the anticancer activity

Chemistry – A European Journal, submitted

Graphical Abstract



Organometallic Ru–arene compounds bearing a maltol ligand were shown to be minimally active in vitro anticancer assays, presumably due to the formation of dimeric Ru(II) species in aqueous solutions, whereas thiopyrone compounds are reasonably active. Studies on the reactivity to amino acids demonstrate different reactivity and stability of the pyrone and thiopyrone complexes, which probably renders them active against human tumor cells

Maltol-derived ruthenium-cymene complexes with tumor inhibiting properties: The impact of ligand-metal bond stability on the anticancer activity

Wolfgang Kandioller^[a], Christian G. Hartinger*^[a], Alexey A. Nazarov*^[a,b], Caroline Bartel^[a], Matthias Skocic^[a], Michael A. Jakupec^[a], Vladimir B. Arion^[a] and Bernhard K. Keppler^[a]

Abstract: Organometallic Ru–arene compounds bearing a maltol ligand were shown to be nearly inactive in *in vitro* anticancer assays, presumably due to the formation of dimeric Ru^{II} species in aqueous solutions. In an attempt to stabilize such complexes, [Ru(η^6 -*p*-cymene)(XY)Cl] (XY = pyrones or thiopyrones) compounds with different substitution pattern of the (thio)pyrone ligands were synthesized, characterized spectroscopically, structurally and in

terms of their aquation behavior as well as their tumor-inhibiting potency. The aquation behavior of pyrone systems with electron-donating substituents and of thiopyrone complexes was found to be significantly different from that of the maltol-type complex reported earlier. However, the formation of the dimer can be excluded as the primary reason for the inactivity of the complex since some of the stable compounds are not active in cancer model systems

either. In contrast, studies on the reactivity to amino acids demonstrate different reactivity of the pyrone and thiopyrone complexes, and the higher stability of the latter probably renders them active against human tumor cells.

Keywords: Amino acids · Antitumor agents · Pyrone ligand · Ruthenium–arene complexes · Thiopyrone ligand

Introduction

Metal complexes play an important role in the treatment of cancer. One of the most important and widely used compound is cisplatin which was developed by Rosenberg in the 1960ies.^[1] Due to severe side effects, activity in a limited spectrum of tumors and the occurrence of resistance,^[2] the development of new antitumor agents with other metal ions as central atom is an area of intensive research.^[1,3-7] Ruthenium complexes have shown the most promising results in preclinical and clinical experiments.^[8-11] NAMI-A and KP1019 are in the most advanced stage of development and are currently undergoing clinical trials (Figure 1).^[8-10] The low general toxicity of these complexes reflects a more selective activity in tumor tissue as compared to platinum-based compounds, mediated by transport into the cell in the form of protein adducts and reduction in the tumor.^[12-16]

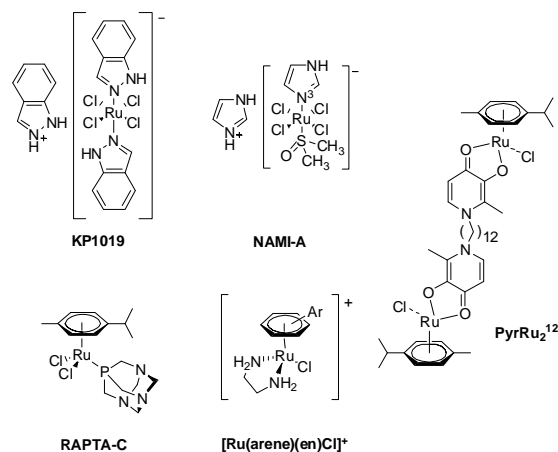


Figure 1. Structures of the investigational anticancer compounds KP1019, NAMI-A, [Ru(η^6 -*p*-cymene)(pta)Cl₂] (RAPTA-C), [Ru(arene)(acac)Cl]⁺, [Ru(arene)(en)Cl]⁺ and the dinuclear compound PyrRu₂¹².

More recently the potential of organometallic Ru^{II}–arene compounds as anticancer agents has been recognized.^[4,7,11,17] This compound type bears an arene ligand which facilitates the diffusion through the cell membrane (and thereby enhances cellular uptake). The coordination sphere is filled with mono- or bidentate ligands, controlling the reactivity to biomolecules, and these moieties also appear to be determinants for the modes of action.^[7,14,18-22]

[a] W. Kandioller, Dr. C. G. Hartinger, Dr. A. A. Nazarov, C. Bartel, M. Skocic, Dr. M. A. Jakupec, Prof. V. B. Arion, Prof. B. K. Keppler
Institute of Inorganic Chemistry, University of Vienna
Währinger Str. 42, Vienna, Austria
Fax: (+) 43-1-4277-9526
E-mail: christian.hartinger@univie.ac.at, alex.nazarov@univie.ac.at

[b] Dr. A. A. Nazarov
Institut des Sciences et Ingénierie Chimiques
Ecole Polytechnique Fédérale de Lausanne (EPFL)
CH-1015 Lausanne, Switzerland

Supporting information for this article is available on the WWW under <http://www.chemeurj.org/> or from the author.

RAPTA (containing the 1,3,5-triaza-7-phoshatricyclo[3.3.1.1]decane [pta] ligand) and Ru^{II}-(arene)(en) complexes (en = 1,2-diaminoethane) are the best studied ruthenium organometallics.^[4,11,23] The pta complexes have been shown to be, similarly to NAMI-A, active against metastasis, but inactive in *in vitro* cell assays,^[24,25] whereas the en complexes have potential as anticancer agents against primary tumors.^[26] Beside pta and en several other ligand systems have been studied in Ru-based organometallics, including moieties containing *O,O*, *N,O*, *N,N* and *S,O* donor sets.^[19,22,27-35] The nature of the donor atoms was shown to influence the *in vitro* anticancer activity significantly, and the low potency of some of the synthesized compounds appears to be related to the instability of the Ru–ligand interaction, causing the formation of dimeric Ru^{II} species, with the arene moiety remaining attached to the metal center. Recently, we have demonstrated that the replacement of the *O,O* donor set of maltol by *S,O* leads to significantly increased stability and the compounds are anticancer active in the low μM range,^[34] and this ligand type found application, *e.g.*, in the removal or supplementation of iron, or in imaging as contrast agents.^[36] However, a switch from the pyrone to a pyridone systems in the case of that particular ligand also afforded stable compounds in aqueous solution with promising anticancer activity.^[21,29,30,33]

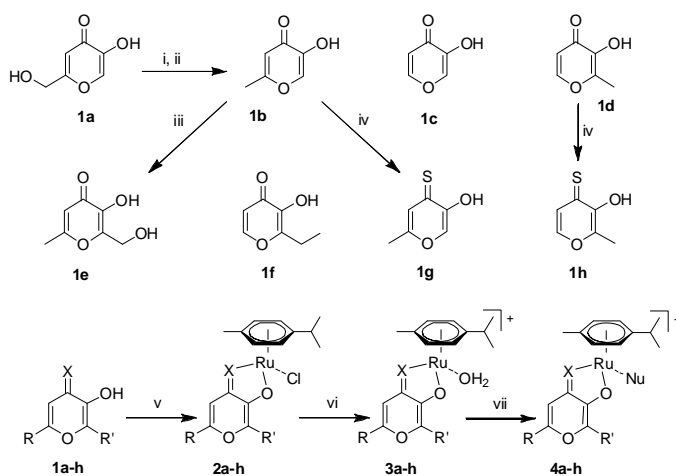
Herein, the synthesis and characterization of a series of (thio)pyrone derived Ru^{II}-cymene complexes is described and compared to recent results.^[34] The molecular structures of the complexes with kojic acid, allomaltol, pyromeconic acid and maltol were determined by single crystal X-ray diffraction analysis. The aquation behavior and the interactions with small biomolecules were investigated, and the cytotoxic activity in different human cancer cell lines was studied. The influence of the substitution pattern of the (thio)pyrone moiety on the stability of the complexes and the anticancer activity in human tumor cell lines is discussed.

Results and Discussion

Synthesis: The synthesis of the ligand **1b** (allomaltol) was achieved in two steps, starting from kojic acid **1a** by reaction with thionyl chloride, followed by a reductive step using Zn/HCl (60%; Scheme 1).^[37] Ligand **1e** was obtained by conversion of **1b** with formaldehyde under alkaline conditions (70%).^[37] The thiopyrones **1g** and **1d** were prepared by reaction of P₄S₁₀ with the corresponding pyrones **1b** and **1d** (40-60%).^[38] Ligands **1a–h** were converted with bis[dichlorido(*η*⁶-*p*-cymene)ruthenium(II)] under alkaline conditions into the respective Ru^{II} complexes **2a–h** in good yields (61–85%) (Scheme 1).^[39] The reaction was performed with a slight excess of ligand to facilitate the purification step.

All complexes were characterized by 1D and 2D NMR spectroscopy, mass spectrometry and elemental analysis. The influence of the solvent on the inversion of the Ru center is significant: In protic solvents, fast inversion of the Ru center was observed, which resulted in the formation of two doublets for the *p*-cymene ligand, whereas in CDCl₃, the aromatic protons are detected as four doublets. A similar behavior was also observed in the ¹³C NMR spectra, which is in agreement with related Ru^{II}-arene complexes.^[39] In the ¹H NMR spectrum of **2e** in CDCl₃, two doublets with a coupling constant of 17 Hz were observed,

which were assigned to the protons of the CH₂ group (see Supporting Information). This geminal splitting can be explained by the formation of an intramolecular hydrogen bond between the hydroxymethyl moiety and the coordinated O3 atom. ESI mass spectra were recorded in methanol, and the predominant peak for the complexes **2a–h** was assigned to [M–Cl]⁺ ions (good agreement of the observed and theoretical isotopic pattern).



Scheme 1. Synthesis of ligands i) SOCl₂; ii) Zn/HCl; iii) formaldehyde, NaOH; iv) P₄S₁₀, dioxane; v) [Ru(*η*⁶-*p*-cymene)Cl₂]₂, NaOMe; vi) H₂O; vii) nucleophiles (Nu) such as 5'-GMP or amino acids.

Molecular structure determination: Single crystals suitable for X-ray diffraction analysis were obtained for the Ru^{II} complexes **2a**, **2c** and **2d** by recrystallization from ethyl acetate (Figure 2). The compounds crystallized in the monoclinic *P*2₁/*n* (**2a**), *P*2₁/*c* (**2d**) and triclinic *P*-1 (**2c**) space groups, respectively. All complexes have piano-stool configuration. The pyrone ligands act as bidentate and form a five-membered chelate cycle with an envelope-like conformation on binding to ruthenium. The Ru–Cl bond lengths are in the same range as those of recently published compounds [2.4200(11)–2.4273(8) Å].^[29,32] The largest torsion angle Ru–O1–C–C (12°) was found for **2c**.

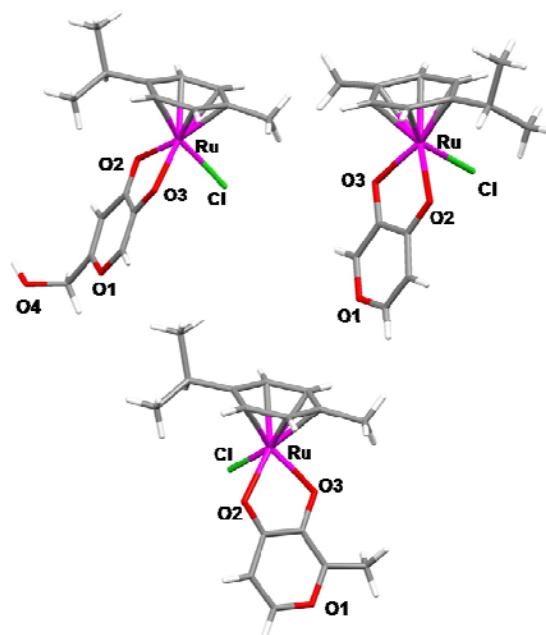


Figure 2. Molecular structures of the Ru^{II} complexes **2a** (top left), **2c** (top right) and **2d** (bottom).

In contrast to a crystal structure report for **2d**,^[19] the two Ru–O bonds in **2a**, **2c** and **2d** were found to be slightly different, and the Ru–O1 distance is marginally shorter than the Ru–O2 bond. The largest difference was found for **2d**, with bond lengths of 2.078(2) (Ru–O1) and 2.117(2) Å (Ru–O2). For complexes **2c** and **2d** short contacts between two independent molecules were found. The H2 of the arene and one proton of the isopropyl group have short contacts to the O3 of the neighboring molecule. Intermolecular hydrogen bonds between the hydroxymethyl group and the O3 of the neighboring molecule were observed for **2a**. The R- and the S-stereoisomers of **2a** are connected in alternating manner *via* hydrogen bonds, forming a syndiotactic chain (Figure 2). The distance between the O3 of the R-enantiomer to the –OH group of the S-isomer is 1.969 Å, whereas the length of the hydrogen bond of the S-O3 to the R-OH is 1.931 Å. Connections between adjacent chains *via* short contacts of the isopropyl protons to O1 (2.527 Å) and *p*-cymene (2.983 Å) are responsible for the observed layer-type structure (see Supporting Information).

Aquation: Aquation and stability in water were investigated by means of ¹H NMR spectroscopy. Due to the higher lipophilicity of the thiopyrone complexes, all experiments for **2g** and **2h** were performed in 10% [D₆]DMSO/D₂O solutions. No coordination of [D₆]DMSO was observed in preliminary experiments, although small amounts of degradation products were detected after 18 h in this solvent mixture.

The complexes **2a–h** hydrolyze in aqueous solution within seconds to the charged complexes **3a–h** by exchange of the chlorido ligand by a neutral water molecule, and identical NMR spectra were obtained after induced release of the chlorido ligands by equimolar amounts of AgNO₃. NMR experiments with **2b** in physiological NaCl solution (100 mM), which should shift the aquation equilibrium back from **3b** to **2b**,^[40] showed no influence on the aquation process. For complexes **3a–d**, the formation of the identical dimeric hydrolysis side product [Ru₂(cym)₂(OH)₃]⁺ was observed (detected in positive ion mode ESI mass and ¹H NMR spectra), which is thought to be responsible for the inactivity of the compound type against cancer cells.^[19] The amount of formed side product depends on the concentration, the incubation time and the pH value of the solution. In contrast to **3a–d**, compounds **3e–h** are stable for more than 24 h in aqueous solution.

In order to stabilize the complexes against hydrolysis and the concomitant dimer formation, **2a–d** were reacted with imidazole in aqueous solution to form the corresponding positively charged complex. The reactions proceeded very quickly (within seconds), and the resulting imidazole complexes did not show the formation of a dimeric species within 18 h (Figure 3).

The p*K_a* values of **3a–f** were determined by stepwise deprotonation of the aqua species with NaOD. The chemical shifts of the *p*-cymene protons were monitored by ¹H NMR spectroscopy and plotted against the pH value of the solution to give the p*K_a* values (corrected as reported recently,^[32] see Table 1 and Supporting Information). The p*K_a* values of the thiopyrone complexes **3g** and **3h** were not detectable due to precipitation of the complexes at pH 10.0; however, the theoretical values obtained by DFT calculation are 12.8 and 12.5 for **3g** and **3h**, respectively. The p*K_a* values for **3a–f** are

comparable to those published recently for other pyrone- and pyridone-based Ru^{II}-arene complexes (8.99–9.64).^[19,32,33] The p*K_a* values implicate that **3a–h** are present as reactive aqua species under physiological conditions.

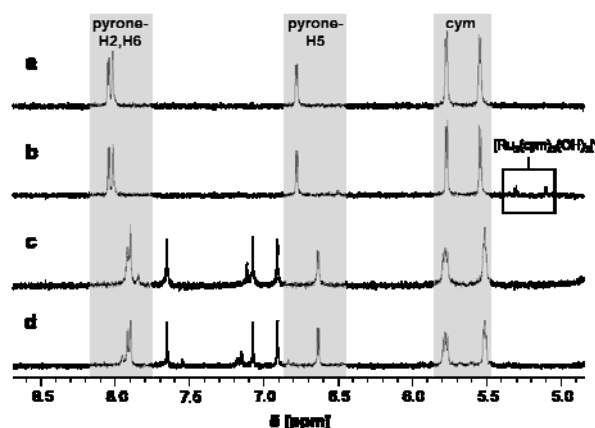


Figure 3. ¹H NMR spectra of the reaction of **3c** with imidazole. (a) **3c** in D₂O after 5 min, (b) **3c** after 18 h, (c) imidazole/**3c** reaction mixture after 5 min (molar ratio 1 : 1) and (d) imidazole/**3c** reaction mixture after 18 h.

Cytotoxicity: Cytotoxic activity was assayed in the human tumor cell lines SW480 (colon carcinoma), CH1 (ovarian carcinoma) and A549 (non-small lung carcinoma) by means of the colorimetric MTT assay (Table 1). It should be noted that the chlorido complexes **2a–h** applied to the medium are rapidly converted into the corresponding aqua complexes **3a–h** prior to contact with cells. The recently reported maltol complex **2d** does not exhibit activity in human tumor cells to a relevant extent. This behavior has been thought to be related to the formation of the inactive [Ru₂(*p*-cymene)₂(OH)₃]⁺ in aqueous solution.^[19,29] Similarly, the structurally related compounds **2a–c** show no relevant cytotoxic activity in the tested cell lines.

Table 1. p*K_a* values of **3a–h** and IC₅₀ values of **2a–h** (96 h exposure).

Complex	p <i>K_a</i>	IC ₅₀ [μM]		
		CH1	SW480	A549
a	8.93 ± 0.02	234 ± 21	429 ± 10	n.d.
b ^[34]	9.01 ± 0.03	239 ± 22	359 ± 119	518 ± 65
c	8.91 ± 0.02	112 ± 50	206 ± 94	490 ± 43
d ^[34]	9.23 ^[19]	81 ± 14	159 ± 41	482 ± 20
e	8.92 ± 0.02	242 ± 39	457 ± 33	510 ± 29
f	9.12 ± 0.04	81 ± 8	165 ± 31	389 ± 37
g ^[34]	>10 (12.8 ^a)	35 ± 8	20 ± 7	n.d.
h ^[34]	>10 (12.5 ^a)	13 ± 4	5.1 ± 0.5	n.d.

^a obtained by DFT calculation.

In contrast to **2a–d**, **2e–h** do not form such dimeric species. However, the *in vitro* activity of **2e** and **2f** was in a similar dimension as that of **2a–d**. Switching from pyrone to the analogous thiopyrone compounds **2g** and **2h** results in IC₅₀ values in the low μM range. Notably these compounds are more active in the SW480 cell line than in the otherwise more chemosensitive CH1 cells. This data set suggests that dimer formation is not responsible for the inactivity of **2a–f** (Table 1).

Reaction with small biomolecules: The interactions of the aqua species **3a–h** with small biomolecules, like the DNA model compound 5'-GMP and amino acids, were investigated by ¹H NMR spectroscopy.

The reaction of 5'-GMP can easily be monitored in ¹H NMR spectroscopy due to the shift of the N7 atom of 5'-GMP from 8.1 to approximately 7.9.^[41] The reaction was completed within seconds, and the formed adducts were stable in solution for more than 18 h. Accordingly, DNA is a possible target for this kind of Ru^{II}-cymene complexes, as suggested for related organometallic ruthenium(II) compounds.^[19]

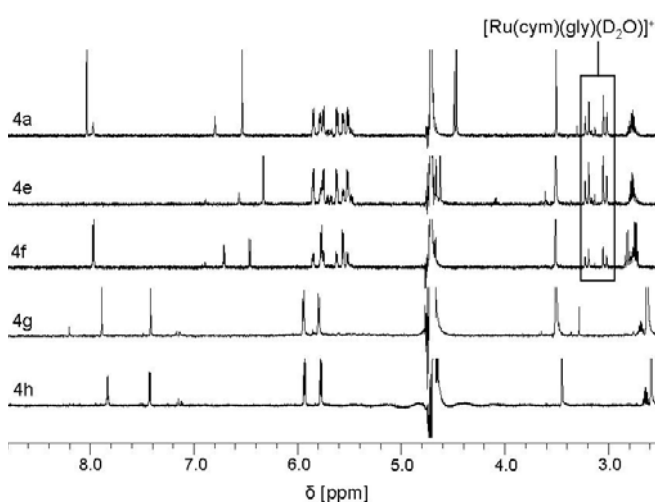


Figure 4. The reactions of **3a** and **3e–h** with glycine to **4a** and **4e–h** monitored by ¹H NMR spectroscopy for 18 h.

However, many drugs are administered intravenously, and amino acids and proteins are the first potential binding partners for the complexes in the bloodstream. Therefore, the reaction with the amino acids glycine, L-histidine, L-methionine and L-cysteine was investigated to gain insight into possible interactions with proteins and pharmacokinetic pathways. Complexes **3a–h** were treated with an equimolar amount of the respective amino acid, and the reaction progress was monitored for 18 h. The addition of L-cysteine led to fast decomposition of all complexes within minutes, most probably due to the strong *trans*-effect exhibited by the thiol functionality. The reactions of the pyrone-derived complexes **3a–f** with L-methionine, L-histidine and glycine to give **4a–f** differ significantly from those of the thiopyrone complexes **3g** and **3h**. All compounds reacted immediately with 1 eq L-methionine by replacing the aqua ligand with the amino acid (bound *via* the thioether moiety; see below). In the case of **3a–f**, the pyrone ligands **1a–f** were cleaved off quantitatively by the amino acid within 18 h. In contrast, **4g** and **4h** were stable in solution over the analysis time and no free ligands were detected. Similar results were obtained for the

reaction with L-histidine. All Ru(II) centers coordinated to the amino acid at a ratio of 1 : 1 *via* the N1 or N3 atoms of the imidazole moiety. As in the case with L-Met, the pyrone ligands **1a–f** were released upon coordination of the amino acid, whereas for **3g** and **3h** stable species were obtained. The reaction of glycine with **3a–h** was significantly slower than with the other investigated amino acids: after 18 h incubation time, the ¹H NMR spectra of reaction mixtures showed the formation of two doublets at approximately 3.1 ppm with a geminal coupling of 17 Hz (Figure 4). Those signals were assigned to the CH₂ group of glycine which acts as a chelating ligand and is coordinated *via* the amino and the carboxylic group to the Ru(II) center to form a five-membered ring structure. No adducts of **3g** and **3h** with glycine were observed, probably due to the inability of bidentate coordination of the amino acid. This also demonstrates the higher stability of the thiopyrone complexes.

Notably, no ruthenium dimer signals (at approximately 5.0 and 5.5 ppm) were observed in the NMR experiments within 18 h, when amino acids were present. The high reactivity to amino acids and the prevention of the formation of dimeric species by coordination to amino acids make it unlikely that the dimerization is the reason for the anticancer inactivity of the maltol complex and the related pyrone-based compounds. In contrast, the slower degradation in presence of amino acids might allow the thiopyrone complexes to enter the cells to a higher degree in their unmodified form.

In order to characterize the coordination compound obtained upon reaction of **3c** with L-methionine by NMR spectroscopy, **3c** was reacted with an equimolar amount of the L-Met analogous *Se*-methyl-L-selenocysteine. ¹H, ¹³C and ⁷⁷Se NMR spectra were recorded over a period of 18 h. The selenium signal of *Se*-methyl-L-selenocysteine at -419 ppm vanished within 10 min after addition of **3c**, and two new signals at -283 and -265 ppm appeared (Figure 5 and Supporting Information). The signal at -283 ppm disappears over time, probably due to completion of the *N,Se*-chelation to the Ru^{II} center (Figure 5, C). The ¹³C NMR spectrum contained after 18 h signals at 176.3 ppm, assignable to the carbonyl functionality of the free pyrone, and at 180.5 ppm, which corresponds to the uncoordinated carboxylate of the amino acid. Therefore it is proposed that the amino acid binds in a bidentate fashion *via* Se and N to the Ru^{II} center under release of the pyrone ligand.

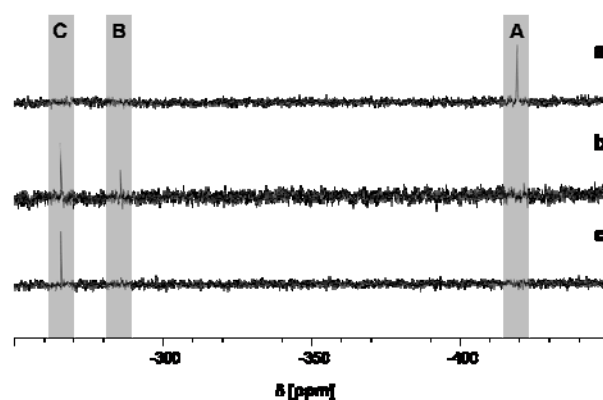


Figure 5. Time course of the reaction of *Se*-methyl-L-selenocysteine (A) with **3c** followed by ⁷⁷Se NMR spectroscopy. (a) *Se*-methyl-L-selenocysteine, (b) *Se*-methyl-L-selenocysteine/**3c** reaction mixture after 5 min and (c) after 18 h to form the intermediate [Ru(cym)(*Se*-methyl-L-selenocysteine-κ*Se*)(1c)] (B) and eventually [Ru(cym)(*Se*-methyl-L-selenocysteine-κ²*N,Se*)(D₂O)] (C).

In an attempt to overcome the rapid decomposition of **3g** and **3h** in the presence of L-cysteine, the chlorido ligands in the Ru^{II} complexes were exchanged by L-histidine *in situ*. The new compounds were, similarly to the reactions with imidazole, significantly more stable under the applied conditions, and no degradation products were observed in the ¹H NMR spectra after addition of an equimolar amount of L-cysteine (monitored for 18 h).

Conclusion

Biorganometallic chemistry is an emerging topic of research, and especially the use of Ru–arene compounds as anticancer agents appears promising. The Ru–arene complex with the *O,O*-bound maltol ligand was shown to be inactive in *in vitro* anticancer assays. The inactivity of the compound was assumed to be related to the formation of dimeric Ru^{II} species in aqueous solutions.^[19] In contrast, the analogous thiomaltol complexes exhibit anticancer activity in the low μM range and are not prone to the dimer formation.^[34] The formation of the dimeric species can also be inhibited by modification of the substitution pattern of the pyrone scaffold. The introduction of electron-donating groups leads to compounds with higher stability. However, these compounds were found to be also inactive *in vitro*, demonstrating that the dimer formation is not the main factor for the inactivity of the compound type. The aquation of the Ru center appears to be a prerequisite for the release of the pyrone ligands, and replacement of the chlorido ligand by imidazole was shown to be an effective additional option to obtain Ru^{II}–(arene)(pyrone) complexes stable in aqueous solutions.

In order to gain deeper insight into the chemical behavior of these compounds, reactions with the amino acids Gly, L-His, L-Met and L-Cys were followed by NMR spectroscopy. These studies revealed a significantly higher stability of the thiopyrone complexes. This property gives them more time to be taken up into the tumor cells, whereas the pyrone complexes decompose to compound mixtures involving amino acid coordination. It is assumed that *N,O* and *S,O* chelates are thermodynamically preferred over the *O,O* coordination of pyrone ligands, causing the release of the pyrone ligand if appropriate molecules are present, as is the case in a biological environment.

Experimental Section

All solvents were dried and distilled prior to use.^[42] Ruthenium(III) chloride (Johnson Matthey), kojic acid **1a** (Fluka), maltol **1d** (Aldrich), ethylmaltol **1f** (Aldrich), formaldehyde solution (Aldrich), P₄S₁₀ (Aldrich) and sodium methoxide (Aldrich) were purchased and used without further purification. Bis[dichlorido(*η*⁶-*p*-cymene)ruthenium(II)], 2-chloromethyl-5-hydroxypyran-4(*1H*)-one (chlorokojic acid), 5-hydroxy-2-methyl-pyran-4(*1H*)-one (**1b**), 3-hydroxy-pyran-4(*1H*)-one (**1c**), 2-hydroxymethyl-3-hydroxy-6-methyl-pyran-4(*1H*)-one (**1e**), 5-hydroxy-2-methyl-pyran-4(*1H*)-thione (**1g**) and 3-hydroxy-2-methyl-pyran-4(*1H*)-thione (**1h**) were synthesized as described elsewhere.^[37,38] Melting points were determined with a Büchi B-540 apparatus and are uncorrected. Elemental analyses were carried out with a Perkin Elmer 2400 CHN Elemental Analyzer at the Microanalytical Laboratory of the University of Vienna. NMR spectra were recorded at 25 °C using a Bruker FT-NMR spectrometer Avance IIITM 500 MHz at 500.10 MHz (¹H), 125.75 MHz (¹³C), 202.44 MHz (³¹P) and 95.38 MHz (⁷⁷Se, referenced to diphenyl diselenide) in [D₆]DMSO, D₂O or CDCl₃. The 2D NMR spectra were measured in a gradient-enhanced mode. An esquire₃₀₀₀ ion trap mass spectrometer (Bruker Daltonics, Bremen, Germany), equipped with an orthogonal ESI ion source, was used for MS measurements. The solutions were introduced *via* flow injection using a Cole-Parmer 74900 single-syringe infusion pump (Vernon Hills, IL).

X-ray diffraction measurements were performed with single crystals of **2a–d** on a Bruker X8 APEXII CCD diffractometer at 100 K. The single crystals were positioned at 40 mm from the detector and measured under the following conditions: (**2a**) 2710 frames for 5 sec over 2°, (**2b**) 622 frames for 20 sec over 2°, (**2c**) 1007 frames for 10 sec over 1° and (**2d**) 2173 frames for 4 sec over 1°. The data were processed using the SAINT software package.^[43] Crystal data, data collection parameters, and structure refinement details are given in Table S1–S4 (Supporting Information). The structures were solved by direct methods and refined by full-matrix least-squares techniques. Non-hydrogen atoms were refined with anisotropic displacement parameters. H atoms were inserted at calculated positions and refined with a riding model. The following computer programs were used: structure solution, SHELXS-97;^[44] refinement, SHELXL-97;^[45] molecular diagrams, ORTEP-3;^[46] computer, Pentium IV; scattering factors.^[47] Crystallographic data for the structural analysis has been deposited with the Cambridge Crystallographic Data Centre, CCDC No. 739426 for **2a**, CCDC No. 739427 for **2c**, CCDC No. 739425 for **2d**. These data can be obtained free of charge from The Cambridge Crystallographic Data Centre via www.ccdc.cam.ac.uk/data_request/cif.

General procedure for the synthesis of the ruthenium(II)(*η*⁶-*p*-cymene) complexes: Ligand (1 eq) and sodium methoxide were dissolved in methanol and stirred for 5 min under inert atmosphere (clear solution). A solution of [Ru(*η*⁶-*p*-cymene)Cl₂]₂ in MeOH/CH₂Cl₂ (1 : 1) was added, and the reaction mixture was stirred for 5–18 h. The reaction mixture was concentrated under reduced pressure, and the residue was extracted with CH₂Cl₂. The combined organic layers were filtered, and the solvent was removed. The crude product was purified by recrystallization.

Chlorido[2-hydroxymethyl-5-(oxo-κO)-4-(1H)-pyronato-κO⁴](*η*⁶-*p*-cymene)-ruthenium(II) (2a**):** The reaction was performed according to the general complexation protocol, using **1a** (113.2 mg, 0.73 mmol, 1 eq), NaOMe (43 mg, 0.8 mmol, 1.1 eq) and [Ru(*η*⁶-*p*-cymene)Cl₂]₂ (200 mg, 0.33 mmol, 0.45 eq). The crude product was recrystallized from acetone/*n*-hexane, affording an orange powder (200 mg, 67%). Single crystals were grown from ethyl acetate, suitable for X-ray diffraction analysis. Mp: > 180 °C (decomp.); ¹H NMR (500.10 MHz, CDCl₃): δ = 1.31 (d, ³J(H,H) = 7 Hz, 6H, CH_{3,Cym}), 2.29 (s, 3H, CH_{3,Cym}), 2.90 (m, 1H, CH_{2,Cym}), 3.83 (bs, 1H, OH), 4.40 (d, ²J(H,H) = 17 Hz 1H, CH₂), 4.46 (d, ²J(H,H) = 17 Hz 1H, CH₂), 5.30 (dd, ³J(H,H) = 5 Hz, ³J(H,H) = 5 Hz, 2H, H3/H5_{Cym}), 5.53 (dd, ³J(H,H) = 5 Hz, ³J(H,H) = 5 Hz, 2H, H2/H6_{Cym}), 6.63 (s, 1H, H3), 7.65 (s, 1H, H6); ¹³C NMR (125.75 MHz, CDCl₃): δ: 18.6 (CH_{3,Cym}), 22.3 (CH_{3,Cym}), 31.1 (CH_{2,Cym}), 60.7 (CH₂), 78.0 (C3/C5_{Cym}), 79.6 (C2/C6_{Cym}), 95.6 (C4_{Cym}), 100.1 (C1_{Cym}), 107.5 (C3), 141.1 (C6), 159.3 (C2), 167.9 (C5), 185.7 (C4); elemental analysis calcd for C₁₆H₁₉ClO₄Ru: C 46.66 H 4.65; found C 46.43 H 4.56.

Chlorido[2-methyl-5-(oxo-κO)-4-(1H)-pyronato-κO⁴](*η*⁶-*p*-cymene)-ruthenium(II) (2b**):** The reaction was performed according to the general complexation procedure, using **1b** (98 mg, 0.73 mmol, 1 eq), NaOMe (43 mg, 0.8 mmol, 1.1 eq) and [Ru(*η*⁶-*p*-cymene)Cl₂]₂ (200 mg, 0.33 mmol, 0.45 eq). The crude product was recrystallized from MeOH/*n*-hexane, affording a deep red crystalline solid (207 mg, 73%). Single crystals were grown from ethyl acetate, suitable for X-ray diffraction analysis. Mp: > 200 °C (decomp.); ¹H NMR (500.10 MHz, CDCl₃): δ = 1.33 (d, ³J(H,H) = 7 Hz, 6H, CH_{3,Cym}), 2.26 (s, 3H, CH₃), 2.32 (s, 3H, CH_{3,Cym}), 2.93 (m, 1H, CH_{2,Cym}), 5.32 (dd, ³J(H,H) = 5 Hz, ³J(H,H) = 5 Hz, 2H, H3/H5_{Cym}), 5.53 (dd, ³J(H,H) = 5 Hz, ³J(H,H) = 5 Hz, 2H, H2/H6_{Cym}), 6.34 (s, 1H, H3), 7.66 (s, 1H, H6); ¹³C NMR (125.75 MHz, CDCl₃): δ = 18.6 (CH_{3,Cym}), 19.8 (CH₃), 22.3 (CH_{3,Cym}), 31.1 (CH_{2,Cym}), 78.8 (C3/C5_{Cym}), 79.8 (C2/C6_{Cym}), 95.6 (C4_{Cym}), 100.1 (C1_{Cym}), 109.6 (C3), 141.1 (C6), 159.3 (C2), 165.2 (C5), 185.7 (C4); elemental analysis calcd (%) for C₁₆H₁₉ClO₃Ru·0.25 H₂O: C 48.00, H 4.91 found: C 47.94, H 4.76.

Chlorido[3-(oxo-κO)-4-(1H)-pyronato-κO⁴](*η*⁶-*p*-cymene)ruthenium(II) (2c**):** The reaction was performed according to the general complexation procedure, using pyroneconic acid (81 mg, 0.72 mmol, 1 eq), NaOMe (43 mg, 0.8 mmol, 1.1 eq) [Ru(*η*⁶-*p*-cymene)Cl₂]₂ (200 mg, 0.326 mmol, 0.45 eq). The crude product was recrystallized from ethyl acetate/*n*-hexane, affording a deep red crystalline solid (202 mg, 73%). Single crystals were grown from ethyl acetate, suitable for X-ray diffraction analysis. Mp: > 200 °C (decomp.); ¹H NMR (500.10 MHz, CDCl₃): δ = 1.34 (d, ³J(H,H) = 7 Hz, 6H, CH_{3,Cym}), 2.32 (s, 3H, CH_{3,Cym}), 2.90–2.96 (m, 1H, CH_{2,Cym}), 5.32 (dd, ³J(H,H) = 5 Hz, ³J(H,H) = 5 Hz, 2H, H3/H5_{Cym}); 5.55 (dd, ³J(H,H) = 5 Hz, ³J(H,H) = 5 Hz, 2H, H2/H6_{Cym}), 6.57 (d, ³J(H,H) = 7 Hz, 1H, H5), 7.66 (d, ³J(H,H) = 7 Hz, 1H, H6), 7.77 (s, 1H, H2); ¹³C NMR (125.75 MHz, CDCl₃): δ = 18.6 (CH_{3,Cym}), 22.3 (CH_{2,Cym}), 31.1 (CH_{3,Cym}), 76.9 (C3/C5_{Cym}), 79.6 (C2/C6_{Cym}), 95.6 (C4_{Cym}), 100.1 (C1_{Cym}), 111.4 (C5), 142.6 (C2), 153.8 (C6), 161.0 (C3), 185.3 (C4); elemental analysis calcd (%) for C₁₅H₁₇ClO₃Ru·0.5 H₂O: C 46.10, H 4.64; found C 45.92, H 4.37.

Chlorido[2-methyl-3-(oxo-κO)-4-(1H)-pyronato-κO⁴](*η*⁶-*p*-cymene)-ruthenium(II) (2d**):** The reaction was performed according to the general complexation procedure, using **1d** (98 mg, 0.73 mmol, 1 eq), NaOMe (43 mg,

0.8 mmol, 1.1 eq) and $[\text{Ru}(\eta^6\text{-}p\text{-cymene})\text{Cl}_2]_2$ (200 mg, 0.33 mmol, 0.45 eq). The crude product was recrystallized from ethyl acetate/*n*-hexane, affording a deep red crystalline solid (164 mg, 64%). Single crystals were grown from ethyl acetate, suitable for X-ray diffraction analysis. Mp: > 200 °C (decomp.); ^1H NMR (500.10 MHz, CDCl_3): δ = 1.32 (d, $^3J(\text{H,H})$ = 7 Hz, 6H, CH_3 , C_{Cym}), 2.32 (s, 3H, CH_3), 2.41 (s, 3H, CH_3), 2.91 (m, 1H, CH_{Cym}), 5.30 (dd, $^3J(\text{H,H})$ = 6 Hz, $^2J(\text{H,H})$ = 6 Hz, 2H, $\text{H}_3/\text{H}_{5\text{Cym}}$), 5.52 (dd, $^3J(\text{H,H})$ = 6 Hz, $^2J(\text{H,H})$ = 6 Hz, 2H, $\text{H}_2/\text{H}_{6\text{Cym}}$), 6.51 (d, $^3J(\text{H,H})$ = 5 Hz, 1H, H_5), 7.56 (d, $^3J(\text{H,H})$ = 5 Hz, 1H, H_6); ^{13}C NMR (125.75 MHz, CDCl_3): δ = 14.6 (CH_3), 18.6 (CH_3 , C_{Cym}), 22.3 (CH_3 , C_{Cym}), 31.1 (CH_{Cym}), 77.8 ($\text{C}_3/\text{C}_{5\text{Cym}}$), 79.6 ($\text{C}_2/\text{C}_{6\text{Cym}}$), 95.8 ($\text{C}_{4\text{Cym}}$), 99.7 ($\text{C}_{1\text{Cym}}$), 111.1 (C5), 151.7 (C6), 153.9 (C2), 157.8 (C3), 182.7 (C4); elemental analysis calcd (%) for $\text{C}_{16}\text{H}_{19}\text{ClO}_3\text{Ru}$: C 48.55, H 4.84; found C 48.45, H 4.63.

Chlorido[2-hydroxymethyl-6-methyl-3-(oxo- κO)-4-(1H-pyronato- κO^4)](η^6 -*p*-cymene)ruthenium(II) (2e): The reaction was performed according to general complexation protocol, using 2-hydroxymethyl-3-hydroxy-6-methyl-pyran-4(1H)-one **1e** (113 mg, 0.73 mmol, 1 eq), NaOMe (43 mg, 0.8 mmol, 1.1 eq) and $[\text{Ru}(\eta^6\text{-}p\text{-cymene})\text{Cl}_2]_2$ (200 mg, 0.33 mmol, 0.45 eq). The crude product was recrystallized from ethyl acetate/*n*-hexane, affording a red crystalline solid (250 mg, 81%). Mp: 193–196 °C (decomp.); ^1H NMR (500.10 MHz, CDCl_3): δ = 1.33 (d, $^3J(\text{H,H})$ = 7 Hz, 6H, CH_3 , C_{Cym}), 2.27 (s, 3H, CH_3 , C_{Cym}), 2.31 (s, 3H, CH_3 , C_{Cym}), 2.88 (m, 1H, CH_{Cym}), 4.05 (brs, 1H, OH), 4.63 (d, $^3J(\text{H,H})$ = 14 Hz, 1H, CH_2), 4.80 (d, $^3J(\text{H,H})$ = 14 Hz, 1H, CH_2), 5.30 (dd, $^3J(\text{H,H})$ = 4 Hz, $^2J(\text{H,H})$ = 4 Hz, 2H, $\text{H}_3/\text{H}_{5\text{Cym}}$), 5.53 (dd, $^3J(\text{H,H})$ = 6 Hz, $^2J(\text{H,H})$ = 6 Hz, 2H, $\text{H}_2/\text{H}_{6\text{Cym}}$), 6.31 (s, 1H, H_5); ^{13}C NMR (125.75 MHz, CDCl_3): δ = 19.1 (CH_3 , C_{Cym}), 20.3 (CH_3), 22.8 (CH_3 , C_{Cym}), 31.5 (CH_{Cym}), 59.4 (CH_2), 78.1 ($\text{C}_3/\text{C}_{5\text{Cym}}$), 80.3 ($\text{C}_2/\text{C}_{6\text{Cym}}$), 96.2 ($\text{C}_{4\text{Cym}}$), 100.0 ($\text{C}_{1\text{Cym}}$), 109.9 (C5), 152.1 (C6), 156.5 (C2), 164.5 (C3), 185.3 (C4); elemental analysis calcd (%) for $\text{C}_{17}\text{H}_{21}\text{ClO}_4\text{Ru}$: C 47.94, H 4.97; found C 48.00, H 5.02.

Chlorido[2-ethyl-3-(oxo- κO)-4-(1H-pyronato- κO^4)](η^6 -*p*-cymene)ruthenium(II) (2f): The reaction was performed according to the general complexation procedure, using ethylmaltol **1g** (102 mg, 0.72 mmol, 1 eq), NaOMe (43 mg, 0.8 mmol, 1.1 eq) and $[\text{Ru}(\eta^6\text{-}p\text{-cymene})\text{Cl}_2]_2$ (200 mg, 0.33 mmol, 0.45 eq). The crude product was dissolved in a minimum amount of CH_2Cl_2 and precipitated with diethyl ether, affording a deep red solid (181 mg, 61%). Mp: > 140 °C (decomp.); ^1H NMR (500.10 MHz, CDCl_3): δ = 1.22 (t, $^3J(\text{H,H})$ = 7 Hz, 3H, CH_3 , C_{Cym}), 1.32 (d, $^3J(\text{H,H})$ = 7 Hz, 6H, CH_3 , C_{Cym}), 2.34 (s, 3H, CH_3), 2.80 (m, 1H, CH_{Cym}), 2.91 (q, $^3J(\text{H,H})$ = 7 Hz, 2H, CH_2), 5.30 (dd, $^3J(\text{H,H})$ = 6 Hz, $^2J(\text{H,H})$ = 6 Hz, 2H, $\text{H}_3/\text{H}_{5\text{Cym}}$), 5.52 (dd, $^3J(\text{H,H})$ = 6 Hz, $^2J(\text{H,H})$ = 6 Hz, 2H, $\text{H}_2/\text{H}_{6\text{Cym}}$), 6.52 (d, $^3J(\text{H,H})$ = 5 Hz, 1H, H_5), 7.59 (d, $^3J(\text{H,H})$ = 5 Hz, 1H, H_6); ^{13}C NMR (125.75 MHz, CDCl_3): δ = 10.8 (CH_3), 18.6 (CH_3 , C_{Cym}), 21.6 (CH_2), 22.3 (CH_3 , C_{Cym}), 31.1 (CH_{Cym}), 77.8 ($\text{C}_3/\text{C}_{5\text{Cym}}$), 79.6 ($\text{C}_2/\text{C}_{6\text{Cym}}$), 95.9 ($\text{C}_{4\text{Cym}}$), 99.6 ($\text{C}_{1\text{Cym}}$), 111.0 (C5), 151.6 (C6), 157.3 (C2), 158.3 (C3), 182.9 (C4); elemental analysis calcd (%) for $\text{C}_{17}\text{H}_{21}\text{ClO}_3\text{Ru}$: C 49.81, H 5.16; found C 49.49, H 5.10.

Chlorido[2-methyl-5-(oxo- κO)-pyran-4(1H)-thionato- κS](η^6 -*p*-cymene)-ruthenium(II) (2g): The reaction was performed according to the general complexation protocol, using thiomaltol **1g** (103 mg, 0.72 mmol, 1 eq), NaOMe (43 mg, 0.8 mmol, 1.1 eq) and $[\text{Ru}(\eta^6\text{-}p\text{-cymene})\text{Cl}_2]_2$ (200 mg, 0.33 mmol, 0.45 eq). The crude product was recrystallized from ethyl acetate/*n*-hexane, affording a red crystalline solid (230 mg, 85%). Mp: > 190 °C (decomp.); ^1H NMR (500.10 MHz, CDCl_3): δ = 1.26 (d, $^3J(\text{H,H})$ = 7 Hz, 6H, CH_3), 2.23 (s, 3H, CH_3 , C_{Cym}), 2.27 (s, 3H, CH_3), 2.76 (m, 1H, CH_{Cym}), 5.51 (d, $^3J(\text{H,H})$ = 5 Hz, 2H, H_3'/H_5'), 5.71 (d, $^3J(\text{H,H})$ = 6 Hz, 2H, H_2'/H_6'), 7.09 (s, 1H, H_5), 7.87 (s, 1H, H_2); ^{13}C NMR (125.75 MHz, CDCl_3): δ = 18.6 (CH_3 , C_{Cym}), 19.0 (CH_3), 22.1 (CH_3 , C_{Cym}), 30.9 (CH_{Cym}), 80.5 ($\text{C}_3/\text{C}_{5\text{Cym}}$), 81.3 ($\text{C}_2/\text{C}_{6\text{Cym}}$), 99.5 ($\text{C}_{4\text{Cym}}$), 100.9 ($\text{C}_{1\text{Cym}}$), 119.4 (C3), 139.6 (C6), 157.1 (C2), 166.0 (C5), 187.0 (C4); elemental analysis calcd (%) for $\text{C}_{16}\text{H}_{19}\text{ClO}_2\text{RuS}$: C 46.65, H 4.65, S 7.78; found C 46.24, H 4.61, S 8.04.

Chlorido[2-methyl-3-(oxo- κO)-pyran-4(1H)-thionato- κS](η^6 -*p*-cymene)-ruthenium(II) (2h): The reaction was performed according to the general complexation protocol, using thiomaltol **1h** (103 mg, 0.72 mmol, 1 eq), NaOMe (43 mg, 0.8 mmol, 1.1 eq) and $[\text{Ru}(\eta^6\text{-}p\text{-cymene})\text{Cl}_2]_2$ (200 mg, 0.33 mmol, 0.45 eq). The crude product was recrystallized from ethyl acetate/*n*-hexane, affording a red crystalline solid (200 mg, 74%). Mp: > 190 °C (decomp.); ^1H NMR (500.10 MHz, CDCl_3): δ = 1.28 (d, $^3J(\text{H,H})$ = 7 Hz, 6H, CH_3 , C_{Cym}), 2.21 (s, 3H, CH_3 , C_{Cym}), 2.50 (s, 3H, CH_3), 2.76 (m, 1H, CH_{Cym}), 5.49 (brs, 2H, $\text{H}_3/\text{H}_{5\text{Cym}}$), 5.71 (brs, 2H, $\text{H}_2/\text{H}_{6\text{Cym}}$), 7.18 (d, $^3J(\text{H,H})$ = 5 Hz, 1H, H_5), 7.43 (d, $^3J(\text{H,H})$ = 5 Hz, 1H, H_6); ^{13}C NMR (125.75 MHz, CDCl_3): δ = 15.4 (CH_3), 18.4 (CH_3 , C_{Cym}), 22.1 (CH_3 , C_{Cym}), 31.0 (CH_{Cym}), 80.5 ($\text{C}_3/\text{C}_{5\text{Cym}}$), 81.3 ($\text{C}_2/\text{C}_{6\text{Cym}}$), 98.2 ($\text{C}_{4\text{Cym}}$), 100.0 ($\text{C}_{1\text{Cym}}$), 120.2 (C5), 143.9 (C6), 153.3 (C2), 165.4 (C3), 180.5 (C4); elemental analysis calcd (%) for $\text{C}_{16}\text{H}_{19}\text{ClO}_2\text{SRu}$: C 46.65, H 4.65, S 7.75; found C 47.03, H 4.57, S 7.67.

pK_a determination. For the pK_a value determination, **2a–f** were dissolved in D_2O and the pH of the solution in the NMR tube was determined with an Eco Scan pH6 pH meter equipped with a glass-micro combination pH electrode (Orion 9826BN) and calibrated with standard buffer solutions of pH 4.00, 7.00 and 10.00. The pH titration was performed by addition of NaOD (0.4–0.0004% in D_2O) to a DNO_3 -

acidified solution (0.4–0.0004% in D_2O). The observed shifts of the H_2/H_6 cymene protons in the ^1H NMR spectra were plotted against the pH value, and the obtained curves were fitted using the Henderson-Hasselbalch equation with Excel software (Microsoft® Office Excel 2003, SP3, Microsoft Corporation). The experimentally obtained pK_a^* values were corrected with equation 1,^[48] in order to convert the pK_a^* in D_2O to the corresponding pK_a values in aqueous solutions.

$$pK_a = 0.929 pK_a^* + 0.42 \quad (1)$$

Computational details. The full geometry optimization of all structures has been carried out at the DFT level of theory using Becke's three-parameter hybrid exchange functional^[49] in combination with the gradient-corrected correlation functional of Lee, Yang and Parr^[50] (B3LYP) with the help of the Gaussian-03^[51] program package. Symmetry operations were not applied for all structures. The geometry optimization was carried out using a quasi-relativistic Stuttgart pseudopotential described 28 core electrons and the appropriate contracted basis set (8s7p6d)/[6s5p3d]^[52] for the ruthenium atom and the 6-31G(d) basis set for other atoms. Then single-point calculations were performed in the basis of the found equilibrium geometries using the 6-31+G(d,p) basis set for non-metal atoms. The experimental X-ray structure of **2h**^[34] was chosen as the starting geometry for the optimizations. The Hessian matrix was calculated analytically for all optimized structures in order to prove the location of correct minima (no "imaginary" frequencies) and to estimate thermodynamic parameters, the latter were calculated at 25 °C.

Solvent effects were taken into account at the single-point calculations based on the gas-phase equilibrium geometries at the CPCM-B3LYP/6-31+G(d,p)/gas-B3LYP/6-31G(d) level of theory using the polarizable continuum model in the CPCM version^[53,54] with H_2O as a solvent and UAKS atomic radii. The Gibbs free energies in solution (G_s) were estimated by addition of the solvation energy δG_{solv} to gas-phase Gibbs free energies (G_g).

pK_a values have been calculated for the reaction $\text{HA}^+ + \text{H}_2\text{O} \rightarrow \text{A} + \text{H}_3\text{O}^+$ (HA^+ – cationic complexes **3'b**, **3'd**, **3'g** and **3'h**, A – corresponding neutral hydroxo-complexes **5'b**, **5'd**, **5'g** and **5'h**, 1 atm standard state) using equation 2.

$$pK_a = \frac{\Delta G_s}{2.303RT} - 1.74 \quad (2)$$

The vertical heterolytic bond energies in solution have been calculated at the CPCM-B3LYP/6-31+G(d,p)/gas-B3LYP/6-31G(d) level of theory.

Interaction with small biomolecules. Complexes **2a–h** (1–2 mg/ml) were dissolved in D_2O (containing 5% $[\text{D}_6]$ -DMSO for **2g** and **2h**), yielding the aqua species **3a–h**, titrated with 5'-GMP solution (10 mg/mL) in 50 μL steps, and the reaction was monitored by ^1H and ^{31}P NMR spectroscopy until unreacted 5'-GMP was detected.

For the investigation of the reactivity towards amino acids and imidazole, the aqua-complexes **3a–h** (1 mg/mL) were reacted with an equimolar amount of amino acid and the ^1H NMR spectra were recorded after 5 min and 18 h.

Cytotoxicity in cancer cell lines

Cell lines and culture conditions. CH1 cells originate from an ascites sample of a patient with a papillary cystadenocarcinoma of the ovary and were a generous gift from Lloyd R. Kelland, CRC Centre for Cancer Therapeutics, Institute of Cancer Research, Sutton, UK. SW480 (adenocarcinoma of the colon, human), and A549 (non-small cell lung cancer, human) cells were kindly provided by Brigitte Marian (Institute of Cancer Research, Department of Medicine I, Medical University of Vienna, Austria). All cell culture reagents were obtained from Sigma-Aldrich Austria. Cells were grown in 75 cm^2 culture flasks (Iwaki) as adherent monolayer cultures in Minimal Essential Medium (MEM) supplemented with 10% heat-inactivated fetal calf serum, 1 mM sodium pyruvate, 4 mM L-glutamine and 1% non-essential amino acids (100 \times). Cultures were maintained at 37 °C in a humidified atmosphere containing 95% air and 5% CO_2 .

MTT assay conditions. Cytotoxicity was determined by the colorimetric MTT (3-(4,5-dimethyl-2-thiazolyl)-2,5-diphenyl-2H-tetrazolium bromide, purchased from Fluka) microculture assay. For this purpose, cells were harvested from culture flasks by trypsinization and seeded in 100 μL aliquots into 96-well microculture plates (Iwaki). Cell densities of 1.5×10^3 cells/well (CH1), 2.5×10^3 cells/well (SW480) and 4×10^3 cells/well (A549) were chosen in order to ensure exponential growth of untreated controls throughout the experiment. Cells were allowed to settle and resume exponential growth in drug-free complete culture medium for 24 h. Stocks of the test compounds in DMSO were appropriately diluted in complete culture medium such that the maximum DMSO content did not exceed 1% (this procedure

yielded opaque but colloidal solutions from which no precipitates could be separated by centrifugation). These dilutions were added in 100 μL aliquots to the microcultures (if necessary due to limited solubility, the maximum concentration tested was added in 200 μL aliquots after removal of the pre-incubation medium), and cells were exposed to the test compounds for 96 hours. At the end of exposure, all media were replaced by 100 μL /well RPMI1640 culture medium (supplemented with 10% heat-inactivated fetal bovine serum) plus 20 μL /well MTT solution in phosphate-buffered saline (5 mg/ml). After incubation for 4 h, the supernatants were removed, and the formazan crystals formed by vital cells were dissolved in 150 μL DMSO per well. Optical densities at 550 nm were measured with a microplate reader (Tecan Spectra Classic), using a reference wavelength of 690 nm to correct for unspecific absorption. The quantity of vital cells was expressed in terms of T/C values by comparison to untreated control microcultures, and 50% inhibitory concentrations (IC_{50}) were calculated from concentration-effect curves by interpolation. Evaluation is based on means from at least three independent experiments, each comprising at least three replicates per concentration level.

Acknowledgements

We thank the Hochschuljubiläumstiftung Vienna, the Theodor-Körner-Fonds, COST D39 and the Austrian Science Fund (Schrodinger Fellowship J2613-N19 [C.G.H.] and project P18123-N11) for financial support and the computer center of the University of Vienna for computer time at the Linux-PC cluster Schroedinger III. We gratefully acknowledge Alexander Roller for collecting the X-ray diffraction data and Dr. Maxim L. Kuznetsov for the DFT calculations.

- [1] M. A. Jakupec, M. Galanski, V. B. Arion, C. G. Hartinger, B. K. Keppler, *Dalton Trans.* **2008**, 183-194.
- [2] P. Heffeter, U. Jungwirth, M. Jakupec, C. Hartinger, M. Galanski, L. Elbling, M. Micksche, B. Keppler, W. Berger, *Drug Res. Upd.* **2008**, *11*, 1-16.
- [3] M. J. Clarke, F. Zhu, D. R. Frasca, *Chem. Rev.* **1999**, *99*, 2511-2533.
- [4] W. H. Ang, P. J. Dyson, *Eur. J. Inorg. Chem.* **2006**, 4003-4018.
- [5] P. J. Dyson, G. Sava, *Dalton Trans.* **2006**, 1929-1933.
- [6] K. Strohfeldt, M. Tacke, *Chem. Soc. Rev.* **2008**, *37*, 1174-1187.
- [7] C. G. Hartinger, P. J. Dyson, *Chem. Soc. Rev.* **2009**, *38*, 391-401.
- [8] J. M. Rademaker-Lakhai, D. Van Den Bongard, D. Pluim, J. H. Beijnen, J. H. M. Schellens, *Clin. Cancer Res.* **2004**, *10*, 3717-3727.
- [9] C. G. Hartinger, M. A. Jakupec, S. Zorbas-Seifried, M. Groessl, A. Egger, W. Berger, H. Zorbas, P. J. Dyson, B. K. Keppler, *Chem. Biodiversity* **2008**, *5*, 2140-2155.
- [10] C. G. Hartinger, S. Zorbas-Seifried, M. A. Jakupec, B. Kynast, H. Zorbas, B. K. Keppler, *J. Inorg. Biochem.* **2006**, *100*, 891-904.
- [11] A. F. A. Peacock, P. J. Sadler, *Chem. Asian J.* **2008**, *3*, 1890-1899.
- [12] M. Pongratz, P. Schluga, M. A. Jakupec, V. B. Arion, C. G. Hartinger, G. Allmaier, B. K. Keppler, *J. Anal. At. Spectrom.* **2004**, *19*, 46-51.
- [13] M. Sulyok, S. Hann, C. G. Hartinger, B. K. Keppler, G. Stingeder, G. Koellensperger, *J. Anal. At. Spectrom.* **2005**, *20*, 856-863.
- [14] P. Schluga, C. G. Hartinger, A. Egger, E. Reisner, M. Galanski, M. A. Jakupec, B. K. Keppler, *Dalton Trans.* **2006**, 1796-1802.
- [15] M. A. Jakupec, E. Reisner, A. Eichinger, M. Pongratz, V. B. Arion, M. Galanski, C. G. Hartinger, B. K. Keppler, *J. Med. Chem.* **2005**, *48*, 2831-2837.
- [16] M. Groessl, C. G. Hartinger, K. Polec-Pawlak, M. Jarosz, B. K. Keppler, *Electrophoresis* **2008**, *29*, 2224-2232.
- [17] G. Jaouen, Wiley-VCH, Weinheim, **2006**, p. 444.
- [18] C. S. Allardyce, P. J. Dyson, D. J. Ellis, S. L. Heath, *Chem. Commun.* **2001**, 1396-1397.
- [19] A. F. A. Peacock, M. Melchart, R. J. Deeth, A. Habtemariam, S. Parsons, P. J. Sadler, *Chem. Eur. J.* **2007**, *13*, 2601-2613.
- [20] H. Chen, J. A. Parkinson, S. Parsons, R. A. Coxall, R. O. Gould, P. J. Sadler, *J. Am. Chem. Soc.* **2002**, *124*, 3064-3082.
- [21] O. Nováková, A. A. Nazarov, C. G. Hartinger, B. K. Keppler, V. Brabec, *Biochem. Pharmacol.* **2009**, *77*, 364-374.
- [22] R. Fernandez, M. Melchart, A. Habtemariam, S. Parsons, P. J. Sadler, *Chem. Eur. J.* **2004**, *10*, 5173-5179.
- [23] P. J. Dyson, *Chimia* **2007**, *61*, 698-703.
- [24] C. Scolaro, A. Bergamo, L. Brescacin, R. Delfino, M. Cocchietto, G. Laurenczy, T. J. Geldbach, G. Sava, P. J. Dyson, *J. Med. Chem.* **2005**, *48*, 4161-4171.
- [25] S. Chatterjee, S. Kundu, A. Bhattacharyya, C. G. Hartinger, P. J. Dyson, *J. Biol. Inorg. Chem.* **2008**, *13*, 1149-1155.
- [26] R. E. Aird, J. Cummings, A. A. Ritchie, M. Muir, R. E. Morris, H. Chen, P. J. Sadler, D. I. Jodrell, *Br. J. Cancer* **2002**, *86*, 1652-1657.
- [27] A. Habtemariam, M. Melchart, R. Fernandez, S. Parsons, I. D. H. Oswald, A. Parkin, F. P. A. Fabbiani, J. E. Davidson, A. Dawson, R. E. Aird, D. I. Jodrell, P. J. Sadler, *J. Med. Chem.* **2006**, *49*, 6858-6868.
- [28] W. H. Ang, E. Daldini, C. Scolaro, R. Scopelliti, L. Juillerat-Jeannerat, P. J. Dyson, *Inorg. Chem.* **2006**, *45*, 9006-9013.
- [29] M. G. Mendoza-Ferri, C. G. Hartinger, R. E. Eichinger, N. Stolyarova, M. A. Jakupec, A. A. Nazarov, K. Severin, B. K. Keppler, *Organometallics* **2008**, *27*, 2405-2407.
- [30] M. G. Mendoza-Ferri, C. G. Hartinger, A. A. Nazarov, W. Kandioller, K. Severin, B. K. Keppler, *Appl. Organomet. Chem.* **2008**, *22*, 326-332.
- [31] R. Schuecker, R. O. John, M. A. Jakupec, V. B. Arion, B. K. Keppler, *Organometallics* **2008**, *27*, 6587-6595.
- [32] W. Kandioller, C. G. Hartinger, A. A. Nazarov, J. Kasser, R. John, M. A. Jakupec, V. B. Arion, P. J. Dyson, B. K. Keppler, *J. Organomet. Chem.* **2009**, *694*, 922-929.
- [33] M. G. Mendoza-Ferri, C. G. Hartinger, M. A. Mendoza, M. Groessl, A. E. Egger, R. E. Eichinger, J. B. Mangrum, N. P. Farrell, M. Maruszak, P. J. Bednarski, F. Klein, M. A. Jakupec, A. A. Nazarov, K. Severin, B. K. Keppler, *J. Med. Chem.* **2009**, *52*, 916-925.
- [34] W. Kandioller, C. G. Hartinger, A. A. Nazarov, M. L. Kuznetsov, R. John, C. Bartel, M. A. Jakupec, V. B. Arion, B. K. Keppler, *Organometallics* **2009**, in press.
- [35] W. H. Ang, Z. Grote, R. Scopelliti, L. Juillerat-Jeanneret, K. Severin, P. J. Dyson, *J. Organomet. Chem.* **2009**, *694*, 968-972.
- [36] K. H. Thompson, C. A. Barta, C. Orvig, *Chem. Soc. Rev.* **2006**, *35*, 545-556.
- [37] Z. D. Liu, H. H. Khodr, D. Y. Liu, S. L. Lu, R. C. Hider, *J. Med. Chem.* **1999**, *42*, 4814-4823.
- [38] J. A. Lewis, D. T. Puerta, S. M. Cohen, *Inorg. Chem.* **2003**, *42*, 7455-7459.
- [39] R. Lang, K. Polborn, T. Severin, K. Severin, *Inorg. Chim. Acta* **1999**, *294*, 62-67.
- [40] I. Berger, M. Hanif, A. A. Nazarov, C. G. Hartinger, R. O. John, M. L. Kuznetsov, M. Groessl, F. Schmitt, O. Zava, F. Biba, V. B. Arion, M. Galanski, M. A. Jakupec, L. Juillerat-Jeanneret, P. J. Dyson, B. K. Keppler, *Chem. Eur. J.* **2008**, *14*, 9046-9057.
- [41] A. Dorcier, C. G. Hartinger, R. Scopelliti, R. H. Fish, B. K. Keppler, P. J. Dyson, *J. Inorg. Biochem.* **2008**, *102*, 1066-1076.
- [42] W. L. F. Armarego, C. Chai, *Purification of Laboratory Chemicals*, 5th ed., Butterworth Heinemann, Oxford, **2003**.
- [43] M. R. Pressprich, J. Chambers, *SAINT + Integration Engine, Program for Crystal Structure Integration*, Bruker Analytical X-ray systems, Madison, **2004**.
- [44] G. M. Sheldrick, *SHELXS-97, Program for Crystal Structure Solution*, University Göttingen (Germany), **1997**.
- [45] G. M. Sheldrick, *SHELXL-97, Program for Crystal Structure Refinement*, University Göttingen (Germany), **1997**.
- [46] L. J. Farrugia, *J. Appl. Crystallogr.* **1997**, *30*, 565.
- [47] *International Tables for X-ray Crystallography, Vol. C*, Kluwer Academic Press, Dordrecht, The Netherlands, **1992**.
- [48] A. Krezel, W. Bal, *J. Inorg. Biochem.* **2004**, *98*, 161-166.
- [49] A. D. Becke, *J. Chem. Phys.* **1993**, *98*, 5648-5652.
- [50] C. Lee, W. Yang, R. G. Parr, *Phys. Rev. B: Condens. Matter* **1988**, *37*, 785-789.
- [51] M. J. Frisch, G. W. Trucks, H. B. Schlegel, G. E. Scuseria, M. A. Robb, J. R. Cheeseman, J. Montgomery, J. A., T. Vreven, K. N. Kudin, J. C. Burant, J. M.

Millam, S. S. Iyengar, J. Tomasi, V. Barone, B. Mennucci, M. Cossi, G. Scalmani, N. Rega, G. A. Petersson, H. Nakatsuji, M. Hada, M. Ehara, K. Toyota, R. Fukuda, J. Hasegawa, M. Ishida, T. Nakajima, Y. Honda, O. Kitao, H. Nakai, M. Klene, X. Li, J. E. Knox, H. P. Hratchian, J. B. Cross, V. Bakken, C. Adamo, J. Jaramillo, R. Gomperts, R. E. Stratmann, O. Yazyev, A. J. Austin, R. Cammi, C. Pomelli, J. W. Ochterski, P. Y. Ayala, K. Morokuma, G. A. Voth, P. Salvador, J. J. Dannenberg, V. G. Zakrzewski, S. Dapprich, A. D. Daniels, M. C. Strain, O. Farkas, D. K. Malick, A. D. Rabuck, K. Raghavachari, J. B. Foresman, J. V. Ortiz, Q. Cui, A. G. Baboul, S. Clifford, J. Cioslowski, B. B. Stefanov, G. Liu, A. Liashenko, P. Piskorz, I. Komaromi, R. L. Martin, D. J. Fox, T. Keith, M. A. Al-Laham, C. Y. Peng, A. Nanayakkara, M. Challacombe, P. M. W. Gill, B. Johnson, W. Chen, M. W. Wong, C. Gonzalez, J. A. Pople, *Gaussian 03, Revision D.01*, Gaussian, Inc., Wallingford CT, **2004**.

-
- [52] D. Andrae, U. Haeussermann, M. Dolg, H. Stoll, H. Preuss, *Theor. Chim. Acta* **1990**, *77*, 123-141.
[53] J. Tomasi, M. Persico, *Chem. Rev.* **1994**, *94*, 2027-2094.
[54] V. Barone, M. Cossi, *J. Phys. Chem. A* **1998**, *102*, 1995-2001.

Received: ((will be filled in by the editorial staff))
Revised: ((will be filled in by the editorial staff))
Published online: ((will be filled in by the editorial staff))

Supporting Information

Maltol-derived ruthenium-cymene complexes with tumor inhibiting properties: The impact of ligand-metal bond stability on the anticancer activity

Wolfgang Kandioller^[a], Christian G. Hartinger^[a], Alexey A. Nazarov*^[a,b], Caroline Bartel^[a], Matthias Skocic^[a], Michael A. Jakupec^[a], Vladimir B. Arion^[a] and Bernhard K. Keppler^[a]*

^a University of Vienna, Institute of Inorganic Chemistry, Austria

^b Institut des Sciences et Ingénierie Chimiques, Ecole Polytechnique Fédérale de Lausanne,
Switzerland

Table of contents

1. Characterization of the complexes 2a and 2e by ^1H NMR spectroscopy.....	3
2. Single crystal X-ray diffraction analysis data.....	4
3. <i>In vitro</i> anticancer activity.....	8
4. $\text{p}K_a$ determination.....	10
4.1. NMR titration.....	10
4.2. Computational details.....	11
5. Reactions of complexes 3a–h with amino acids.....	24
6. The reaction of 3h with amino acids.....	27
6.1. Glycine with an equimolar amount of 3h	27
6.2. L-Histidine with an equimolar amount of 3h	28
6.3. L-Methionine with an equimolar amount of 3h	29
6.4. L-Cysteine with an equimolar amount of 3h	30
7. References.....	31

1. Characterization of the complexes **2a** and **2e** by ^1H NMR spectroscopy

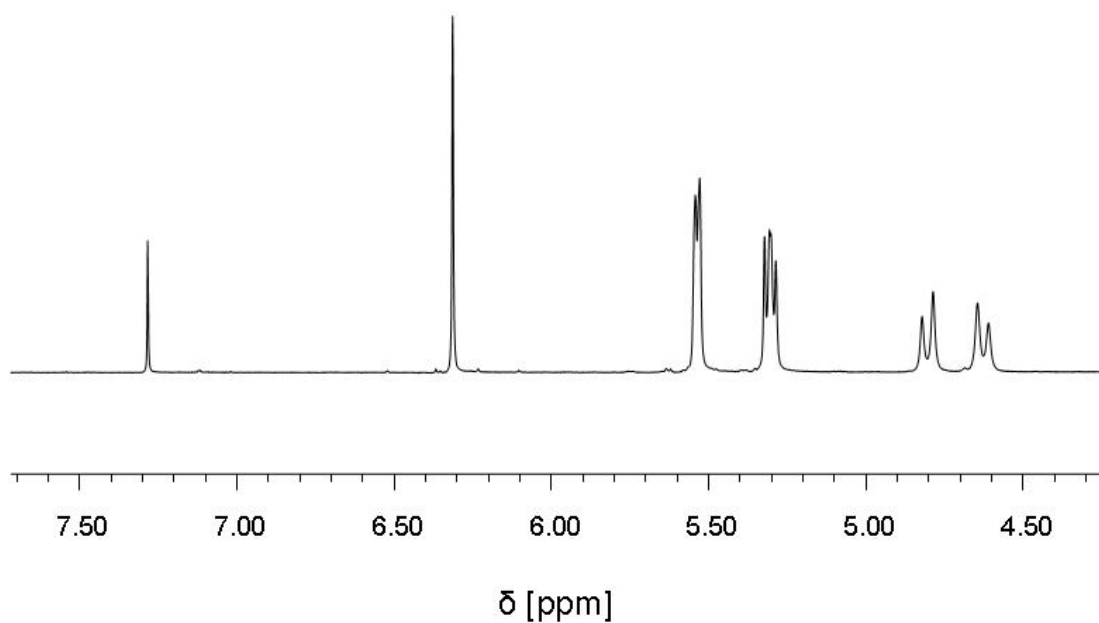


Figure S1: Geminal splitting of the CH_2 group in the ^1H NMR spectrum of **2e** in CDCl_3 , due to the formation of a hydrogen bond between $-\text{OH}$ and O_3 .

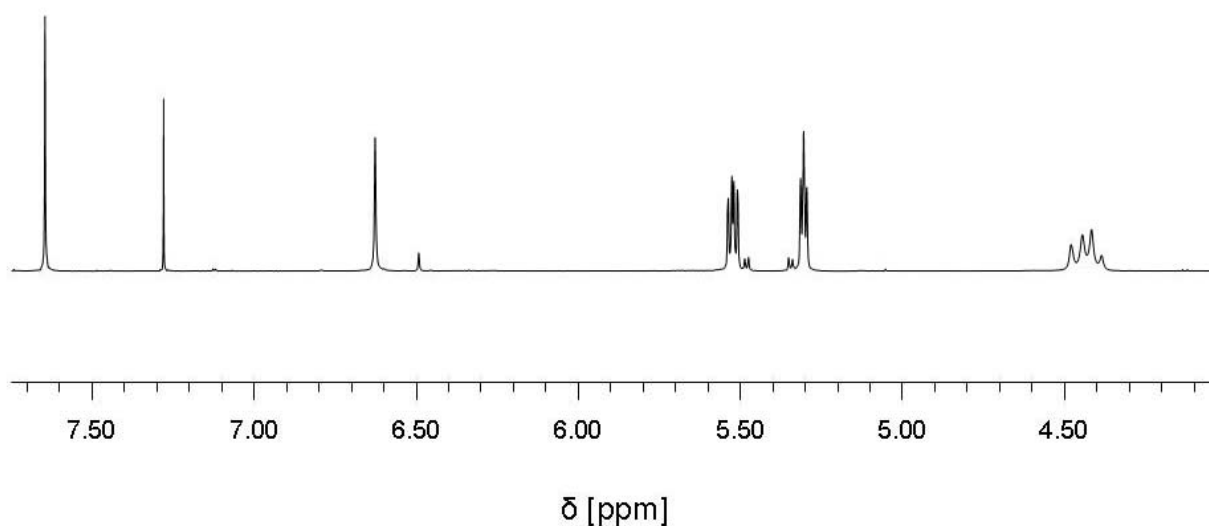


Figure S2: Geminal splitting of the CH_2 group in the ^1H NMR spectrum of **2a** in CDCl_3 , due to the formation of a hydrogen bond between $-\text{OH}$ and O_1 .

2. Single crystal X-ray diffraction analysis data

Table S1: Crystallographic data of **2a**.

Chemical formula 2a	C ₁₆ H ₁₉ ClO ₄ Ru
M (g mol ⁻¹)	411.85
Temperature (K)	100(2)
Crystal size (mm ³)	0.20 × 0.15 × 0.10
Crystal color, shape	red, block
Crystal system	monoclinic
Space group	<i>P2₁/n</i>
<i>a</i> (Å)	10.7989(4)
<i>b</i> (Å)	14.1722(8)
<i>c</i> (Å)	21.0364(10)
β (°)	90.003(3)
<i>V</i> (Å ³)	3207.2(3)
<i>Z</i>	8
D _c (g cm ⁻³)	1.706
μ (cm ⁻¹)	11.58
F(000)	1664
θ range for data collection (°)	2.05–25.71
<i>h</i> range	-13/13
<i>k</i> range	-17/17
<i>l</i> range	-25/25
No. refls. used in refinement	6091
No. parameters	401
<i>R</i> _{int}	0.1015
<i>R</i> ₁ ^a	0.0412
w <i>R</i> ₂ ^b	0.1107
GOF ^c	1.001

^a $R_1 = \Sigma||F_o| - |F_c||/\Sigma|F_o|$.

^b $wR_2 = \{\Sigma[w(F_o^2 - F_c^2)^2]/w\Sigma(F_o^2)^2\}^{1/2}$.

^c $GOF = \{\Sigma[w(F_o^2 - F_c^2)^2]/(n - p)\}^{1/2}$, where *n* is the number of reflections and *p* is the total number of parameters refined.

Table S2: Crystallographic data of **2c**.

Chemical formula 2c	C ₁₅ H ₁₇ ClO ₃ Ru
M (g mol ⁻¹)	381.81
Temperature (K)	100(2)
Crystal size (mm ³)	0.18 × 0.16 × 0.12
Crystal color, shape	red, block
Crystal system	triclinic
Space group	<i>P</i> -1
a (Å)	8.0776(7)
b (Å)	8.4215(10)
c (Å)	11.2342(14)
α (°)	83.675(9)
β (°)	73.624(6)
γ (°)	89.712(7)
V (Å ³)	728.48
Z	2
D _c (g cm ⁻³)	1.741
μ (cm ⁻¹)	12.63
F(000)	384
θ range for data collection (°)	2.43–25.70
h range	-9/9
k range	-10/10
l range	-13/13
No. refls. used in refinement	2771
No. parameters	182
<i>R</i> _{int}	0.0643
<i>R</i> ₁ ^a	0.0271
w <i>R</i> ₂ ^b	0.0634
GOF ^c	1.024

^a $R_1 = \frac{\sum ||F_o| - |F_c||}{\sum |F_o|}$

^b $wR_2 = \left\{ \frac{\sum [w(F_o^2 - F_c^2)^2]}{w \sum (F_o^2)^2} \right\}^{1/2}$

^c $GOF = \left\{ \frac{\sum [w(F_o^2 - F_c^2)^2]}{(n - p)} \right\}^{1/2}$, where *n* is the number of reflections and *p* is the total number of parameters refined.

Table S3: Crystallographic data of **2d**.

Chemical formula 2d	C ₁₆ H ₁₉ ClO ₃ Ru
M (g mol ⁻¹)	395.85
Temperature (K)	296(2)
Crystal size (mm ³)	0.30 × 0.25 × 0.20
Crystal color, shape	red, block
Crystal system	monoclinic
Space group	<i>P</i> 2 ₁ / <i>c</i>
<i>a</i> (Å)	11.8660(5)
<i>b</i> (Å)	9.2496(4)
<i>c</i> (Å)	15.5200(6)
β (°)	109.523(2)
<i>V</i> (Å ³)	1605.48(12)
<i>Z</i>	4
D _c (g cm ⁻³)	1.638
μ (cm ⁻¹)	11.49
F(000)	800
θ range for data collection (°)	2.61–26.42
<i>h</i> range	-14/14
<i>k</i> range	-11/11
<i>l</i> range	-19/19
No. refls. used in refinement	3305
No. parameters	190
<i>R</i> _{int}	0.0534
<i>R</i> ₁ ^a	0.0355
w <i>R</i> ₂ ^b	0.0931
GOF ^c	1.037

^a $R_1 = \Sigma||F_o| - |F_c||/\Sigma|F_o|.$

^b $wR_2 = \{\Sigma[w(F_o^2 - F_c^2)^2]/w\Sigma(F_o^2)^2\}^{1/2}.$

^c GOF = $\{\Sigma[w(F_o^2 - F_c^2)^2]/(n - p)\}^{1/2}$, where *n* is the number of reflections and *p* is the total number of parameters refined.

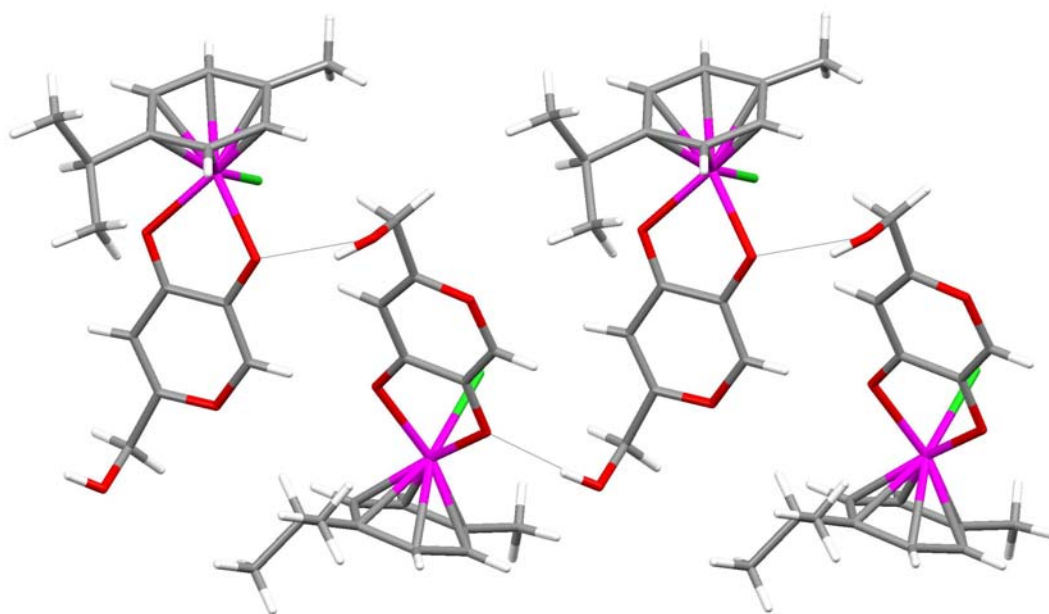


Figure S3: Syndiotactic chain formed by the R- and S-enantiomers of **2a**.

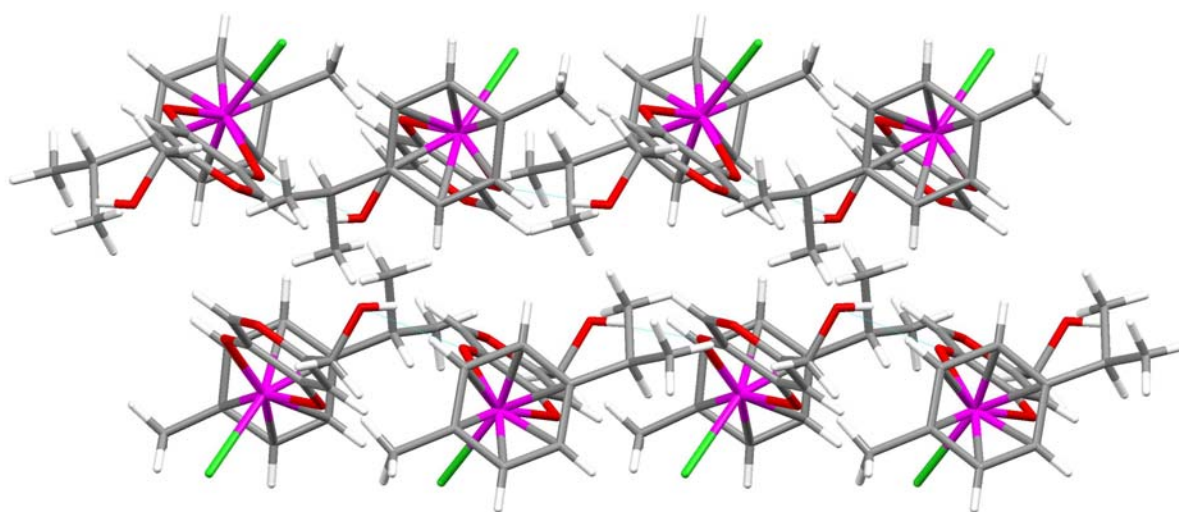


Figure S4: Layer structure of **2a** in the crystal.

3. *In vitro* anticancer activity

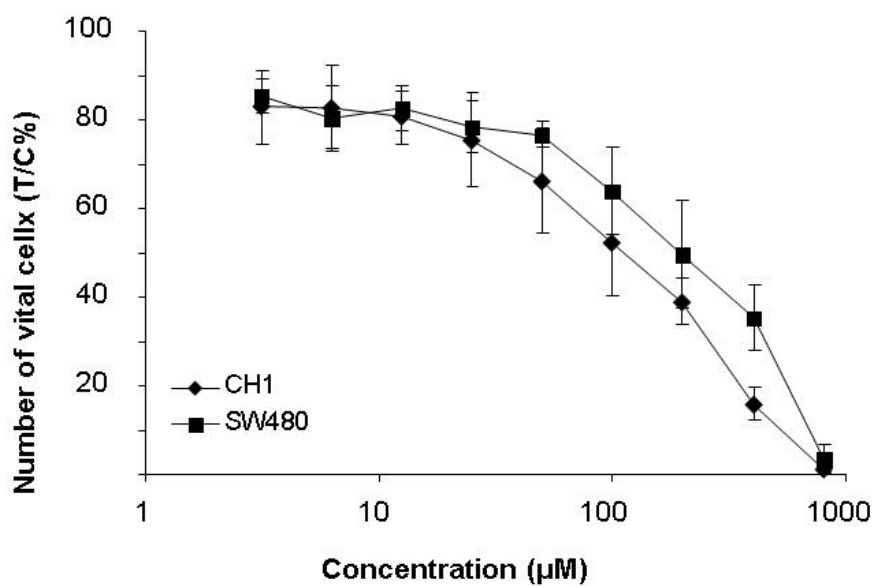


Figure S5: Concentration-effect curves of 3c in CH1 and SW480 cell lines.

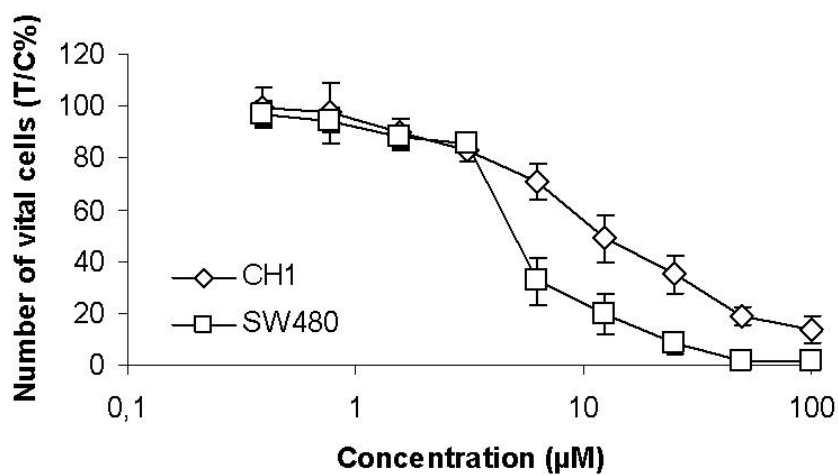


Figure S6: Concentration-effect curves of 3h in CH1 and SW480 cell lines.

Table S4: Solubility of **3a–h** in PBS.

Complex	Solubility in PBS (mg/mL)
3a	> 10
3b ^{S1}	> 10
3c	> 10
3d ^{S1}	> 10
3e	> 10
3f	5
3g ^{S1}	< 1 ^a
3h ^{S1}	< 1 ^a

^a in 1% DMSO/PBS solution: > 10 mg/mL.

4. pK_a determination

4.1. NMR titration

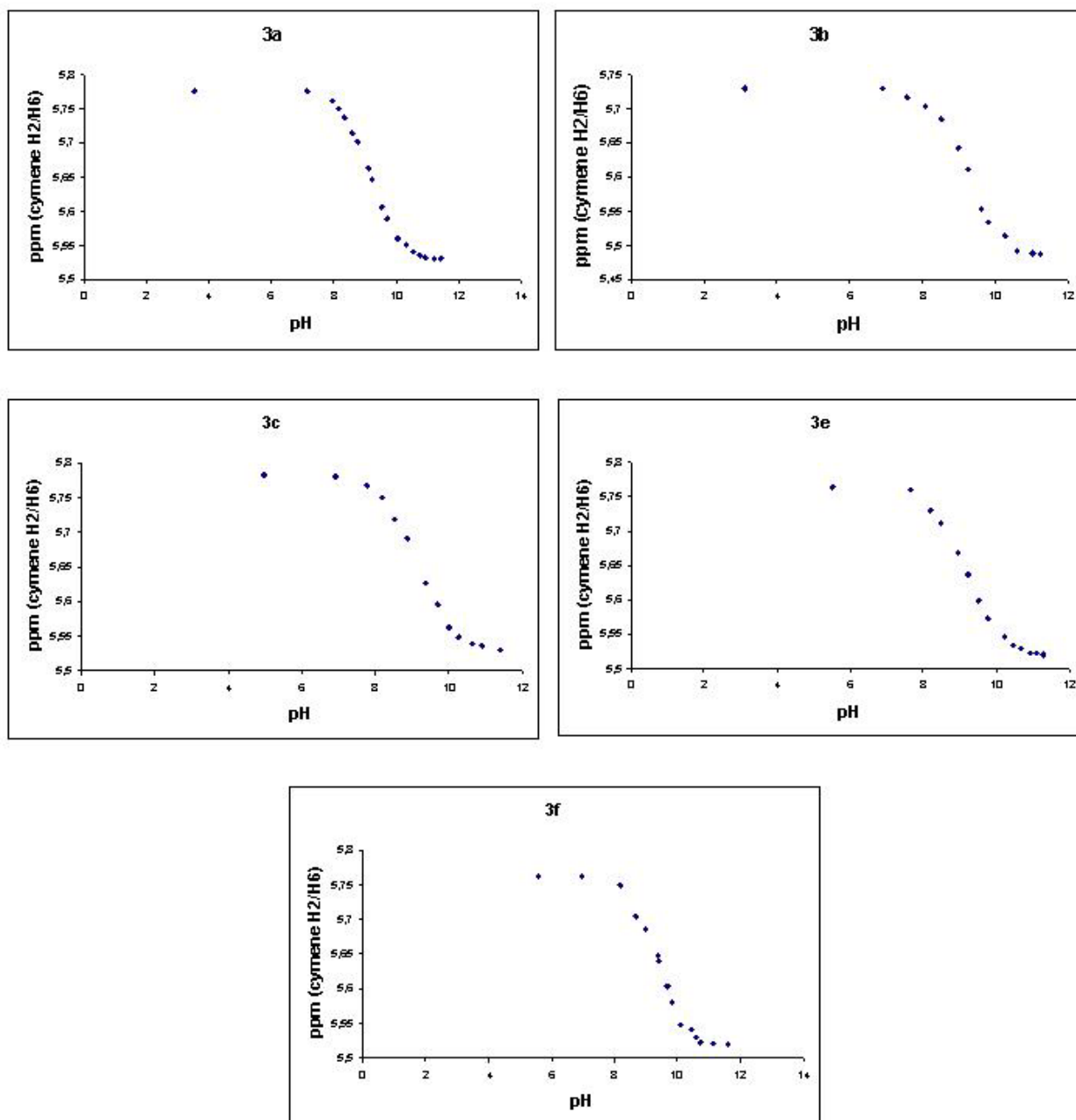


Figure S7: Titration curves for the pK_a determination by means of ^1H NMR spectroscopy.

4.2. Computational details

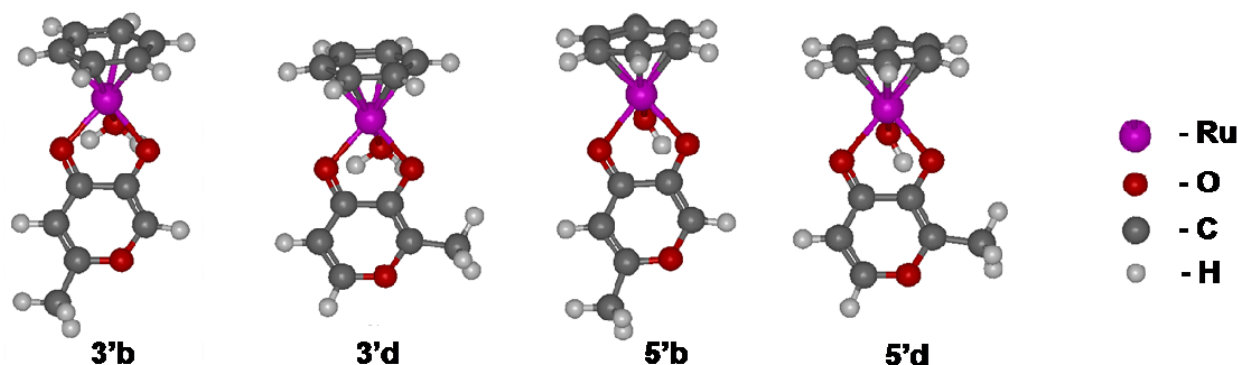


Figure S8. Equilibrium structures of the calculated pyrone complexes with numbering of selected atoms. Structures of the thiopyrone species are similar.

Table S5. Total energies, enthalpies and Gibbs free energies for the gas-phase and H₂O solution (Hartree) of the calculated structures.

	$E_g(6-31G^*)$	$E_g(6-31+G^{**})$	E_s	H_g	G_g	G_s
H ₂ O	-76.408953	-76.433933	-76.445244	-76.384013	-76.406114	-76.417425
H ₃ O ⁺	-76.689084	-76.707574	-76.880432	-76.650930	-76.673921	-76.846779
Cl ⁻	-460.252233	-460.274726	-460.388702	-460.249873	-460.267256	-460.381232
2'd	-1244.752725	-1244.785467	-1244.808913	-1244.528795	-1244.589480	-1244.612926
3'd	-860.753112	-860.793688	-860.870726	-860.503495	-860.565452	-860.642490
5'd	-860.334699	-860.375987	-860.401011	-860.099002	-860.160042	-860.185066
2'h	-1567.725128	-1567.756490	-1567.779352	-1567.503125	-1567.566512	-1567.589374
3'h	-1183.730680	-1183.769920	-1183.844267	-1183.482906	-1183.545901	-1183.620248
5'h	-1183.306404	-1183.346214	-1183.370216	-1183.072593	-1183.135279	-1183.159281
2'b	-1244.752547	-1244.785001	-1244.810377	-1244.528703	-1244.589490	-1244.614866
3'b	-860.753388	-860.793873	-860.871775	-860.503809	-860.565338	-860.643240
5'b	-860.334962	-860.375987	-860.402292	-860.099323	-860.159878	-860.186183
2'g	-1567.724717	-1567.755941	-1567.780854	-1567.502724	-1567.565314	-1567.590227
3'g	-1183.730836	-1183.769955	-1183.844913	-1183.483090	-1183.545807	-1183.620765
5'g	-1183.305917	-1183.345628	-1183.371532	-1183.072164	-1183.134632	-1183.160536

Table S6. Cartesian coordinates (Å) of the calculated equilibrium structures of the complexes.**2'b**

Ru	-1.151625	0.008824	-0.011704
Cl	-0.529393	2.337869	-0.011134
O	3.941668	-0.150756	0.973138
O	0.350649	-0.249553	1.414042
O	0.559083	-0.245173	-1.247858
C	-2.257874	-1.525794	-1.124459
H	-1.829779	-2.141372	-1.909460
C	-2.175773	-1.957723	0.224155
H	-1.706814	-2.902648	0.473799
C	-2.818445	-0.250902	-1.461588
C	1.545361	-0.198260	0.878599
C	-3.123316	0.218972	0.947565
H	-3.352854	0.924950	1.736720
C	-3.232982	0.614668	-0.423011
H	-3.527238	1.630929	-0.659553
C	2.720385	-0.165406	1.585370
C	1.642077	-0.218542	-0.572679
H	2.801174	-0.138805	2.662921
C	-2.571788	-1.052529	1.257840
C	2.937307	-0.230092	-1.158556
H	3.037444	-0.248889	-2.237712
C	4.048836	-0.181882	-0.362313
C	5.469139	-0.148971	-0.830593
H	-2.819485	0.089184	-2.490771
H	-2.372576	-1.307805	2.293789
H	5.966748	0.766294	-0.489553
H	5.512981	-0.184888	-1.921247
H	6.031111	-0.998978	-0.426422

2'd

Ru	1.263322	0.694785	-0.519390
Cl	1.374085	-0.465312	-2.629825
O	-0.416880	-4.063596	0.661424
O	1.691882	-1.147331	0.357558
O	-0.675472	-0.156716	-0.366232
C	0.514582	2.612129	0.215428
H	-0.525502	2.801025	0.462731
C	1.386707	2.093188	1.216396
H	1.025632	1.911221	2.222159
C	0.960126	2.817668	-1.124385
C	0.654991	-1.955006	0.333449
C	3.150286	1.839025	-0.511609
H	4.116683	1.451678	-0.811736
C	2.270846	2.404604	-1.479495
H	2.567746	2.416597	-2.522253
C	0.716202	-3.293023	0.665089
C	-0.627787	-1.390052	-0.036275
C	1.945719	-4.042041	1.044665
C	2.686740	1.666359	0.826154
C	-1.772412	-2.236598	0.008715
H	-2.751390	-1.850441	-0.250400
C	-1.605752	-3.543512	0.347178
H	-2.395156	-4.284071	0.388949
H	0.270580	3.164560	-1.884815
H	3.305871	1.127837	1.536769
H	2.810721	-3.388637	0.917558
H	2.074586	-4.930063	0.414116
H	1.907385	-4.378948	2.089088

2'g

Ru	-1.231863	-0.015157	0.007590
Cl	-0.680801	-1.222759	2.034205
O	3.968665	-0.986851	-0.720975
O	0.377358	-1.042998	-0.849886
S	0.513373	1.524754	0.621406
C	-2.773611	1.547767	-0.079924
H	-2.692489	2.531021	0.371626
C	-2.293755	1.339614	-1.417663
H	-1.852753	2.162051	-1.969024
C	-3.285753	0.467857	0.678823
C	1.588285	-0.647267	-0.580181
C	-2.805744	-1.071592	-1.187955
H	-2.726602	-2.079703	-1.578384
C	-3.305278	-0.848522	0.109910
H	-3.593579	-1.689516	0.729834
C	2.694119	-1.386209	-0.959248
C	1.849064	0.600079	0.103658
H	2.645964	-2.341401	-1.462920
C	-2.279022	0.030414	-1.945517
C	3.196325	0.981885	0.304096
H	3.425140	1.914838	0.807563
C	4.226396	0.175746	-0.102890
C	5.687667	0.435654	0.076102
H	-3.576341	0.612269	1.712226
H	-1.806202	-0.160367	-2.903074
H	6.148853	-0.346781	0.690023
H	5.845213	1.399357	0.564910
H	6.203869	0.442509	-0.891019

2'h

Ru	1.311265	1.074878	-0.584596
Cl	1.585380	0.268461	-2.853205
O	0.199127	-4.111449	-0.092515
O	1.756894	-0.889542	-0.016866
S	-0.923355	0.187195	-0.684385
C	0.626566	3.105734	-0.092816
H	-0.381855	3.477768	-0.242354
C	0.968193	2.454108	1.140894
H	0.221299	2.332404	1.917449
C	1.572633	3.203882	-1.140782
C	0.832516	-1.800777	-0.152710
C	3.210563	1.957615	0.218089
H	4.157778	1.436866	0.303131
C	2.875177	2.627813	-0.974360
H	3.558666	2.608682	-1.815571
C	1.151731	-3.148082	0.000793
C	-0.535299	-1.458826	-0.439011
C	2.523238	-3.659617	0.274238
C	2.238548	1.853998	1.272011
C	-1.485600	-2.508966	-0.497450
H	-2.530512	-2.298922	-0.697998
C	-1.079855	-3.797919	-0.329182
H	-1.713150	-4.674206	-0.378468
H	1.288608	3.629337	-2.095956
H	2.463328	1.255175	2.148550
H	3.244729	-3.142351	-0.366324
H	2.573882	-4.736334	0.093249
H	2.820276	-3.464546	1.313727

3'b

Ru	0.582223	1.957559	-0.498825
O	0.859757	0.932151	-2.440570
O	0.261203	-2.871958	1.328016
O	1.598215	0.254869	0.097622
O	-1.006426	0.610536	-0.291805
C	-0.655681	3.696221	0.076705
H	-1.735105	3.675683	0.187099
C	0.172687	3.307771	1.179375
H	-0.274819	3.026118	2.125950
C	-0.086422	3.994761	-1.181372
C	0.769416	-0.719394	0.453009
C	2.165405	3.512222	-0.271452
H	3.229648	3.372889	-0.424125
C	1.327409	3.875317	-1.353039
H	1.754837	3.991263	-2.343935
C	1.158750	-1.907428	1.013762
C	-0.641831	-0.517963	0.223457
H	2.176894	-2.192962	1.242125
C	1.576391	3.216503	0.995178
C	-1.539708	-1.555543	0.567148
H	-2.603353	-1.432255	0.399398
C	-1.055909	-2.716819	1.116914
C	-1.859491	-3.901326	1.539468
H	-0.721503	4.227425	-2.028778
H	2.198614	2.831107	1.796408
H	0.031021	0.494391	-2.708050
H	1.484378	0.217220	-2.206498
H	-1.533103	-4.798667	1.001856
H	-2.920134	-3.736506	1.340989
H	-1.725601	-4.092836	2.610190

3'd

Ru	0.542595	0.869164	-1.297307
O	0.863722	-0.284744	-3.158545
O	0.568095	-3.801425	0.917138
O	1.675126	-0.716227	-0.592778
O	-0.946313	-0.558204	-0.966198
C	-0.821978	2.589070	-0.990829
H	-1.905151	2.527369	-0.973834
C	-0.080028	2.336034	0.210515
H	-0.601733	2.109000	1.133685
C	-0.149981	2.801675	-2.212459
C	0.914244	-1.712020	-0.142083
C	2.025665	2.517168	-1.070826
H	3.104591	2.419233	-1.115509
C	1.280326	2.747157	-2.248637
H	1.791765	2.805761	-3.203994
C	1.415848	-2.816790	0.517402
C	-0.502166	-1.616212	-0.367688
C	2.844982	-3.079115	0.837987
C	1.334853	2.299114	0.163227
C	-1.334745	-2.678081	0.071837
H	-2.406663	-2.648670	-0.085351
C	-0.749521	-3.734996	0.701903
H	-1.267748	-4.603953	1.087337
H	-0.712460	2.923592	-3.131534
H	1.895782	2.020470	1.049194
H	0.060002	-0.792540	-3.374001
H	1.532081	-0.938949	-2.873121
H	3.434668	-2.181570	0.643601
H	3.242332	-3.898571	0.225732
H	2.957788	-3.368209	1.888475

3'g

Ru	0.891711	1.867919	-0.069241
O	1.112943	1.254112	-2.194564
O	0.175806	-3.340433	0.756447
O	1.562461	-0.090642	0.117317
S	-1.245989	0.810892	-0.142065
C	0.194553	3.956200	0.328314
H	-0.755764	4.388235	0.034662
C	0.306125	3.230676	1.557622
H	-0.566547	3.104085	2.189322
C	1.302562	4.012521	-0.544457
C	0.675659	-1.050072	0.304048
C	2.660789	2.711035	1.035862
H	3.572769	2.173574	1.273274
C	2.553539	3.413642	-0.177621
H	3.384853	3.431570	-0.873982
C	1.063216	-2.340567	0.604473
C	-0.734966	-0.804650	0.187702
H	2.088180	-2.664877	0.727965
C	1.523602	2.596558	1.903909
C	-1.623690	-1.886282	0.354426
H	-2.693838	-1.735548	0.265433
C	-1.147747	-3.144263	0.638183
C	-1.953464	-4.381942	0.847623
H	1.197398	4.476450	-1.519618
H	1.585393	1.994175	2.803528
H	0.240101	1.020195	-2.563044
H	1.591518	0.407967	-2.087381
H	-1.664439	-5.156755	0.128522
H	-3.017475	-4.169394	0.727863
H	-1.785476	-4.785803	1.852600

3'h

Ru	0.417749	1.437329	-0.680957
O	0.690447	0.616449	-2.732596
O	-0.353340	-3.657867	0.631411
O	1.066015	-0.499848	-0.284624
S	-1.720534	0.389320	-0.716314
C	-0.337352	3.517909	-0.403714
H	-1.318483	3.886937	-0.682231
C	-0.140818	2.892866	0.870979
H	-0.976230	2.782742	1.553723
C	0.724806	3.554930	-1.331917
C	0.165310	-1.433785	-0.029450
C	2.209943	2.427504	0.272977
H	3.156077	1.951336	0.506673
C	2.013185	3.027914	-0.982714
H	2.808169	3.021037	-1.720745
C	0.564343	-2.692832	0.417590
C	-1.230471	-1.190308	-0.215629
C	1.968525	-3.116537	0.666736
C	1.117229	2.334539	1.198702
C	-2.140883	-2.246358	0.023592
H	-3.207721	-2.109826	-0.114418
C	-1.662220	-3.452238	0.441511
H	-2.251814	-4.332234	0.662687
H	0.557153	3.944916	-2.330248
H	1.244199	1.800222	2.134027
H	-0.177494	0.357521	-3.096427
H	1.154013	-0.220284	-2.529789
H	2.397713	-3.596155	-0.223470
H	2.010656	-3.837722	1.487722
H	2.581348	-2.244516	0.903923

5'b

Ru	0.683632	1.979794	-0.451454
O	1.099876	1.003903	-2.139870
O	0.179014	-2.893896	1.426807
O	1.584894	0.312634	0.496917
O	-0.977948	0.602034	-0.262145
C	-0.592273	3.650685	0.211440
H	-1.645597	3.563932	0.459592
C	0.381234	3.485088	1.228659
H	0.082130	3.284210	2.251122
C	-0.212934	3.867057	-1.155469
C	0.750186	-0.679461	0.682441
C	2.155258	3.589879	-0.515356
H	3.193761	3.466585	-0.799386
C	1.161739	3.839431	-1.504493
H	1.446715	3.865595	-2.550881
C	1.082714	-1.881468	1.256548
C	-0.638006	-0.504099	0.262168
H	2.067194	-2.148317	1.615219
C	1.745697	3.379812	0.841211
C	-1.538169	-1.589686	0.473093
H	-2.573006	-1.489642	0.165633
C	-1.098145	-2.751460	1.043201
C	-1.920933	-3.973038	1.306713
H	-0.971381	3.949199	-1.925435
H	2.486106	3.075219	1.574262
H	1.410027	0.124844	-1.865273
H	-1.522610	-4.834383	0.757746
H	-2.956037	-3.810520	0.998537
H	-1.906397	-4.227973	2.372724

5'd

Ru	0.666795	0.911335	-1.291045
O	1.192454	-0.092283	-2.930925
O	0.478820	-3.898491	0.789796
O	1.663356	-0.647456	-0.257866
O	-0.889001	-0.575433	-1.081271
C	-0.744957	2.502950	-0.714590
H	-1.792844	2.343760	-0.479684
C	0.219501	2.452611	0.322782
H	-0.082047	2.267869	1.347580
C	-0.358573	2.695025	-2.083365
C	0.896989	-1.692115	-0.041895
C	2.011859	2.628574	-1.396816
H	3.062027	2.578196	-1.659564
C	1.020017	2.760870	-2.410226
H	1.321306	2.768726	-3.452336
C	1.326847	-2.836856	0.600918
C	-0.484192	-1.631283	-0.499489
C	2.696633	-3.070763	1.137627
C	1.595034	2.438856	-0.039656
C	-1.315192	-2.768421	-0.261548
H	-2.347620	-2.767258	-0.591990
C	-0.788119	-3.851241	0.368876
H	-1.321800	-4.767922	0.589289
H	-1.107305	2.688597	-2.867089
H	2.343197	2.223576	0.716819
H	1.530155	-0.948833	-2.620310
H	3.299705	-2.177086	0.967567
H	3.180502	-3.922445	0.642197
H	2.672427	-3.285990	2.213557

5'g

Ru	0.830690	1.932275	-0.040419
O	0.620333	1.601591	-2.006970
O	0.307819	-3.408883	0.486267
O	1.558715	-0.066380	0.060701
S	-1.289649	0.775911	0.272915
C	0.457922	4.105144	0.051779
H	-0.348833	4.626441	-0.449840
C	0.255253	3.529133	1.348452
H	-0.718093	3.618902	1.820949
C	1.696772	3.886108	-0.610550
C	0.725490	-1.044480	0.236396
C	2.481787	2.545756	1.296018
H	3.213371	1.860826	1.713044
C	2.715871	3.109819	-0.002236
H	3.616506	2.860868	-0.551022
C	1.151180	-2.362219	0.304196
C	-0.703037	-0.825378	0.374024
H	2.182077	-2.673839	0.207255
C	1.291112	2.815684	2.013669
C	-1.533646	-1.953220	0.575746
H	-2.604602	-1.820820	0.686180
C	-1.012687	-3.219871	0.623483
C	-1.774642	-4.491827	0.815314
H	1.812018	4.203798	-1.641492
H	1.113124	2.360399	2.981140
H	0.114964	0.782002	-2.128312
H	-1.639777	-5.161203	-0.042544
H	-2.840537	-4.282109	0.929070
H	-1.425821	-5.026047	1.706951

5'h

Ru	0.586766	1.401966	-0.737999
O	1.161099	0.539890	-2.459334
O	-0.497575	-3.664910	0.695515
O	1.032362	-0.476585	0.155264
S	-1.570701	0.330685	-1.049646
C	-0.340369	3.314239	-0.204793
H	-1.406692	3.515194	-0.242256
C	0.236906	2.833924	1.005978
H	-0.379420	2.666573	1.881835
C	0.448075	3.507798	-1.383820
C	0.129896	-1.410170	0.154133
C	2.398260	2.575537	-0.191770
H	3.414865	2.200393	-0.209466
C	1.819579	3.130338	-1.360432
H	2.391414	3.147414	-2.282199
C	0.431647	-2.676953	0.660814
C	-1.199833	-1.194614	-0.362378
C	1.766527	-3.062556	1.196818
C	1.581829	2.395921	0.975006
C	-2.127104	-2.263332	-0.277679
H	-3.142656	-2.141482	-0.638768
C	-1.741089	-3.460745	0.245505
H	-2.361684	-4.341978	0.343293
H	-0.011336	3.854014	-2.302090
H	1.994052	1.872718	1.832124
H	0.550442	-0.188740	-2.655542
H	1.955146	-2.587083	2.168868
H	2.552673	-2.715310	0.518225
H	1.833934	-4.146706	1.318228

5. Reactions of complexes **3a–h** with amino acids

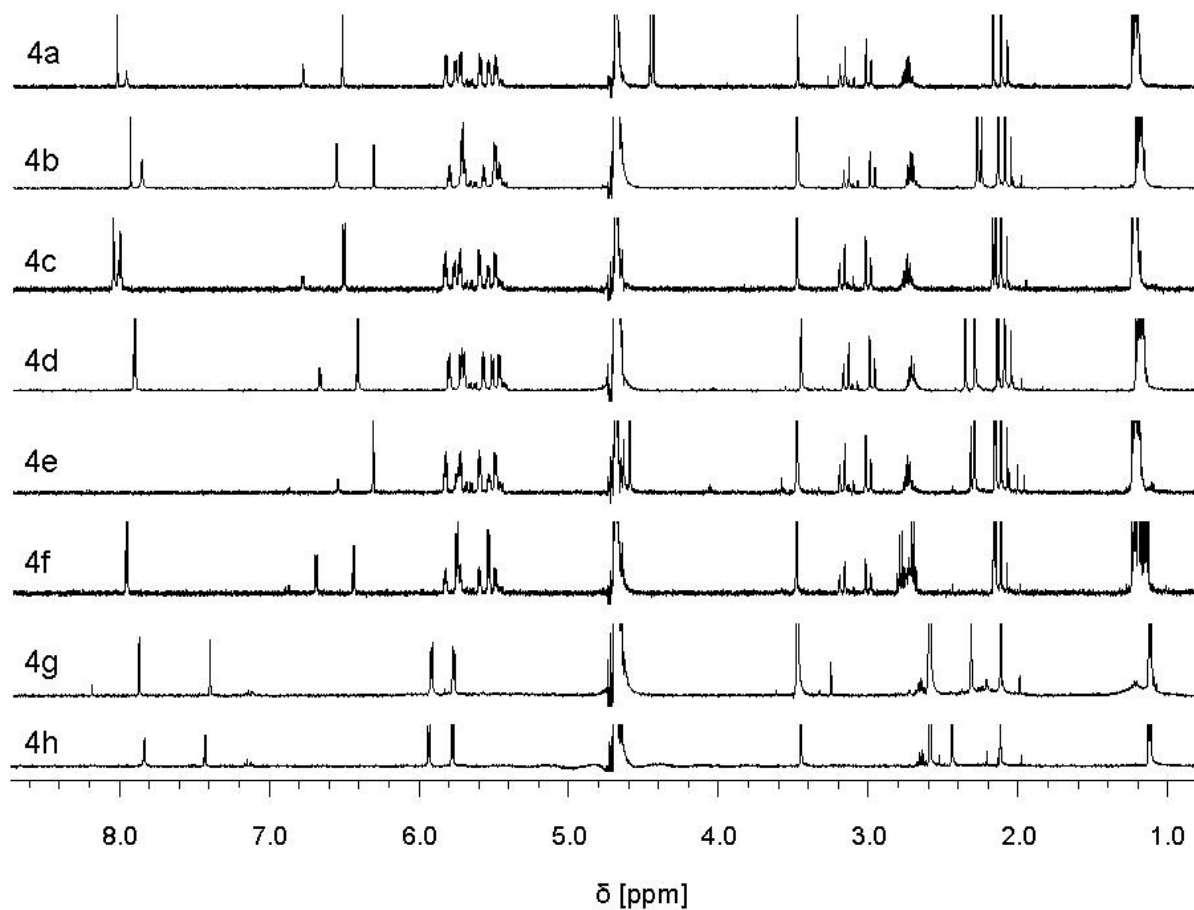


Figure S9: ¹H NMR spectra of the reaction products **4a–h** obtained by the incubation of **3a–h** with equimolar amounts of glycine after 18 h.

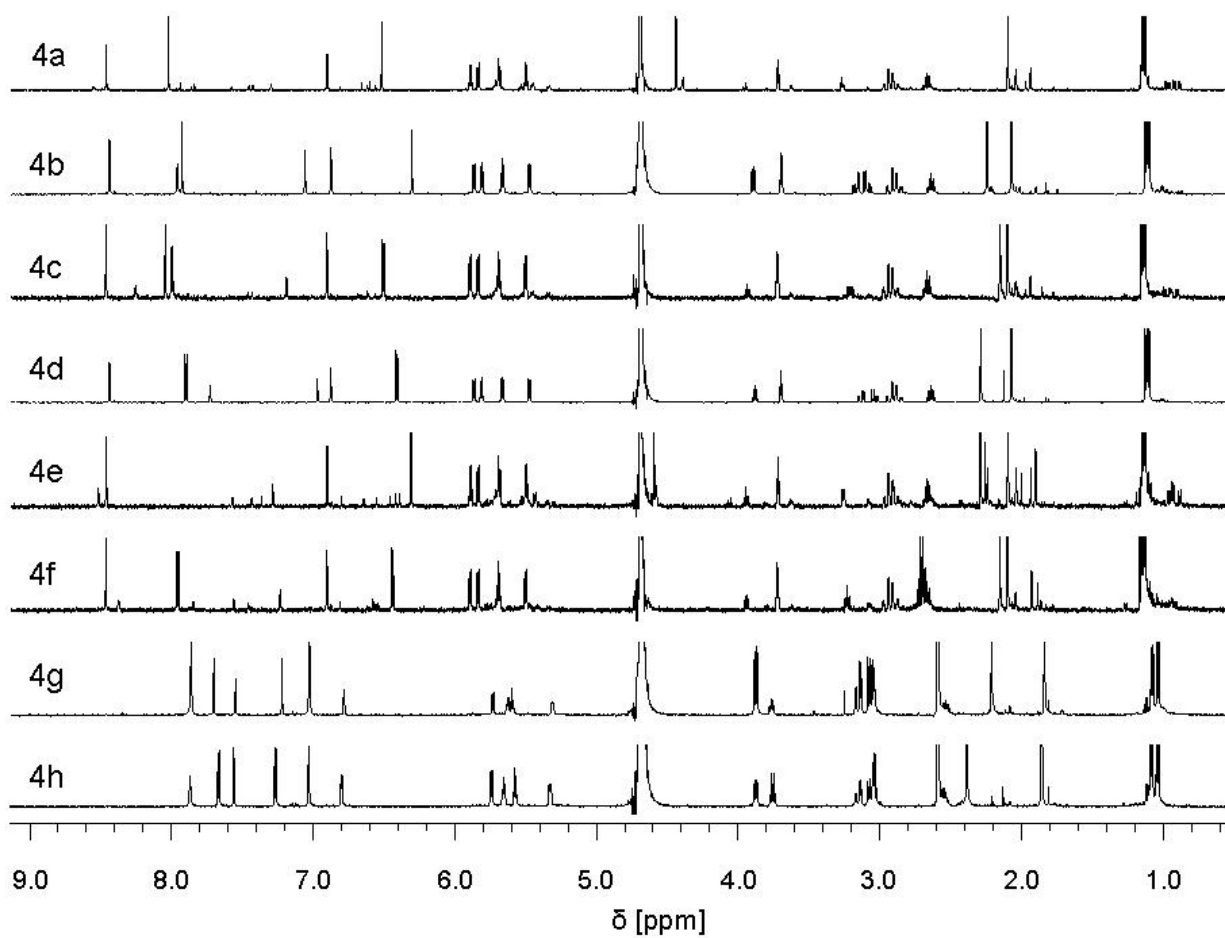


Figure S10: ¹H NMR spectra after 18 h of the reactions of **3a–h** with an equimolar amount of L-histidine.

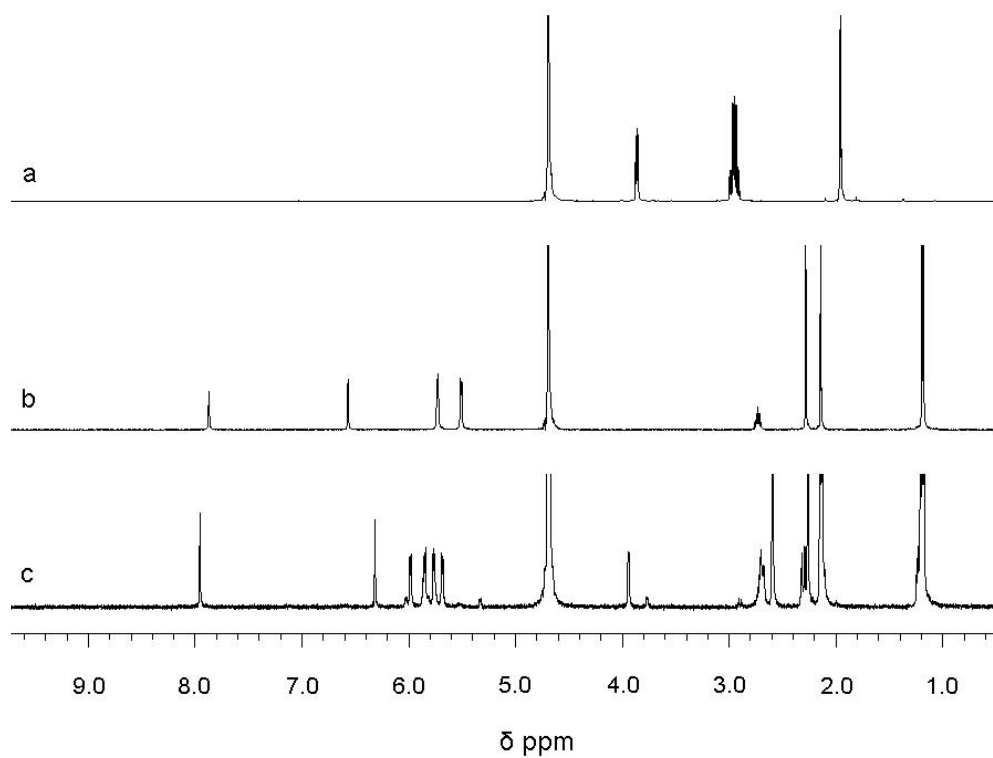


Figure S11: (a) *Se*-Methyl-L-selenocysteine, (b) **3b** and (c) the reaction of **3b** with an equimolar amount of *Se*-methyl-L-selenocysteine after 18 h.

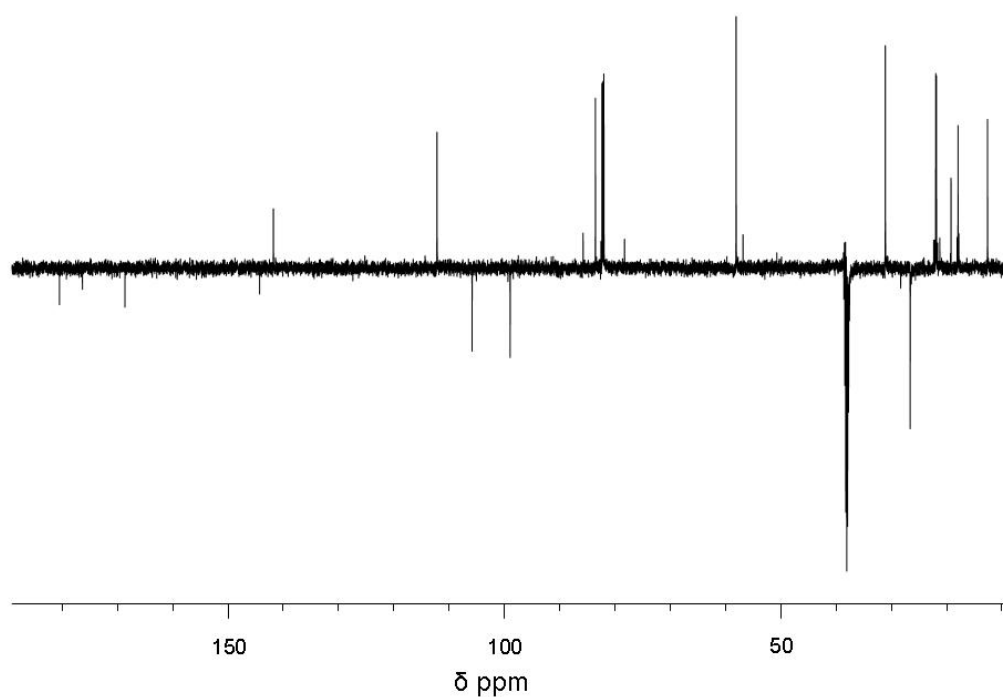


Figure S12: ^{13}C NMR spectrum of **3b** with an equimolar amount of *Se*-methyl-L-selenocysteine measured after 18 h.

6. The reaction of 3h with amino acids

6.1. Glycine with an equimolar amount of 3h

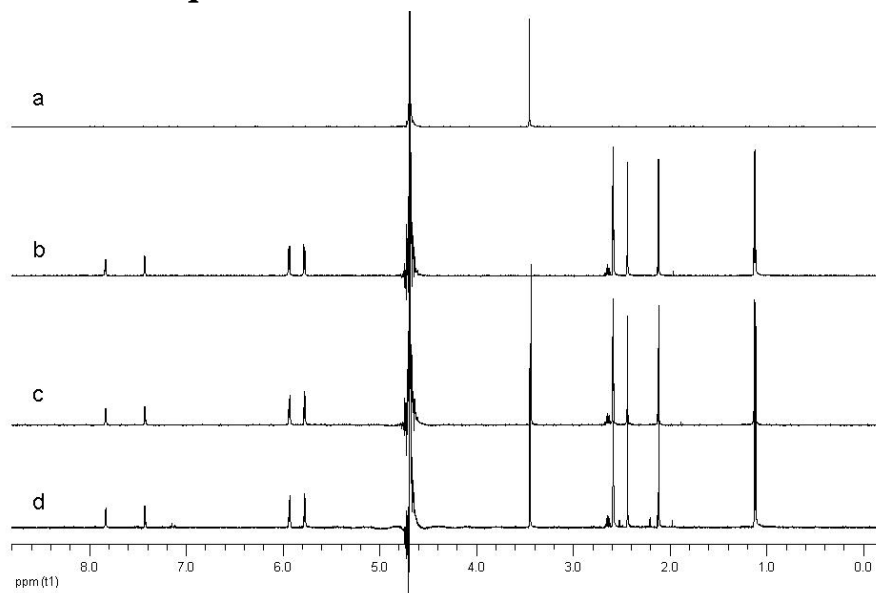


Figure S13: a) Glycine, b) 3h, c) 3h + 1 eq glycine after 5 min and d) after 18 h.

6.2. L-Histidine with an equimolar amount of **3h**

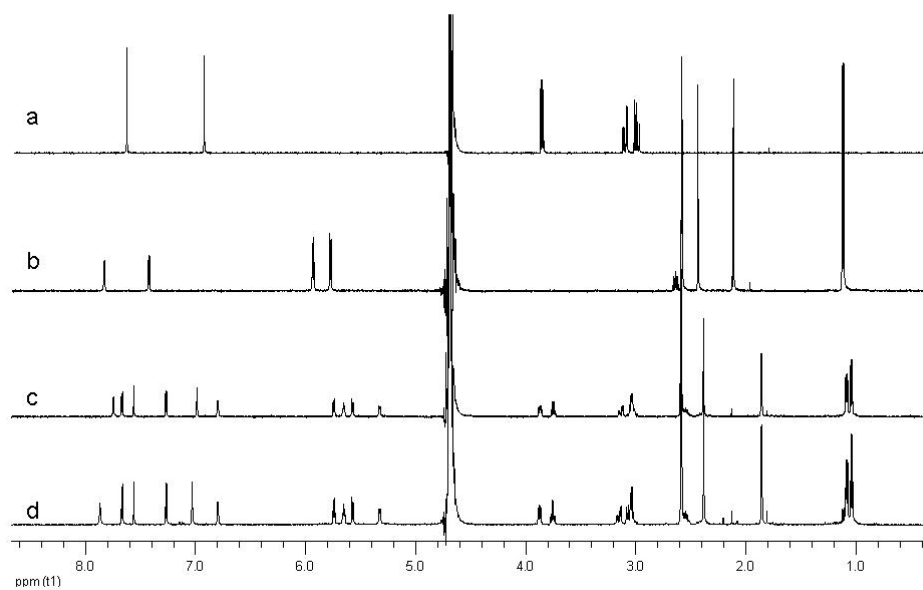


Figure S14: a) L-Histidine, b) **3h**, c) **3h** + 1 eq L-histidine after 5 min and d) after 18 h.

6.3. L-Methionine with an equimolar amount of **3h**

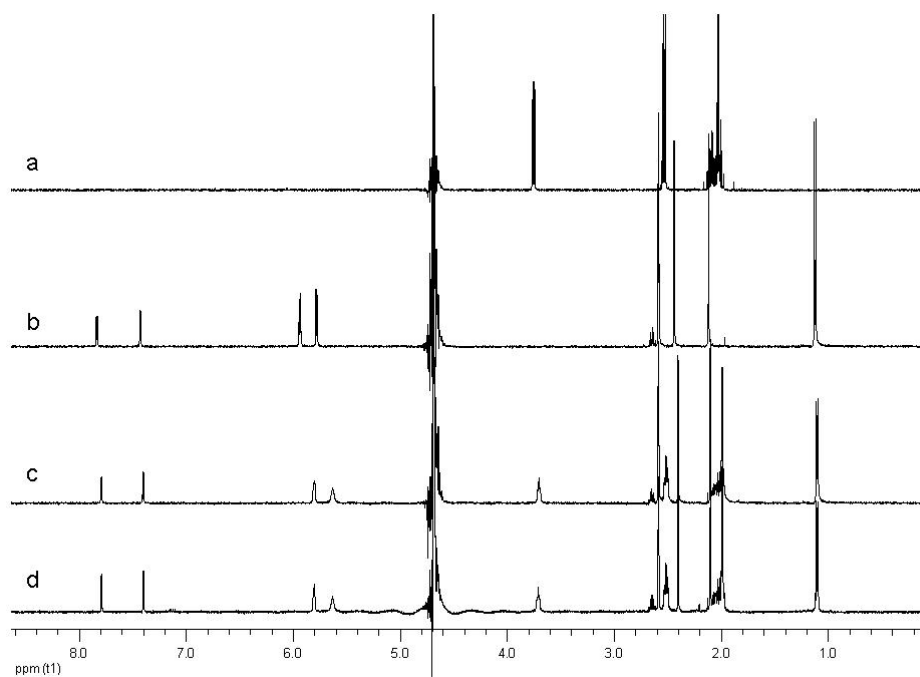


Figure S15: a) L-Methionine, b) **3h**, c) **3h** + 1 eq L-methionine after 5 min and d) after 18 h.

6.4. L-Cysteine with an equimolar amount of **3h**

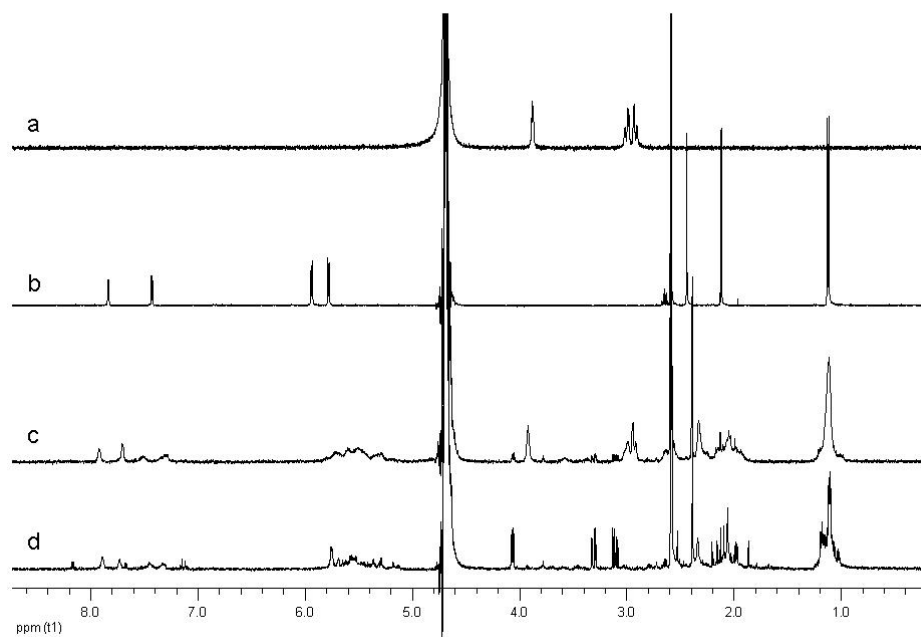


Figure S16: a) L-Cysteine, b) **3h**, c) **3h** + 1 eq L-cysteine after 5 min, d) **3h** + 1 eq L-cysteine after 18 h.

7. References

1. Kandioller, W.; Hartinger, C. G.; Nazarov, A. A.; Kuznetsov, M. L.; John, R.; Bartel, C.; Jakupec, M. A.; Arion, V. B.; Keppler, B. K. *Organometallics* **2009**, in press.

4. Conclusion and Outlook

Within this PhD thesis a series of novel pyrone and thiopyrone derived Ru(II) *p*-cymene complexes has been synthesized and their behavior in aqueous solution and reactivity towards small biomolecules was investigated. The cytotoxic activity in different human cancer cell lines was determined and structure-activity relationships were established.

Organometallic 2-hydroxymethylaryl-5-hydroxy-6-methyl-pyran-4(1*H*)-one derived Ru(II) *p*-cymene complexes were prepared, which hydrolyzed quick to form the charged aqua species by replacing the chlorido ligand by a water molecule. The more reactive aqua complex was found to be stable in solution for more than 18 h and in the presence of nucleophilic agents like 5'-GMP, selective binding over the *N7* of the purine ring was observed. Furthermore, the pK_a values (8.99–9.64) of the compounds were determined by means of ^1H NMR spectroscopy. These values implicate that the complexes are present as more reactive aqua species under physiological conditions. The compounds exhibit moderate cytotoxic activity and were found to be more active against CH1 cells (ovarian cancer cell line) than against SW480 (colon carcinoma) or A549 (non-small lung cancer) cells. The aryl moiety seems to be relevant for cytotoxic activity, because electron withdrawing groups decreased the IC_{50} value in contrast to electron donating groups.

The effect of thiopyrone coordination on the cytotoxic activity and on the behavior in aqueous solution was investigated. The aquation behavior of the thiopyrone complexes was found to be quite different to that of the earlier reported maltol complex. In contrast to the maltol complex, no formation of the dimeric species $[\text{Ru}_2(\textit{p}\text{-cymene})_2(\text{OH})_3]^+$ was observed. This side reaction was supposed to be responsible for the minimal activity of the substance. DFT calculations have been performed to explain the observed results. The replacement of the chlorido ligand by an imidazole molecule prevents the dimer formation of the pyrone complexes. The organometallic thiopyrone compounds were found to be by an order of magnitude more cytotoxic compared to the pyrone analogues and slightly more active in SW480 cells as compared to CH1 cells, though the latter are in general more chemosensitive to the majority of metal-based and other tumor-inhibiting compounds tested so far. Furthermore, the behavior in aqueous solution and the interaction with small biomolecules like 5'-GMP and amino acids was assayed. It was found, that the observed Ru dimer $[\text{Ru}_2(\textit{p}\text{-cymene})_2(\text{OH})_3]^+$ could not be the main factor for the minimal activity of the pyrone complexes, because the formation of the

dimeric species can also be inhibited by modification of the substitution pattern of the pyrone scaffold. Replacement of the chlorido ligand by imidazole was shown to be an effective additional option to obtain in aqueous solutions stable Ru(II)-(p-cymene)(pyrone) complexes. Therefore, the interactions of the amino acids Gly, L-His, L-Met and L-Cys were investigated and it was observed, that the pyrone ligands of the corresponding complexes were cleaved off and the amino acid was bound in a bidentate manner within 18 h. In contrast, the pyrone compounds, the thiopyrone complexes formed quickly adducts with L-His and L-Met and were stable in solution for more than 18 h. The reaction with L-Cys led to fast decomposition and Gly did not coordinate to the metal center. This feature gives the thiopyrone complexes more time to be taken up into the tumor cells, whereas the pyrone complexes decompose to compound mixtures involving amino acid coordination. These results have important implications on the mode of action of the compounds and considerably active thiopyrone vs. minimally active pyrone complexes were obtained.

Further research will be on the synthesis of thiopyrones and on the evaluation of their anti-cancer potential. The cellular uptake of these compounds should be investigated to get a deeper insight into the relationship between cytotoxic activity and cellular uptake. The change of the metal center and derivatization of the arene moiety is another direction opening interesting opportunities. Another possibility is the exchange of the chlorido ligand by more strongly coordinating ligands to prevent hydrolysis and cleavage of the pyrone in aqueous solution and investigations on the cytotoxic activity of this class of compounds. With regard to studies on the mode-of-action at the molecular level, the interactions with oligonucleotides and proteins will be investigated.

5. Curriculum vitae

Dipl. Ing. Wolfgang Kandioller

Penzinger Str. 157/2/15

1140 Wien

Tel. 0664 4254374

Email: wolfgang.kandioller@univie.ac.at



Nationality: Austria
Date of Birth: 21.06.1977
Marital status: single

Education

2008 to date	Teaching assistant (Assistent in Ausbildung) at the Institute of Inorganic Chemistry, University of Vienna
2004 to date	Ph.D. Research at the University of Vienna (Institute of Inorganic Chemistry) <i>“Synthesis of “piano-stool” configured ruthenium(II) arene complexes”</i>
28. November 2003	Graduation with Dipl. Ing.
1996 - 2003	Studies of Technical Chemistry Diploma Thesis under the supervision of Prof. Peter Stanetty (University of Technology of Vienna, Institute of Organic Chemistry): <i>„Microbial Baeyer-Villiger Oxidation of Bridged Bicyclic Ketones”</i>
June 1995	High-school graduation
1991 – 1995	High-school at the BORG Mistelbach
1987 – 1991	Hauptschule Poysdorf
1983 – 1987	Elementary school Herrnbaumgarten

Professional Experience

- 2005 – 2008 Lector at the Institute of Inorganic Chemistry, University of Vienna
- 2003 – 2008 Tutor at the Institute of Inorganic Chemistry, University of Vienna
- 2003 – 2008 Chemistry Teacher (HBLVA für Chemische Industrie)

Publications

“Maltol-derived ruthenium-cymene complexes with tumor inhibiting properties: The impact of ligand-metal bond stability on the anticancer activity”

Wolfgang Kandioller, Christian G. Hartinger, Alexey A. Nazarov, Caroline Bartel, Matthias Skocic, Michael A. Jakupec, Vladimir B. Arion and Bernhard K. Keppler, *Chemistry – A European Journal*, submitted

“From pyrone to thiopyrone ligands – rendering maltol-derived Ru(II)-arene complexes anticancer active in vitro”

Wolfgang Kandioller, Christian G. Hartinger, Alexey A. Nazarov, Maxim L. Kuznetsov, Roland John, Caroline Bartel, Michael A. Jakupec, Vladimir B. Arion and Bernhard K. Keppler, *Organometallics* **2009**, in press

„Tuning the anticancer activity of maltol-derived ruthenium complexes by derivatization of the 3-hydroxy-4-pyrone moiety”

Wolfgang Kandioller, Christian G. Hartinger, Alexey A. Nazarov, Johanna Kasser, Roland John, Michael A. Jakupec, Vladimir B. Arion, Paul J. Dyson, Bernhard K. Keppler, *Journal of Organometallic Chemistry*, **2009**, *694*, 922-929

“Modifying the structure of dinuclear ruthenium complexes with anti-tumor activity”

Maria G. Mendoza-Ferri, Christian G. Hartinger, Alexey A. Nazarov, Wolfgang Kandioller, Kay Severin, Bernhard K. Keppler, *Applied Organic Chemistry*, **2008**, 22, 326

„The Hydration of Chloroacetonitriles Catalyzed by Mono- and Dinuclear Ru(II) and Os(II) Arene Complexes“

Shaheen M. Ashraf, Wolfgang Kandioller, Maria-Grazia Mendoza Ferri, Alexey A. Nazarov, Christian G. Hartinger, Bernhard K. Keppler, *Chemistry & Biodiversity*, **2008**, 5, 2060

“Recombinant Whole-Cell Mediated Baeyer-Villiger Oxidation of Perhydropyran-Type Ketones”

Marko D. Mihovilovic, Birgit Grötzl, Wolfgang Kandioller, Adel Muskotal, Radka Snajdova, Florian Rudriff, Helmut Spreitzer, *Chemistry & Biodiversity*, **2008**, 5, 490

“Facile Synthesis and Ring-Opening Cross Metathesis of Carbo- and Heterocyclic Bicyclo(3.2.1)oct-6-en-3-ones Using Gaseous Olefinic Reaction Partners”

Marko D. Mihovilovic, Birgit Grötzl, Wolfgang Kandioller, Radka Snajdrova, Adel Muskotal, Dario A. Bianchi, Peter Stanetty, *Advanced Synthesis and Catalysis*, **2006**, 348, 463

“Synthesis and Enantioselective Baeyer-Villiger Oxidation of Prochiral Perhydropyranones with Recombinant E. Choli Producing Cyclohexanonemonooxygenase”

Marko D. Mihovilovic, Florian Rudroff, Wolfgang Kandioller, Birgit Grötzl, Peter Stanetty, Helmut Spreitzer, *Synlett*, **2003**, 13, 1973